Correlation of Corrosion Measurements and Bridge Conditions with NBIS Deck Rating

By
Andrei Ramniceanu

Thesis submitted to the faculty of the

Department of Civil and Environmental Engineering

Virginia Polytechnic Institute and State University

in partial fulfillment of the requirements for the degree of

Master of Science

In

Civil and Environmental Engineering

Committee Members

Richard E. Weyers, Co – Chair

Christine Anderson – Cook, Co – Chair

Carin L. Roberts – Wollmann

David Mokarem

Michael M. Sprinkel

October 11, 2004
Blacksburg, Virginia

Keywords: bridge deck, NBIS, resistivity, potentials, cover depths

Correlation of Corrosion Measurements and Bridge Conditions with NBIS Deck Rating

Andrei Ramniceanu

Abstract

Since the use of epoxy coated steel has become mandatory starting in the 1980s, recent studies have shown that epoxy coating does not prevent corrosion, but instead will debond from the steel reinforcement in as little as 4 years (Weyers RE et al, 1998) allowing instead a much more insidious form of corrosion to take place known as crevice corrosion. Therefore, it is important to determine if the nondestructive corrosion activity detection methods are applicable to ECR as well as institute guidelines for interpreting the results. Since the corrosion of reinforcing steel is directly responsible for damage to concrete structures, it is surprising that nondestructive corrosion assessment methods are not part of regular bridge inspection programs such as PONTIS and NBIS. Instead, the inspection and bridge rating guidelines of federally mandated programs such as NBIS are so vague as to allow for a relatively subjective application by the field inspectors.

Clear cover depths, resistance, corrosion potentials, linear polarization data, as well as environmental exposure and structural data were collected from a sample of 38 bridge decks in the Commonwealth of Virginia. These structures were further divided in three subsets: bridge decks with a specified w/c ratio of 0.47, bridge decks with a specified w/c ratio of 0.45 and bridge decks with a specified w/cm ratio of 0.45. This data was then correlated to determine which parameters are the most influential in the assignment of NBIS condition rating. Relationships between the non-destructive test parameters were also examined to determine if corrosion potentials and linear polarization are applicable to epoxy coated steel.

Based on comparisons of measurements distributions, there is an indication that corrosion potential tests may be applicable to structures reinforced with epoxy coated steel. Furthermore, these conclusions are supported by statistical correlations between resistivity, half cell potentials and linear polarization measurements. Unfortunately, although apparently applicable, as of now there are no guidelines to interpret the results. Based on the linear corrosion current density data collected, no conclusion can be drawn regarding the applicability of the linear polarization test. As far as the NBIS deck rating is concerned, since the inspection guidelines are so vague, age becomes a very easy and attractive factor to the field personnel to rely on. However, this conclusion is far from definitive since the very large majority of structures used in this particular study had only two rating values out of theoretically ten and realistically five possible rating values.

ACKNOWLEDGMENTS

First, I would like to say how grateful I am to Dr. Richard Weyers for the invaluable opportunity he has given me to continue my education, as well as for his guidance and support during the course of this project.

I am also grateful to Dr. Michael Brown of Virginia Transportation Research Council for his valuable contributions to the content of this report.

I would like to thank Dr Christine Anderson-Cook for her assistance with the statistical analysis portion of this project. Thanks go also to Dr. Carin Roberts-Wollmann, Dr. David Mokarem and Mr. Michael Sprinkel for their evaluation of this report.

I would also like to thank my colleague Wes Keller, as well as Andy Mills and Bill Ordel for all their hard work as well as for making the summer of 2003 positively memorable.

Finally, I would like to thank my wife, Kathryn Clasen, for her love, constant support and sacrifices she made so I could continue my education. Without her unerring belief in me none of this would have been possible.

TABLE OF CONTENTS

LIST OF TABLES

LIST OF FIGURES

INTRODUCTION

According to the Federal Highway Administration (FHWA), there are approximately 600,000 bridges in the United States, and of these more than 50% are made of concrete. Furthermore, according to the latest FHWA inventory dated December 2003, nationwide there are 64,056 structurally deficient or functionally obsolete concrete bridges. Virginia's share is 1099 concrete structures that need to be repaired, replaced or rehabilitated. It is widely known in practice that the primary cause of deterioration of reinforced concrete structures, in this case bridges, is the corrosion of the reinforcing steel induced by chlorides.

In order to assess in-situ the level of corrosion activity in steel reinforced concrete several nondestructive methods have been developed, which when used together may be used to assess the corrosion state of the reinforcing steel in a particular structure. These methods, which are also the subject of this work, are concrete resistivity, half-cell potentials, and unguarded linear polarization measured using a three electrode linear polarization (3LP) instrument. Although these methods have been studied quite extensively, the state agencies and contractors responsible for the maintenance of concrete transportation structures have generally been slow in adopting them as part of their regular inspection programs. A study showed that only 15 states routinely use corrosion potentials in spite of the fact that copper/copper sulfate method for measuring electrical potentials in steel reinforced concrete has been standardized by ASTM (Manning, DG 1985), while no states use resistivity measurements or linear polarization routinely.

One of the most prevalent methods to combat the corrosion problem has been the coating of the reinforcing steel with an organic epoxy resin. However, since this epoxy coating is thought to be dielectric, nondestructive corrosion assessment methods such as potentials and linear polarization have generally been considered inapplicable to epoxy coated reinforcing steel (Brown, MC 2002; Geenen, FM 1991). Epoxy coated steel (ECR) became the prevalent corrosion protection method starting in the early 1980s (Brown, MC 2002). Since then, studies have shown that epoxy coating does not prevent corrosion, but instead will debond from the steel reinforcement in as little as 4 years (Weyers RE et al, 1998) allowing instead a much more insidious form of corrosion to take place under the coating. Therefore, it will be important to determine if the nondestructive corrosion activity detection methods are applicable to ECR as well as institute guidelines for interpreting the results.

Finally, since the corrosion of reinforcing steel is directly responsible for damage to concrete structures, it is surprising that nondestructive corrosion assessment methods are not part of regular bridge inspection programs such as Pontis and National Bridge Inspection Standards (NBIS). Instead, the inspection and bridge rating guidelines of federally mandated programs such as NBIS are so vague as to allow for a relatively subjective application by the field inspectors.

PURPOSE AND SCOPE

Currently, the time to repair, rehabilitate, or replace bridge decks is determined based upon a visual condition rating with values ranging from 9 to 0 (9 being the best and 0 the worst). Since these condition ratings are assigned based upon observations by bridge inspectors and not discrete measurements, they tend to be somewhat subjective and possibly inconsistent.

The scope of this study includes a representative sample of Virginia's bridge decks consisting of 37 structures located in the state's six environmental zones. The sample was divided into two groups: one group consisting of 10 structures reinforced with bare steel and cast using concrete with a specified water/cement ratio (w/c) of 0.47, and one group consisting of 27 structures reinforced with epoxy coated bars. The second group was further subdivided into two subsets: one subset consisting of 16 structures cast using concrete with a specified water/cement ratio (w/c) of 0.45, and another subset consisting of 11 structures cast using concrete with a specified water/cementatious materials ratio (w/cm) of 0.45.

The primary objective of this project is to evaluate the NBIS condition rating based upon environmental and structural parameters, as well as corrosion potential measurements associated with the corrosion of the reinforcing steel.

Secondary objectives include:

- Verification of the theoretical relationships between the different measurements of electrochemical activity associated with corrosion of reinforcing steel in bare bar reinforced concrete decks.
- Determining whether the same theory (and therefore the measurements of electrochemical activity) is applicable to concrete bridge decks which have been reinforced with epoxy coated reinforcing steel.
- Lastly, analyze the variance of corrosion related parameters (i.e. resistivity, corrosion potentials, corrosion current density, and clear concrete cover depths) to determine if there are significant differences between the same parameters in the three different subsets (i.e. 0.47 w/c, 0.45 w/c, 0.45 w/cm), which might be used to assess construction quality, and therefore influence the time to corrosion initiation and subsequent deterioration.

The data was statistically analyzed using Minitab and S-Plus statistical analysis software packages.

LITERATURE REVIEW

A costly maintenance problem bridge engineers have to contend with is the corrosion of the reinforcing steel embedded in the concrete decks, superstructure and substructures. Therefore, to combat this problem, or at the very least minimize it, a fundamental understanding of concrete as well as the mechanism of corrosion of reinforcing steel is necessary.

Concrete

Introduction

Concrete is made of portland cement, aggregate, water, and sometimes mineral and chemical admixtures mixed together to form a liquid which hardens by chemical reactions. The aggregate is a filler material composed of inert ingredients such as sand and stone. Usually concrete is about 70% aggregate.

Whereas the aggregate is the filler, the combination of water and cement provide the binder that keeps the material together. When water is added, the components of portland cement undergo a chemical reaction known as hydration. As hydration occurs, the calcium silicate is transformed into calcium silicate hydrate (CSH) and calcium hydroxide $Ca(OH)_2$ or (CH), and the cement slowly forms a hardened paste. This process is examined in more detail in the following sections.

Portland Cement

Portland cement is a mixture of compounds. It is made by crushing, milling and baking limestone, clay (or shale), sand and iron together. The mixture is heated to approximately 1500°C in kilns that are long rotating steel cylinders on an incline. The kilns may be up to 6 meters in diameter and 180 meters in length. The mixture of raw materials enters at the high end of the cylinder and slowly moves along the length of the kiln due to the constant rotation and inclination. At the low end of the kiln, a fuel is injected and burned, thus providing the heat necessary to make the raw materials react. It can take up to 2 hours for the mixture to pass through the kiln, depending upon the length of the cylinder. The marble-sized pieces produced by the kiln are referred to as clinker. The clinker is cooled, ground, and mixed with a small amount of gypsum (which regulates setting) to produce the general-purpose portland cement. After adding gypsum, the final cement composition is a mixture of tricalcium silicate (Ca_3SiO_5), dicalcium silicate (Ca_2SiO_4), tricalcium aluminate ($Ca_3Al_2O_6$), tetracalciumaluminoferrate ($Ca_4Al_2Fe_2O_{10}$), and gypsum ($CaSO_4 \cdot 2H_2O$) (Young F.J. et al, 1998). The exact proportions of these compounds are manufacturer as well as portland cement type dependent.

Water

Water is the key ingredient, which when mixed with portland cement, forms a paste that binds the aggregate together. The water causes the hardening of concrete through a process called hydration. Hydration is a chemical reaction in which the major compounds in cement form chemical bonds with water molecules and become hydrates or hydration products. The water needs to be free of undesirable ions in order to prevent reactions from occurring which may weaken the concrete or otherwise interfere with the hydration process. The role of water is important because the water to cement ratio is the most critical factor in the production of quality concrete. Too much water reduces concrete strength and increases permeability, while too little will make the concrete unworkable. Because concrete must be strong, impermeable and workable, a careful balance of the water to cement ratio is required when making concrete.

Aggregate

Aggregates are to be chemically inert, solid bodies held together by the cementing compounds. Aggregates come in various shapes, sizes, and materials ranging from fine particles of sand to large, coarse stone. Because portland cement is the most expensive ingredient in making concrete, it is desirable to minimize the amount of portland cement used. Seventy to eighty percent of the volume of concrete is aggregate keeping the cost of the concrete low. The selection of an aggregate is determined, in part, by the desired characteristics of the concrete. For example, the density of concrete is determined by the density of the aggregate. Soft, porous aggregates can result in weak concrete with low wear resistance, while using hard aggregates can make strong concrete with a high resistance to abrasion. Aggregates should be clean, hard, strong and durable. The aggregate is usually washed to remove any dust, silt, clay, organic matter, or other impurities that would interfere with the hydration of the portland cement or bonding reaction with the portland cement paste. It is then separated into various sizes through a sieving process. Furthermore, aggregates have to be carefully selected to avoid adverse reactions with the hydrated portland cement paste such as alkali-silica and alkali-carbonate reactions, which may lead to premature deterioration of the structures (Young F.J. et al, 1998).

Admixtures

Admixtures fall into two categories: mineral and chemical. Mineral admixtures such as flyash, ground granulated blast furnace slag (GGBFS), micro silica, rice husks, and rice hull ash may be used for several reasons: improve workability, lower the heat of hydration, and lower the permeability, thereby increase the durability of Portland cement concrete (Young F.J. et al, 1998). Mineral admixture can be further divided into two categories: pozzolanic or cementing. Pozzolanic mineral additives such as flyash have no stand alone cementing properties like portland cement, but they do react with the calcium hydroxide liberated during the hydration of portland cement to create hydration products similar to portland cement (Lohtia R.P. et al, 1995). In addition to the economic

benefits gained from using less portland cement, studies have shown that some mineral admixtures can increase the workability of fresh mixed portland cement concrete as well as decrease the water demand of the mix (Ferraris C.F. et al, 2001). Another use for minerals admixtures such as flyash and GGBFS is economics since these minerals are industrial waste byproducts. Therefore, substituting fly ash or GGBFS for portland cement decreases the overall cost of the finished product, in this case portland cement concrete, while increasing its overall quality and durability.

Chemical admixtures, unlike mineral admixtures, are not intended to replace portland cement, but rather improve the workability or impart other qualities to the mix or finished product. Chemical admixtures can be accelerators, water reducers/high range water reducers, air entraining admixtures, polymers, dyes, retarders and others (Ramachandran V.S., 2001). Often chemical admixtures are used in conjunction with mineral admixtures. One such example is the use of high range water reducers with micro silica. Unlike fly ash or GGBFS, micro silica particles are several orders of magnitude smaller than portland cement particles. Having such a high surface area, the water required to maintain workability is significantly increased. Therefore, using a water reducer allows the manufacturer to maintain workability as well as the specified maximum w/cm ratio.

Steel Corrosion in Concrete

Exposed steel will corrode in moist atmospheres due to differences in the electrical potential on the steel surface forming anodic and cathodic sites. The metal oxidizes at the anode where corrosion occurs according to (Mehta, P.K.1993):

$$\text{Fe (metal)} \rightarrow Fe^{2+}\text{ (aq.)} + 2e^- \qquad \text{Equation 1}$$

Simultaneously, reduction occurs at cathodic sites, typical cathodic processes being:

$$\tfrac{1}{2}O_2 + H_20 + 2e^-\text{(metal)} \rightarrow 2OH^-\text{(aq.)} \qquad \text{Equation 2}$$

$$2H + \text{(aq.)} + 2e^-\text{ (metal)} \rightarrow H_2\text{ (gas)} \qquad \text{Equation 3}$$

The electrons produced during this process are conducted through the metal while the ions formed are transported through the concrete pore water which acts as the electrolyte.

The environment provided by concrete to steel reinforcement is one of high alkalinity due to the presence of the hydroxides of sodium, potassium and calcium produced during the hydration reactions. Quality concrete acts as a physical barrier to many of the steel's aggressors. In such an environment steel is passive and any small breaks in its protective oxide film are soon repaired. If, however, the alkalinity of its surroundings are reduced, such as by neutralization with atmospheric carbon dioxide, or depassivating anions such as chloride are able to reach the steel then severe corrosion of the reinforcement can occur. This in turn can result in staining of the concrete by rust and spalling of the cover

due to the increase in volume associated with the conversion of iron to iron oxide (Lambert P., 1998).

As previously stated, corrosion is induced by one of two ways: chlorides or carbon dioxide. Chlorides can enter concrete in two ways:

· 1. They may be added during mixing either deliberately as an admixture or as a contaminant in the original constituents

· 2. They may enter the hardened concrete from an external source such sea water or deicing salts.

"Once chlorides have reached the reinforcement in sufficient quantities they will depassivate the embedded steel by breaking down the protective oxide layer normally maintained by the alkaline environment. The concentration of chlorides required to initiate and maintain corrosion is dependant upon the alkalinity and it has been shown that there is an almost linear relationship between hydroxyl ion concentration and the respective threshold level of chloride (Lambert P., 1998)."

Carbon dioxide present in the atmosphere combines with moisture in the concrete to form carbonic acid. This reacts with the calcium hydroxide, other alkaline hydroxides and CSH in the pore water resulting in a reduction in the alkalinity of the concrete. The rate at which this neutralization occurs is influenced by factors such as moisture levels and concrete quality. The depth of carbonation in a structure can be quite easily established by the use of phenolphthalein indicator on freshly exposed material. The distinctive color change, from deep pink in unaffected concrete to clear in the carbonated region, is sufficiently accurate for most practical purposes provided a number of measurements are obtained to allow for local variations.

The microclimate to which the reinforced concrete member is exposed directly affects the likelihood and extent of reinforcement corrosion. Factors such as chloride levels and pH have already been discussed, but another important aspect of the local environment is the moisture level. Carbonation, chloride ingress, resistivity and corrosion rate are all greatly influenced by the degree of saturation.

The permeability of the concrete is important in determining the extent to which aggressive external substances can attack the steel. A thick concrete cover of low permeability will significantly delay the time for chlorides from an external source from reaching the steel and causing depassivation. Where an adequate clear cover depth is difficult to achieve due to design considerations or where aggressive environments are expected such as in marine structures or bridge decks, additional protection may be required for the embedded steel. Protection methods take many and varied forms and commercial interest in this field is strong. The steel reinforcement itself may be made more able to resist corrosion by providing it with a protective coating such as zinc, epoxy resin or stainless steel cladding. Currently, the most commonly used protection methods in the United States are the fusion bonded epoxy coatings (Seymour, R.B. et al 1990).

However, the use of solid stainless steel has been recommended before for use in critical structures located in areas that use a high quantity of deicer salts or coastal zones (Brown, M.C. et al 2002).

There can be little doubt that an effective way of protecting steel which is embedded in concrete is to provide it with an adequate clear cover depth of low permeability concrete free from depassivating ions such as chlorides. However, concrete is placed by the ton in all weathers and environments, exposed to industrial atmospheres, deicing salts and seawater.

Stages of Deterioration

The mechanisms of deterioration are primarily electrochemical in nature and occur in three discrete stages (Lambert P., 1998):

· Stage 1: Initiation – Concentration of aggressive species is insufficient to initiate any electrochemical reactions or the electrochemical reaction is occurring very slowly. No physical damage has occurred. The duration of this stage may vary from a few minutes to the design life of the structure.

· Stage 2: Propagation – Electrochemical reactions begin or are continuing, some physical damage such as cracking and/or spalling of the concrete cover may occur due to stresses induced by corrosion products but is insufficient to cause distress. Acceleration of the deterioration process usually occurs during this stage due to increased accessibility of aggressive ions or modification of the concrete environment.

· Stage 3: Deterioration – Rapid breakdown of the fabric of the structure. The combined effects of the physical and electrochemical processes are of sufficient severity that the structure is no longer serviceable (failure occurs) and major remedial work or, in extreme cases, demolition is required.

Factors Influencing Corrosion Rate of Deterioration

The factors which determine the corrosion rate of steel in concrete are: the presence of an ionically conducting aqueous phase in contact with the steel (i.e. pore water), the existence of anodic and cathodic sites on the metal in contact with this electrolyte, the availability of oxygen, and a conductive path for free movement of electrons.

Inadequate cover is invariably associated with areas of high corrosion risk due to both carbonation and chloride ingress through sound and cracked concrete. By surveying the surface of a structure with an electromagnetic cover meter the low cover high-risk areas can be easily identified. A cover survey of newly completed structures would rapidly identify likely problem areas and permit additional protective measures to be taken.

While this remains an ill-defined area, two forms of cracks are of interest when evaluating the condition of a reinforced concrete structure; those present before the onset

of corrosion which may reduce the time to corrosion initiation and damage (subsidence, shrinkage and structural cracks), and those produced as a direct consequence of corrosion (expansive corrosion products leading to cracking and spalling). The influence of cracking prior to corrosion is currently being studied in an ongoing Virginia Transportation Research Council project.

Others have also studied the influence of the crack width on chloride ingress and subsequent corrosion of the reinforcing steel; however, no consensus has been reached yet. Some studies suggest cracks smaller than 0.30 mm have minimal or no influence on the ingress of chlorides due to the high surface tension of the water (Atimey, E. et al 1974), while others point to crack widths less than 0.10 mm having no effect on chloride ingress. The difference in width being the result of impact loading from traffic which forces the chloride laden water into the cracks (Beeby, A.W 1970 and Takewaka, K. et al 2003).

Corrosion Prevention Methods

Over the years engineers have implemented several methods to deal with the problem of reinforcing steel corroding in concrete. Some of these methods include lowering the specified water/cement ratio; cementing and non-cementing additives, reinforcing steel coatings, and increasing clear cover depths.

Water/Cement Ratio

One way to increase the service life of a bridge deck is to delay the initiation of reinforcing steel corrosion by decreasing the chloride diffusion constant (D_c). Virginia accomplished this by lowering the maximum allowable w/c ratio from 0.47 to 0.45. Decreasing the specified w/c ratio decreases the permeability of the concrete and therefore increases the time for the chlorides to diffuse to the reinforcing steel. Kirkpatrick and others have shown that the decrease in w/c ratio may account for approximately 40% increase in service life (Kirkpatrick, T.J. et al 2002).

Pozzolans

As previously mentioned, pozzolans have no stand alone cementing properties; however, they do hydrate in the presence of water and calcium hydroxide released during the hydration of portland cement. Since the pozzolanic hydration process is not only much slower than the hydration of portland cement, but is also dependant on the calcium hydroxide released by the hydrating portland cement, the pozzolanic hydration products fill the already existent capillary spaces in the cement paste (Zemajtis, J. 1998). This process increases the strength and reduces the permeability of the final product. By reducing the permeability of the portland cement concrete, the ingress of chlorides is significantly reduced and therefore, the corrosion of the reinforcing steel is delayed. It is important to note that the pozzolanic admixtures do not eliminate the capillary porosity, but reduce it by lowering the volume fraction of calcium hydroxide and at the same time

increasing the total amount of calcium silicate hydrates (Bentz, D.P. et al 1991). Two commonly used pozzolanic admixtures are flyash and micro silica.

Slag

Also known as ground granulated blast furnace slag (GGBFS), it is a byproduct of the steel production industry. During steel production, the liquid slag is rapidly quenched in water forming a glassy, granular, non-metallic product consisting of silicates and aluminosilicates of calcium and other bases (Mehta, P.K. 1993). Unlike flyash and micro silica, GGBFS has stand alone cementitious properties. In addition to its benefits with respect to the corrosion of reinforcing steel such as decreased porosity and permeability (Lewis, D.W. 1985), GGBFS has also been used because it improves the workability and reduces the water requirements of the fresh portland cement mix (Fulton, F.S. 1974).

Corrosion Inhibitors

Corrosion inhibitors are chemical admixtures used to retard or delay the corrosion of reinforcing steel in concrete (Zemajtis, J. 1998). Many of these inhibitors are organic compounds; they function by forming an impervious film on the metal surface or by interfering with either the anodic or cathodic reactions or both (Fontana, M.G. 1986).

There are three types of corrosion inhibitors: anodic, cathodic and mixed. Anodic inhibitors react with the corrosion products on the steel and form a protective film on the surface, and cathodic inhibitors react with the hydroxyl ions to precipitate insoluble compounds on the cathodic site and prevent the access of oxygen (Zemajtis, J. 1998).

Anodic corrosion inhibitors may be nitrates, nitrites, chromates, silicates, phosphates, molybdates and borates. Cathodic corrosion inhibitors consist of arsenic, bismuth, antimony, and salts of zinc, magnesium or calcium (Trethewey, K.R. et al 1988).

Epoxy Coating

The significant increase in the use of deicing salts following the implementation of the "bare road policy" by state highway agencies in the 1960s led to a considerable increase in chloride induced corrosion damage of bridge decks (Bennett, J. 1996). To combat this problem, epoxy coatings were introduced in the 1970s and became the prevalent protection methods by the mid 1980s without any significant research into the protection mechanism associated with epoxy coatings (Zemajtis, J. et al 1996).

The most common epoxy coating in the United States is a bisphenol-amine epoxy (Brown, M.C. 2002). This type of epoxy, which is a condensation of bisphenol A and epichlorohydrin, can be cured at ambient temperatures or elevated temperatures with an amino acid (Seymour, R.B. et al 1990). The organic epoxy can be applied in two ways: two-part liquid or powder (Brown, M.C. 2002). The liquid can be applied through brushing, spraying or immersing the bar to be coated, which lends it well to field

applications. The powder is applied using a fusion bonding process at temperatures between 204°C and 230°C (Sagüés, A.A. et al 1990).

Unlike concrete admixtures, epoxy coatings protect the reinforcing steel by forming a physical barrier. This barrier protects by providing electrical resistance to limit current transfer between anodic and cathodic sites, oxygen deprivation and resistance to chloride diffusion (Clear, K.C. 1995 and Brown, M.C. 2002). However, later research has shown that not only is the epoxy coating permeable to oxygen and water to a certain extent, but the total absence of defects, which is essential for the barrier to perform as designed, is unachievable under practical construction conditions (Clear, K.C. et al 1995).

At this time 49 states use epoxy coating reinforcing steel extensively, with the exception of Florida, which discontinued its use after the Long Key Bridge showed signs of corrosion deterioration after only six years (Vermani, P. et al 2001).

Clear Cover Depth

To delay the onset of corrosion, one method is to increase the clear concrete cover depth. American Association of State Highway and Transportation Officials (AASHTO) specifies a minimum cover depth of 50 mm, while the Virginia Department of Transportation (VDOT) requires a minimum clear cover depth between 63 mm to 76 mm, but no less than 63 mm (Weyers, R.E. et al 2003, AASTHO 1994, VDOT 1994). Increasing the cover depth not only increases the chloride diffusion path leading to longer service life, but also leads to longer times to cracking caused by expansive corrosion products (Weyers, R.E. et al 1998).

Corrosion Detection Methods

Since it has been determined that chlorides are at the crux of reinforcing steel corrosion in concrete (Clemeña, G. G. 1992), several invasive and non-destructive methods have been developed to assess the level of corrosion taking place or the potential for corrosion. Because corrosion is an electrochemical process, some of the most commonly used non-destructive field methods for measuring corrosion activity are: resistivity of concrete, half-cell potentials, and linear polarization of steel reinforcement within concrete. The invasive or destructive corrosion assessment methods consist of chloride content analysis from powdered samples, chloride permeability tests and gravimetric loss of steel specimens.

Individually, these methods have been used quite successfully to monitor corrosion activity of reinforcing steel in concrete. Also, the invasive methods mentioned above have been used for many years to model bridge deck service life. "One common service life model for the chloride induced corrosion of reinforcing steel in concrete involves two time periods. The first is the time for chloride ingress to…" reach a concentration necessary "…to initiate corrosion. The second is the time for corrosion activity to the end of functional service life (Weyers, R.E. et al. 1993)." The end of functional service life is defined as: "when 12 percent of worst span lane of a bridge deck has deteriorated

(Fitch, M.G. et al. 1995)." This service life model is based on Fick's second law of diffusion, which uses an apparent diffusion process. A model solution which is used to determine the time for chlorides to "reach and initiate corrosion at first repair and rehabilitation", is described mathematically as follows (Crank, J. 1975):

$$C_{(x,t)} = C_o\left(1 - erf\frac{x}{2\sqrt{D_c t}}\right) \qquad \text{Equation 4}$$

$C_{(x,t)}$ = chloride concentration at depth and time (kg/m^3)
C_o = surface chloride concentration (kg/m^3)
D_c = apparent diffusion coefficient (mm^2/year)
t = time of diffusion (years)
x = concrete cover depth (mm)
erf = statistical error function

When $C_{(x,t)}$ is set equal to the chloride corrosion initiation concentration, and the equation is solved for time, t, the time for diffusion of chlorides to the chloride corrosion initiation concentration can be determined (Kirkpatrick, J. 2001). Weyers and Kirkpatrick, incorporating the statistical nature of the factors affecting the corrosion initiation process, further refined the modeling procedure (Kirkpatrick, J. 2001).

Concrete Resistivity

A non-destructive testing procedure that is becoming increasingly popular due to its low cost and ease of implementation, is measuring the concrete resistivity by the Wenner method, as shown in Figure 1.

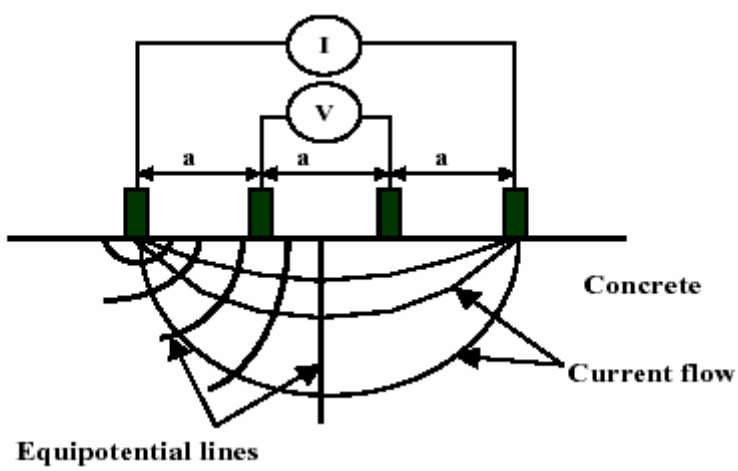

Figure 1 4 – point Wenner Resistivity Apparatus

Originally developed to measure the resistivity of soils by Wenner in 1916, this method uses four equally spaced probes. Although resistivity cannot be used to determine the rate of corrosion, it can be used to assess other concrete properties such as permeability to chlorides and its ability to sustain corrosion. The previous statement can be better understood by examining the corrosion mechanism. For corrosion to take place, four essential elements are necessary:

1. An anode – the actual corrosion site which is the electron donor.

$$Fe \rightarrow 2e^- + Fe^{2+} \qquad \text{Equation 5}$$

$$Fe^{2+} + 2OH^- \rightarrow Fe(OH)_2 \qquad \text{Equation 6}$$

$$4Fe(OH)_2 + O_2 \rightarrow 2Fe_2O_3 \cdot H_2O + 2H_2O \qquad \text{Equation 7}$$

Or

$$6Fe(OH)_2 + O_2 \rightarrow 2Fe_3O_4 \cdot H_2O + 4H_2O \qquad \text{Equation 8}$$

$$Fe_3O_4 \cdot H_2O \rightarrow Fe_3O_4 + H_2O \qquad \text{Equation 9}$$

2. A cathode – the non-corroding site which is the electron acceptor.

$$\tfrac{1}{2}O_2 + H_2O + 2e^- \rightarrow 2(OH)^- \qquad \text{Equation 10}$$

3. Electronic conduction – electron movement through a conductor, in this case the steel reinforcing bars.
4. Ionic conduction – the movement of ions through a solution, the concrete pore water.

The process is illustrated in Figure 2 (Brown, M.C. 2002).

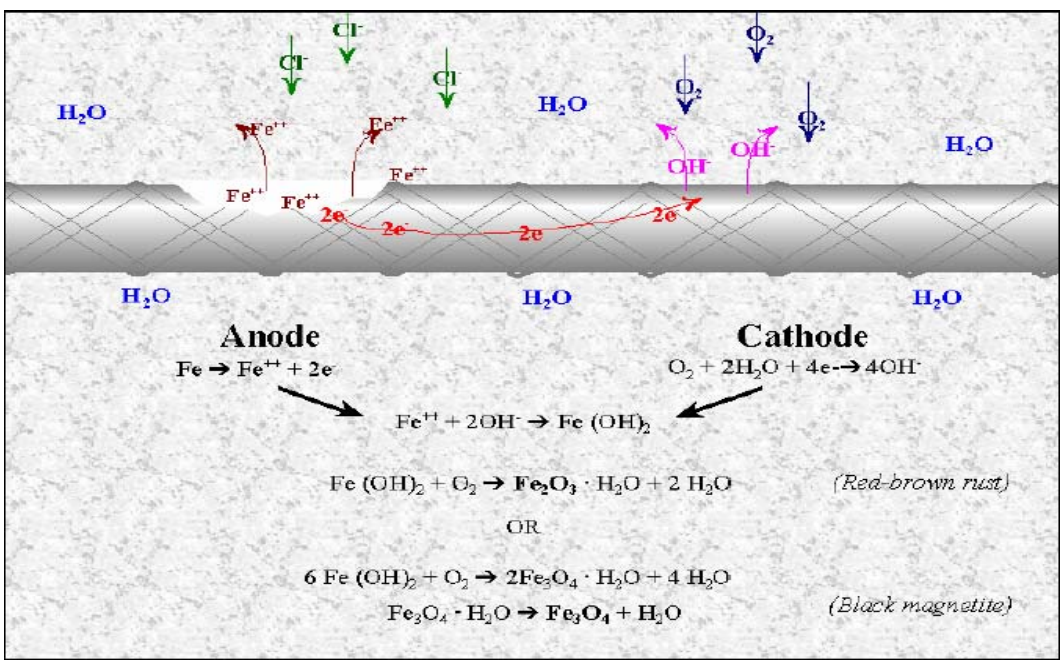

Figure 2 Corrosion Process Diagram

Therefore, the corrosion rate depends on the availability of oxygen for the cathodic reaction and on the electrical resistance of concrete, which controls the movement of ions through the concrete between the anodic and cathodic sites (Malhotra, V.M. and Carino, N.J. 2004).

To minimize the polarization effects to the reinforcing steel, "a small alternating current is applied between the outer electrodes while the potential is measured between the inner electrodes (Nagi, M.A. and Whiting, D.A. 2003)." Thus, we are able to measure the electrical resistance of concrete, which affects the ionic current flow between the anode and the cathode, and the rate at which corrosion can occur (Gowers, K.R. et al 1999). Resistivity is then calculated as follows:

$$\rho = 2\pi aR \qquad \text{Equation 11}$$

ρ = Resistivity in units of ohm-cm or ohm-in
a = spacing between the four probes in cm or in
R = actual measured resistance in ohms

A high concrete resistivity decreases the current flow and impedes the corrosion process. Since concrete resistivity is affected by chlorides (mostly from deicing salts) and other ions, concrete resistivity by the Wenner method has been used to assess other concrete properties such as permeability. A study completed in 2001, by Weyers and Bryant, correlated the permeation properties of low permeability concrete, which is commonly used in the construction of bridge decks in the Commonwealth of Virginia, with the resistivity values obtained using the 4-point Wenner method. The study showed that "electrical resistivity measurements may be able to give an indication of the present penetrability properties of as-built structures (Bryant, J.W. 2001);" however, more research is necessary to better define the procedure. Currently, there are no generally agreed upon interpretation guidelines. Bungey recommends the following guidelines (Bungey, J.H. 1989):

> 20	kΩ-cm	Low corrosion rate
10-20	kΩ-cm	Low to moderate corrosion rates
5 -10	kΩ-cm	High corrosion rate
< 5	kΩ-cm	Very high corrosion rate

Whereas others recommend (Feliu, S. et al, 1996):

>100 to 200	kΩ-cm	Negligible corrosion, or concrete too dry
50 to 100	kΩ-cm	Low corrosion rate
10 to 50	kΩ-cm	Moderate to high corrosion rate
<10	kΩ-cm	Resistivity does not control corrosion rate

And (Manning, D.G. 1985):

>12	kΩ-cm	Corrosion unlikely
5 to 12	kΩ-cm	Corrosion probable
<5	kΩ-cm	Corrosion certain

Potentials

Unlike resistivity, half-cell potentials can in fact indicate the potential of corrosion taking place on the reinforcing steel embedded in concrete. The basic process for the corrosion of steel in concrete is the development of micro and macro cells. That is the coexistence of passive and corroding areas on the same bar or separate bars, respectively. A short-circuited galvanic element with the corroding area as anode and the passive area as cathode is formed (Elsener, B. et al, 1994). The electric field created is then measured using a copper-copper sulfate (CSE) half-cell as an external reference electrode. The half-cell is a copper rod submerged in a saturated copper sulfate solution (Malhotra, V.M. et al, 2004). The measurements are then obtained using a high impedance voltmeter. The illustration below shows the typical apparatus as described in ASTM 876-91.

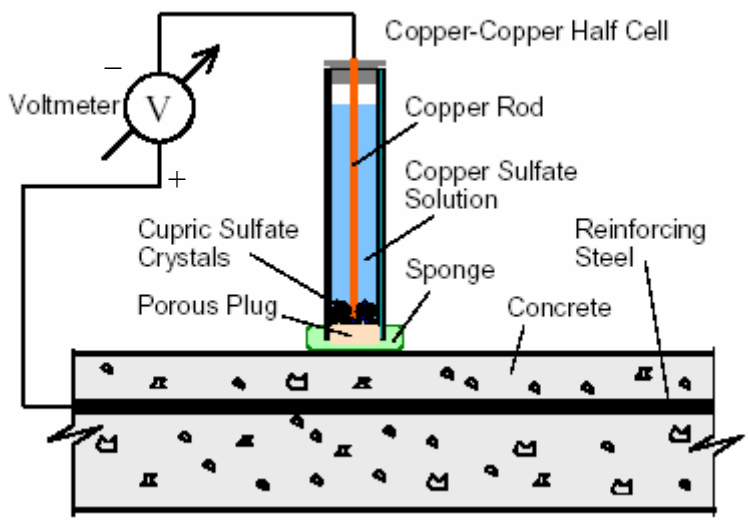

Figure 3 Half-Cell Potential Apparatus

The test results are interpreted using the ASTM C 876-91 standard illustrated in the following table:

Table 1 Potentials Interpretation Guidelines

Voltmeter Reading	Interpretation
Greater than -200mV	90% probability of no active corrosion
Between -200mV and -350mV	Uncertain
Less than -350mV	90% probability of active corrosion

One of the limitations of this method is the fact that it is considered inapplicable to epoxy coated reinforcing steel since the epoxy coating is generally considered to be dielectric. Also due to insufficient research in the field, there are no guidelines available to interpret the results obtained on structures reinforced with epoxy coated steel.

Linear Polarization

A more sophisticated inspection method is the three electrode linear polarization (3LP). The 3LP device appears to be a convenient tool for measuring corrosion current densities. It yields reinforcing steel corrosion current densities that correlate reasonably well with metal losses observed in reinforcing steel specimens extracted from the decks (Clemeña, G.G. 1992).

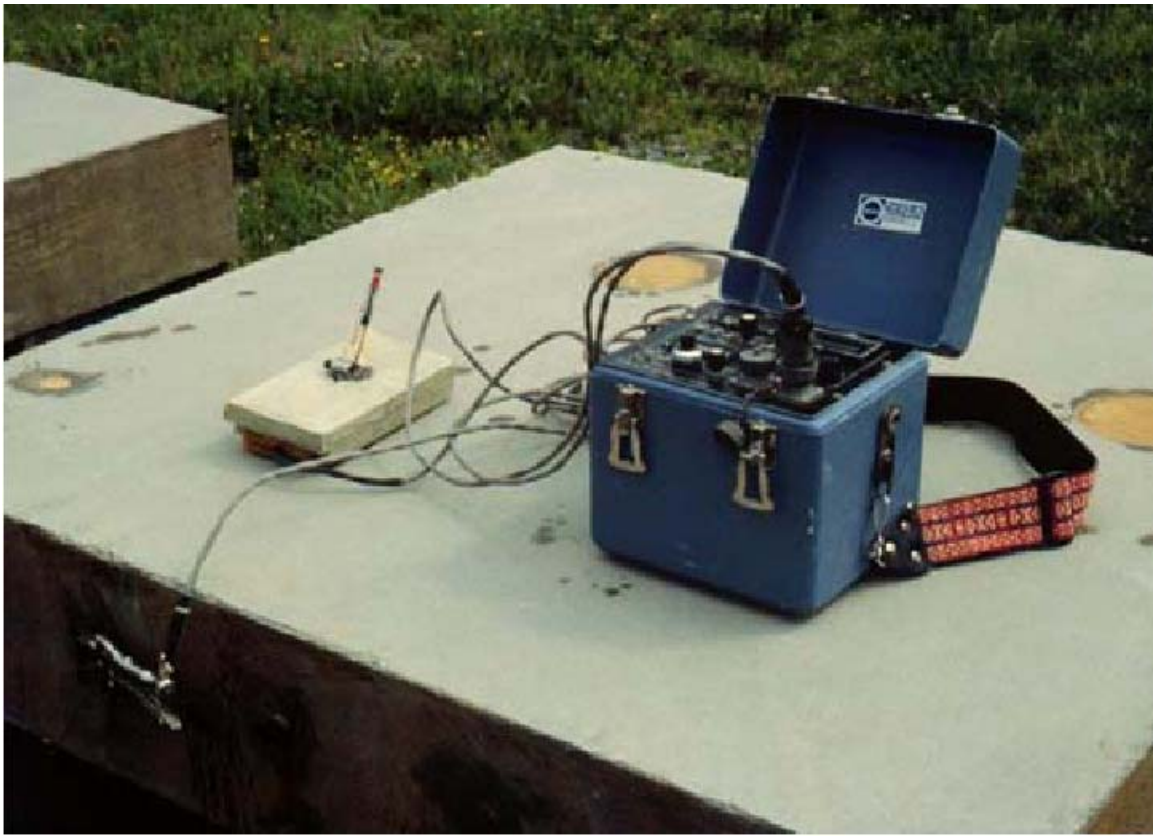

Figure 4 3LP Test Apparatus

"The technique is based upon the fact that a DC current applied to alter the natural electrical half-cell potential of the steel a few millivolts, is proportional to the natural corrosion of the steel. If a high current is required, the corrosion [current density] is high; and vice versa." The development of this device was based on the Stern-Geary equation (Clear, K.C. 1989):

$$I_{corr} = \frac{\Delta I_{appl}(\beta_a \beta_c)}{2.3\Delta\phi(\beta_a + \beta_c)} \qquad \text{Equation 12}$$

I_{corr} = corrosion current in mA
I_{appl} = DC current required to cathodically polarize the bar from its natural electrical half-cell potential

$\Delta\varphi$ = Absolute value of cathodic polarization potential minus the natural electrical half-cell potential
βa = Anodic Tafel constant = 150 mV/decade
βc = Cathodic Tafel constant = 250 mV/decade

The 3LP instrument has been made available commercially; however, it has failed to gain as much popularity as the resistivity or the half-cell potential devices. This may stem from the fact that 3LP readings are more difficult to interpret. Another problem with this method of determining corrosion rates is the fact that it is inapplicable to epoxy coated reinforcing (ECR) steel just as with half-cell potentials. This inability to apply the linear polarization test to epoxy coated steel comes from the fact that the test interpretation is based on an assumed steel surface area. Since the epoxy coating is considered dielectric, as mentioned earlier, any measurements obtained would be from isolated bare areas, the size of which would be unknown (Brown, M.C. 2002). The generally accepted guidelines for interpreting the data obtained using the 3LP test apparatus for bare bar only is shown in Table 2 below (Clear, K.C. 1989):

Table 2 3LP Corrosion Rates

Corrosion State	**Corrosion Current Density ($\mu A/cm^2$)/ (mA/ft^2)**
No Corrosion Damage Expected	< 0.20
Corrosion Damage Possible in the Range of 10 to 15 Years	0.2 – 1.0
Corrosion Damage Expected in 2 to 10 Years	1.0 – 10
Corrosion Damage Expected in 2 or Less	> 10

It must be noted also that these interpretation guidelines are not exact even when applied to structures reinforced with bare bars. Research by Liu and others has shown that the unguarded linear polarization instruments such as the 3LP overestimate the corrosion rate (Liu, Y. 1996). Other studies support these findings showing that the weight loss calculated using this method may be as high as 110% (Law, D.W. et al 2003)
.

Bridge Deck Rating Systems

Currently there are two systems used to rate bridges: National Bridge Inspection Standards (NBIS) and Pontis. Pontis criteria are as follows (Babei, 2002):

Table 3 Pontis Rating System

Deterioration (% of area)	**Pontis Condition State**
0	I
> 0, but ≤ 2	II
> 2, but ≤ 10	III
> 10, but ≤ 25	IV
> 25	V

Whereas the NBIS criteria are as follows (FHWA, 1995):

Table 4 NBIS Rating System

Code	Description
N	Not Applicable
9	Excellent Condition
8	Very Good Condition – no problems noted
7	Good Condition – some minor problems
6	Satisfactory Condition – structural elements show some minor deterioration
5	Fair Condition – all primary elements are sound, but may have minor section loss, cracking or spalling
4	Poor Condition – advanced section loss, deterioration or spalling
3	Serious Condition – loss of section, deterioration or spalling have seriously affected primary structural components. Local failures are possible. Shear cracks in concrete may present
2	Critical Condition – advanced deterioration in primary structural elements. Shear cracks in concrete may be present. Unless closely monitored it may be necessary to close the bridge until corrective action is taken
1	"Imminent" Failure Condition – major deterioration or section loss present in critical structural components or obvious vertical or horizontal movement affecting structure stability. Bridge is closed to traffic, but with corrective action may be put back in light service
0	Failed Condition – out of service – beyond corrective action

There is a fundamental difference between the two systems. NBIS addresses each individual structure, whereas Pontis is a network – wide tool. Under NBIS each individual structure is assigned a value, which is then used by the responsible state agency to prioritize its maintenance activities. By and large, NBIS has proven to be very successful. In this case success can be judged by the fact that "the United States experiences virtually no catastrophic bridge failures due to undetected structural flaws or defects. On the contrary, we continue to receive reports from the Divisions about potential failures that were averted as the result of bridge inspections. By far, most bridge failures occur as a result of natural disasters, such as earthquakes or unusually extreme flooding"; according to James D. Cooper, the FHWA Director of Bridge Technology. One of the problems with the NBIS system, which is immediately noticeable, is a lack of clear, quantitative guidelines for the inspection personnel.

Pontis, as mentioned above, is a network – wide management tool. Unlike NBIS, Pontis rates each component of the bridge, which then incorporates in the network model. "Pontis takes the data stored in its structural and cost databases and models the bridge network. With budget and other constraints, Pontis can form maintenance, repair, rehabilitation, and replacement (MRR&R) recommendations that maximize the effectiveness of such activities. Since it is a network-level model, Pontis is a network-level management tool. It optimizes the level of service of the bridge network, not of each bridge. Pontis uses mathematical models to simulate the bridge network and predict its needs for the future. Pontis uses three sets of models to generate a strategy:

1. *Preservation models.* This set of models develops a picture of the deterioration of the network, the cost for corrective action, and a policy to preserve the agency's investment.

2. *Improvement models.* This set of models finds and predicts functional deficiencies using traffic growth, user costs, and other costs and benefits. The models also generate strategies to meet functional needs of the future.

3. *Project programming model.* This model integrates the results into a set of policies. It uses both preservation and improvement actions in its recommendation (Turner, 1998)."

Although state transportation agencies are introducing Pontis as part of their maintenance programs, NBIS is the federally required bridge inspection and rating program. One of the problems with this rating program is the fact that its rating guidelines are very broad, with no quantitative deterioration ranges, see Table 4 for reference. The Bridge Inspector's Training Manual 90 does not prove to be any less subjective. The Inspection Locations and Procedures section referring to concrete decks reads as follows: "Both the top and the bottom surfaces of concrete decks should be inspected for cracking, scaling, spalling, corroding reinforcement, chloride contamination, delaminations, and full and partial depth failures." This statement is then followed with "the inspection of concrete decks for cracks, spalls, and other defects is primarily a visual activity (Hartle, R.A. et al 1995)." Again, nowhere in the section were there any guidelines as to what kind and how much damage was necessary to change the rating value of a particular deck, leaving the exact inspection procedure at the discretion of each individual state.

In one study designed to examine the condition and performance of epoxy-coated reinforcing steel in bridge decks conducted jointly between PennDOT and NYSDOT, the authors used a modified NBIS rating system in which specific quantitative guidelines were proposed as can be seen in Table 5 (Sohanghpurwala, A.A. et al 2000). It does not appear that these guidelines were ever implemented beyond the scope of the study.

Table 5 Modified NBIS Rating System

Code	Description
N	Not Applicable. Concrete surface is not visible (may be covered by an overlay or sealer)
9	Excellent Condition. No problems noted. Generally used for a new structure.
8	Very Good Condition. No problems noted. Generally used for an old structure.
7	Good Condition – some minor problems
6	Satisfactory Condition – Less than 2% spalls created by corrosion or sum of all deteriorated deck concrete is less than 20%.
5	Fair Condition – Less than 5% spalls created by corrosion or sum of all deteriorated deck concrete is between 20% and 40%.
4	Poor Condition – More than 5% spalls created by corrosion or sum of all deteriorated deck concrete is between 40% and 60%.
3	Serious Condition – More than 5% spalls created by corrosion or sum of all deteriorated deck concrete is greater than 60%.

The authors did not provide any guidelines beyond the modified NBIS condition rating 3 since structures usually get rehabilitated when they reach that stage. In Virginia, the practice of repairing or rehabilitating bridges when they reach an NBIS rating no lower than 3 was confirmed by Hal Coleman, VDOT district bridge engineer, during a personal interview. Furthermore, during the same interview he also indicated that the main

inspection method currently employed in Virginia is the visual inspection, which is augmented with chain drags and hammers to detect delaminations. Non-destructive test methods are not part of the regular inspection program. However, corrosion potentials may be used on select structures that have reached an NBIS condition rating of 3 or 4 and are slated for rehabilitation or repair (Coleman, H. 2004).

METHODS AND MATERIALS

Originally, a total of 40 bridges in Virginia were selected for this study. The selection criteria was based on a generally equal distribution in the three construction eras between 1969 and 1991 as well as the six climate regions in Virginia. More specifically, the bridges were built between 1968 and 1991 with a specified maximum w/c ratio or w/cm ratio of 0.47 or 0.45. The indicated maximum water/cement ratios are the applicable specifications at the time of construction, however they may not be the ones used in the construction of the selected bridge decks. Also, the information regarding the inclusion of flyash or GGBFS was indicated by the appropriate Engineering District personnel. The bridge decks with a w/c ratio of 0.45 were divided into two subsets: one with flyash or slag as supplemental cementing materials and one with only portland cement concrete. Furthermore, the bridge decks selected for the project were distributed throughout six Virginia climate regions, which are outlined in blue in Figure 5.

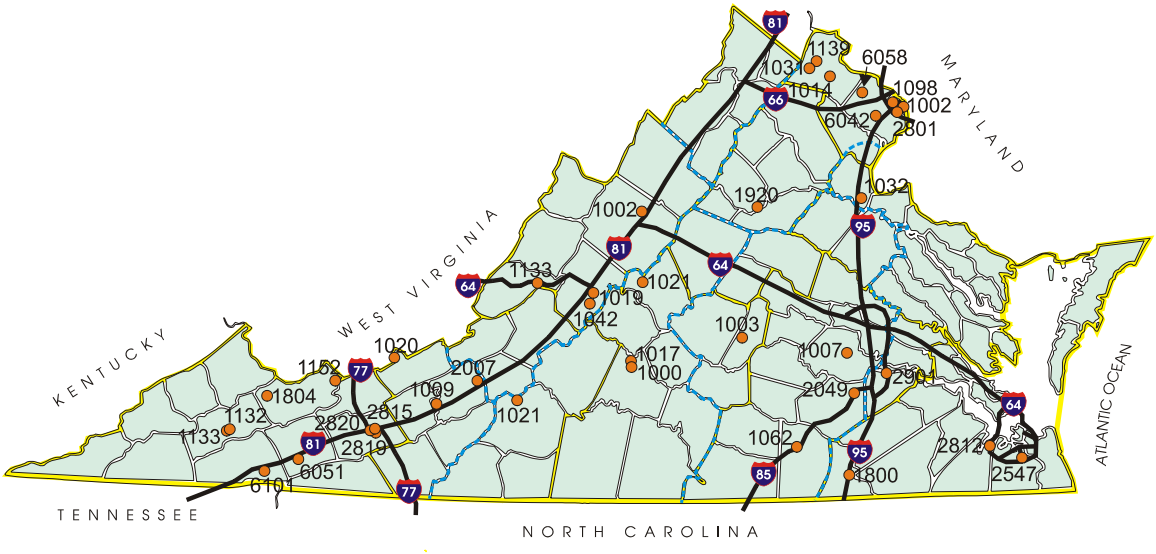

Figure 5 Bridge Locations

The original distribution of the bridges to be sampled included 10 structures with a w/c ratio of 0.47 and 15 structures with 0.45 w/c and w/cm ratios, respectively. Two structures were eliminated due to reasons outside the scope of this study, while one structure was excluded because inclement weather prevented the collection of any electrical measurements. Furthermore, this last structure was a strong slab, meaning that the bridge deck was not supported by a steel or concrete beam superstructure. The lack of an independent superstructure also prevented the collection of core samples that contained reinforcing steel. Later tests performed on core samples from the remaining 37 structures indicated that some of the original information regarding the concrete mixtures used in construction was incorrect. Based on this new information, the 37 bridges remaining were distributed as indicated in Table 6.

Table 6 Bridges selected for study

District	County	Structure Number	Year Built	Age at Survey (Years)	Reinforcement Type	Specified Concrete
4	Dinwiddie	2049	1968	35	Bare Bar	0.47 w/c
4	Brunswick	1062	1969	34	Bare Bar	0.47 w/c
1	Richlands	1804	1969	34	Bare Bar	0.47 w/c
9	Fairfax	6042	1969	34	Bare Bar	0.47 w/c
1	Washington	6101	1969	34	Bare Bar	0.47 w/c
5	Emporia	1800	1970	33	Bare Bar	0.47 w/c
2	Montgomery	2007	1970	33	Bare Bar	0.47 w/c
9	Alexandria	2801	1970	33	Bare Bar	0.47 w/c
3	Nelson	1021	1971	32	Bare Bar	0.47 w/c
6	Stafford	1032	1971	32	Bare Bar	0.47 w/c
8	Rockbridge	1019	1984	19	ECR	0.45 w/c
5	Chesapeake	2547	1984	19	ECR	0.45 w/c
2	Giles	1020	1986	17	ECR	0.45 w/c
1	Wytheville	2820	1986	17	ECR	0.45 w/c
8	Alleghany	1133	1987	16	ECR	0.45 w/c
9	Loudoun	1139	1987	16	ECR	0.45 w/c
9	Loudoun	1014	1987	16	ECR	0.45 w/c
3	Cumberland	1003	1988	15	ECR	0.45 w/c
1	Russell	1132	1988	15	ECR	0.45 w/c
9	Arlington	1098	1988	15	ECR	0.45 w/c
1	Russell	1133	1988	15	ECR	0.45 w/c
9	Loudoun	1031	1990	13	ECR	0.45 w/c
4	Chesterfield	1007	1990	13	ECR	0.45 w/c
1	Smyth	6051	1990	13	ECR	0.45 w/c
7	Orange	1920	1991	12	ECR	0.45 w/c
4	Prince George	2901	1991	12	ECR	0.45 w/c
1	Wytheville	2815	1986	17	ECR	0.45 w/cm
1	Wytheville	2819	1986	17	ECR	0.45 w/cm
9	Arlington	1002	1987	16	ECR	0.45 w/cm
1	Tazewell	1152	1987	16	ECR	0.45 w/cm
8	Augusta	1002	1988	15	ECR	0.45 w/cm
2	Franklin	1021	1988	15	ECR	0.45 w/cm
3	Campbell	1017	1990	13	ECR	0.45 w/cm
8	Rockbridge	1042	1990	13	ECR	0.45 w/cm
5	Suffolk	2812	1991	12	ECR	0.45 w/cm
3	Campbell	1000	1991	12	ECR	0.45 w/cm
9	Fairfax	6058	1991	12	ECR	0.45 w/cm

w/c – water/cement ratio
w/cm – water/cementitious materials ratio
ECR – Epoxy coated reinforcing.

Bridge Deck Samples

The 37 study bridge decks were located on primary and secondary routes. The sample included bridge decks from the following populations of structures:

1. 10 structures built between 1968 and 1972 with a specified maximum w/c ratio of 0.47 and a clear cover depth of 43mm (1.69 in).
2. 16 structures built between 1985 and 1991 with a specified maximum w/c ratio of 0.45 with Portland cement only, and a clear cover depth of 63mm (2.5 in) minus zero, plus 13mm (0.5 in).
3. 11 structures built between 1988 and 1990 with a specified maximum w/cm ratio of 0.45 with flyash or slag as supplemental cementatious materials, and a clear cover depth of 63mm (2.5 in) minus zero, plus 13mm (0.5 in).

None of the bridges chosen for this study had been overlaid; however, during the deck inspection portion part of the study it was determined that two decks had been treated with a polymer sealer.

Deck Survey

The field survey was limited to one traffic lane, to be selected on the basis of traffic and drainage conditions for each individual deck. Under field conditions, however, the right traffic lane was selected for safety and practicality, as this is normally the lane with the most traffic and subsequently deteriorates first. The field survey of each deck included a visual inspection, non-destructive testing of cover depths, half-cell potentials, corrosion current densities, resistance measurements (later used to calculate the resistivity of the concrete) as well as general structural information which included the deck as well as the superstructure. Core samples of the decks, measuring 102 mm (4 in) in diameter were also collected.

Visual Inspection

As part of the visual inspection procedure:

1. The length and the width of the right traffic lane were measured.
2. The deck was “sounded” with a chain drag to determine delaminated area(s).
3. A visual determination of the wheel path locations was made.
4. A crack survey was performed. It consisted of recording the number, length, width and orientation of the cracks in each span.
5. Other structural data included the type of superstructure (i.e. steel, prestressed and cast-in-place concrete), structure type (continuous or simply supported), and the girder spacing. The presence of stay-

in-place forms was recorded. The superelevation condition and the skew angle of the deck were also recorded.

6. Year built and traffic data were provided by the Virginia Department of Transportation.

7. The chloride exposure given in kg-Cl^-/lane-km calculated by Weyers, RE as the average of three winter seasons: 2001, 2002 and 2003, is given in Table 7 below along with the corresponding Virginia environmental zone in Figure 6.

Table 7 Chloride Exposure by Environmental Zone

Zone #	Climatic Zone	kg-Cl^-/lane-km
1	Southwestern Mountain (SM)	688
2	Central Mountain (CM)	671
3	Western Piedmont (WP)	220
4	Northern (N)	4369
5	Eastern Piedmont (EP)	530
6	Tidewater (TW)	225

Figure 6 Virginia Environmental Zones

Cover Depths

Clear cover depth measurements of the top reinforcing steel mat were performed at four-foot intervals in both wheel paths, for a total of 40 measurements per span (Brown, 2002). If the span length did not allow for the collection of 40 measurements, the measurements were taken at two-foot intervals. The data were collected using two Profometer 3 instruments.

Half-cell Potentials

Half-cell potential measurements were collected at the same locations as the cover depth measurements. A copper-copper sulfate half-cell was used, and the test was performed in accordance with ASTM 876-91 (ASTM, 1991).

Linear Polarization

Based on the half-cell potential values and the bridge deck length, four to six corrosion current density measurements were performed. The test was carried out using an

unguarded three electrode linear polarization (3LP) instrument, and the data was usually collected from the right wheel path for safety reasons. Generally, the tests were performed at two locations determined previously, using the copper-copper sulfate half-cell, to have the most negative potential values, two locations with the least negative potential values and if deck length permitted, at two locations with potential values midway between the most and least negative values.

Concrete Resistivity

Generally, the test was performed at nine locations using a four-probe Wenner apparatus. Four to six of the nine locations selected were at the same locations as the corrosion current density measurements, while three locations selected were the same locations from which cores were obtained for petrographic analysis and contained no reinforcing steel. Five measurements were obtained at each test location using due diligence not to conduct the measurements directly over the reinforcing steel bar. For the purpose of calculating the resistivity of the concrete, the spacing between the four probes was maintained at 50.8 mm (2 in). As the depth of the probing alternating current is considered to be equal to the probes' spacing, the measurements should represent an average of the top 50.8 mm (2 in.) of the concrete at the test location. In an effort to reduce the variability of the observations, both the resistivity and corrosion rate measurements were limited to one operator.

Core Samples

Typically, 15 core samples were collected from each bridge deck. Six cores were drilled at the same locations where the corrosion current density measurements were performed, and contained a reinforcing steel bar. Three core samples were obtained for petrographic analysis, and did not contain reinforcing steel. Three core samples obtained included the reinforcing steel, but were located over a crack. Also, three un-cracked "companion" cores were drilled adjacent to the cracked cores. The "companion" cores contained the next parallel reinforcing steel bar that was not cracked. Each specimen measured 102 mm (4 in) in diameter by approximately 152.4 mm (6 in) in length. Also, the cores obtained from the locations where the reinforcing steel was accessed for the corrosion potentials and corrosion current density measurements were used to determine if the in situ concrete contained slag or flyash. Upon coring, each specimen was allowed to air dry only long enough for surface moisture to evaporate. The samples were then wrapped in multiple layers, consisting of a layer of 102-µm (4 mils) polyethylene sheet, followed by a layer of aluminum foil, and another layer of polyethylene sheet. Finally, the specimen and protective layers were wrapped tightly with duct tape. The purpose of the immediate wrapping of the cores was to maintain as closely as practical the in-place moisture condition of the concrete during transport and storage (Brown, 2002). Since corrosion current density measurements as well as resistivity and corrosion potentials measurements were performed at all the core sample locations with the exception of the cracked cores, inclement weather conditions that prevented the collection of electrochemical measurements also prevented the collection of the associated core samples.

Laboratory Testing

The Virginia Transportation Research Council (VTRC) at their facility located in Charlottesville, Virginia are to conduct the following laboratory tests:

1. Chloride content analysis.
2. Resistivity measurements using a two probe method across the diameter of the specimen at various depths.
3. Carbonation depth.
4. Corroded area measurements for both the bare bars and the ECR bars.
5. ECR bars only:
   - Epoxy coating adhesion.
   - Bar color and epoxy coating color
   - Epoxy coating thickness
   - Epoxy coating holidays
6. Concrete moisture content.
7. Concrete permeability

Data Analysis

Pending the completion of the laboratory testing as discussed above within an adequate time period, the following relationships will be assessed: Resistivity and concrete permeability as related to the apparent diffusion constant (D_c); 3LPs and bar corrosion state; and 3LPs and chloride concentration at bar depth. However, if the laboratory testing is not completed as scheduled, which was the case because of equipment and personnel problems, then the significance of the following relationships based on non-destructive test data alone will be assessed:

Primary objective – The non-destructive test data, as well as the environmental and structural data, will be correlated with the NBIS deck rating.

Secondary objectives – Test if the non-destructive corrosion assessment methods are applicable to concrete bridge decks which have been reinforced with epoxy coated reinforcing steel. This will be accomplished by comparing the data collected on ECR reinforced structures with data collected on bare bar reinforced structures. Lastly, analyze the variance of corrosion related parameters (i.e. resistivity, corrosion potentials, corrosion current density, and clear concrete cover depths) to determine if there are significant differences between the same parameters in the three different subsets (i.e. 0.47 w/c, 0.45 w/c, 0.45 w/cm), which might be used to assess construction quality, and therefore influence the time to corrosion initiation and subsequent deterioration.

The data obtained from the laboratory testing portion of the study will then be used in future projects to assess the accuracy and better define the previously mentioned non-destructive methods. For the statistical analysis, the program Minitab Release 14 will be used primarily. The program will be used to determine the correlation values that may exist between the different parameters, as well as the corresponding P-value. The Pearson correlation coefficient measures the degree of linear relationship between two variables. The correlation coefficient assumes a value between –1 and +1. If one variable tends to increase as the other decreases, the correlation coefficient is negative. Conversely, if the two variables tend to increase together the correlation coefficient is positive. "The P-value is a formal measure of the correlation and relates to the viability of the null hypothesis, or the contention that there is no relationship between the response and the explanatory variable. Thus it tests the reliability and strength of the predictor-response relationship. P-values are measures of how likely the observed data are under the null hypothesis. The smaller the p-value, the greater confidence there exists in the predictor-response relationship. For the purpose of this study, parameters were determined to be statistically significant if their p-values were below or equal to a predetermined threshold value of 0.10 (Keller W.J., 2004)."

In addition to Minitab, S-Plus 2000 will also be used. S-Plus is necessary because it has the ability to perform non-parametric classification analyses on categorical values such as the NBIS deck rating value. The classification method employed in this study will be the classification tree. "The classification tree is a statistical tool for partitioning the range of explanatory variables into a unique classification of the response (Anderson-Cook C.M. 2002)." "The model is fitted using binary recursive partitioning whereby the data are successively split along coordinate axes of the predictor variables so that at any node, the split which maximally distinguishes the response variable in the left and the right branches is selected. Splitting continues until nodes are pure or data are too sparse; terminal nodes are called leaves, while the initial node is called the root (Breiman L. et al. 1984)." In other words, tree models are fit by successively splitting the data to form homogeneous subsets.

RESULTS

For the purpose of statistical analysis, some of the discrete pieces of information were changed to "indicator variables" as follows:

Table 8 Structural Parameter Value Assignments

	Structural Parameter	Assigned Value
Beam Material	Steel	1
	Concrete	2
Design Type	Simply supported	1
	Continuous	2
Concrete Mixture	0.47 w/c	1
	0.45 w/c	2
	0.45 w/cm	3

Subset 1: Bridge Decks Constructed Between 1968 and 1971 with Bare Bar and Specified Maximum W/C Ratio of 0.47

Cover Depths

To correlate the non-destructive test data with the NBIS deck rating as well as the other parameters available for each individual structure, it was necessary to condense the large number of measurements available for each structure into one value, such as the mean.

The clear cover depth number of observations, the mean, the standard deviation, and the percent of observations less than 51 mm based on a normal distribution for each individual structure in subset 1 is summarized in Table 9. The structures in subset 1 had a mean clear cover depth ranging from 39 to 62 mm. For the 10 structures, 100% of the measurements performed on one bridge deck, 2007_2, were less than 51 mm, while the majority (80% and 65%, respectively) of the measurements performed on bridge decks 2801_9 and 1800_5 were less than 51 mm. The percent of measurements less than 51 mm performed on the remaining decks ranged between 3% and 41%.

Table 9 Cover Depths for Structures with a Specified Maximum W/C Ratio of 0.47

Bridge Number_District	Number of Observations	Cover Depth Mean/Bridge (mm.)	Standard Deviation (mm.)	Cover Depths % < 51 mm.
2049_4	60	53	6.9	38
1062_4	80	58	9.9	28
1804_1	102	57	6.8	18
6042_9	42	61	6.2	7
6101_1	62	53	6.9	41
1800_5	40	45	10	65
2007_2	80	39	2.7	100
2801_9	80	41	8.5	80
1021_3	72	62	6.3	33
1032_6	80	62	7.8	3

As shown in Figures 7 through 9, the clear cover depth measurements for each individual structure in subset 1 were approximately normally distributed with the exception of structures 1021_3, 1800_5 and 6042_9 that failed to fit a normal distribution as well as the rest of the structures, see Figures 7 and 9. The approximate normal distribution of the clear cover depth measurements is supported by previous studies (Weed R.M., 1974 and Pyc W.A., 1998).

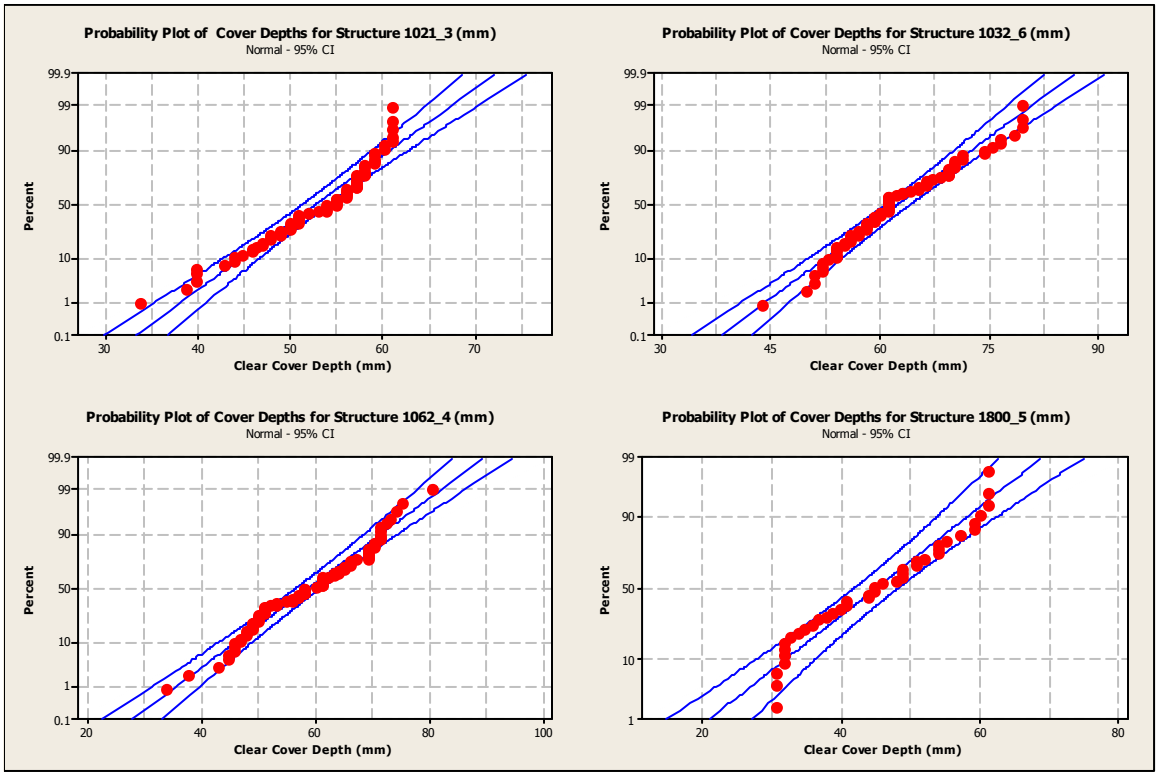

Figure 7 Cover Depth Distributions for Structures 1021_3, 1032_6, 1062_4 and 1800_5

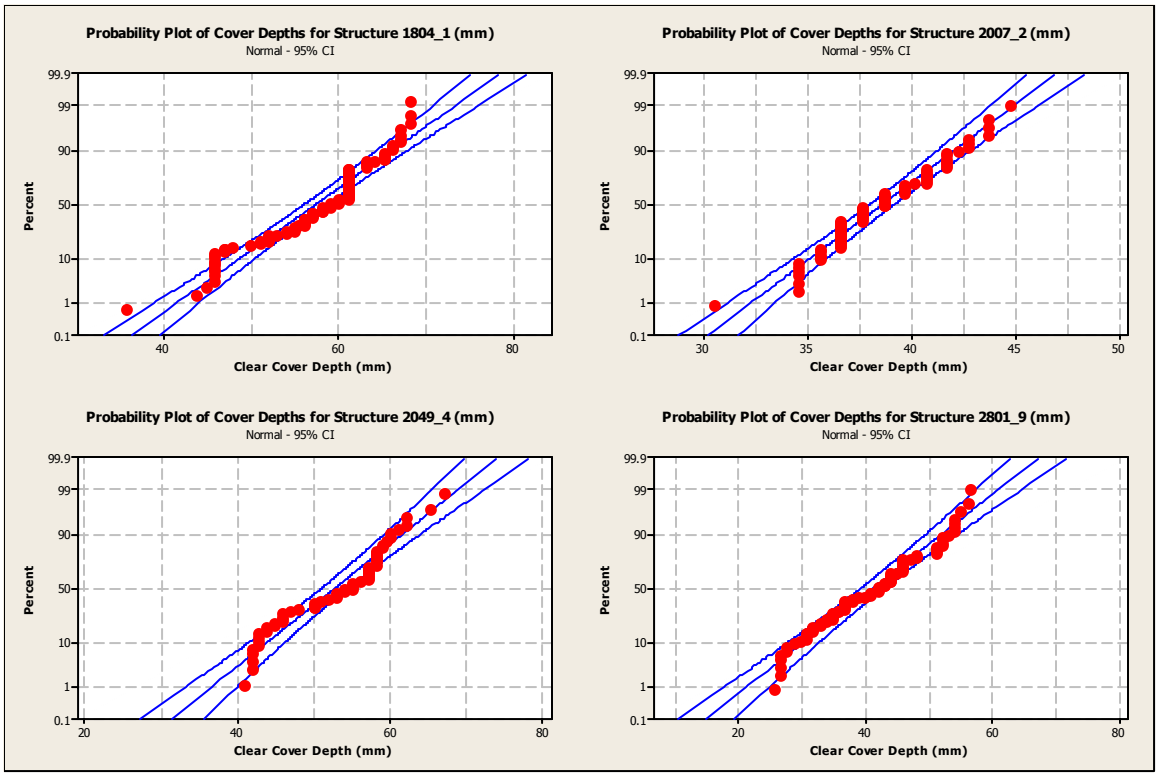

Figure 8 Cover Depth Distributions for Structures 1804_1, 2007_2, 2049_4 and 2801_9

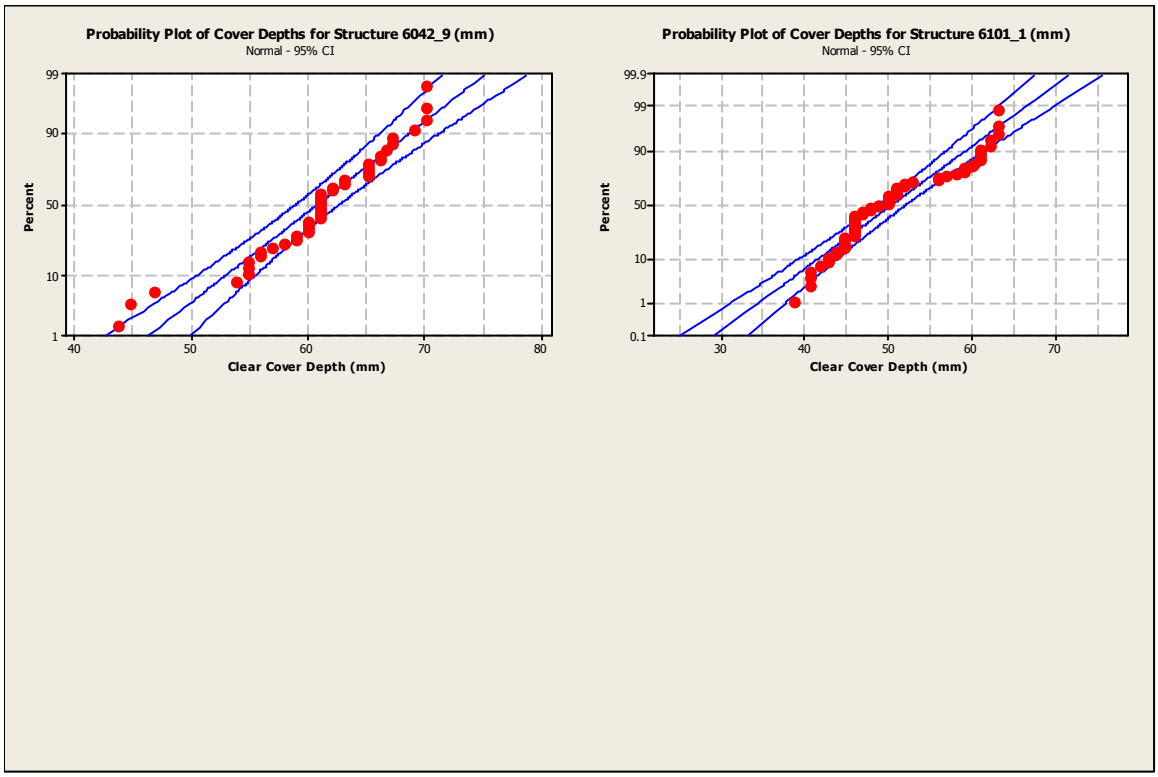

Figure 9 Cover Depth Distributions for Structures 6042_9 and 6101_1

Resistivity Measurements

As with the cover depth measurements, the resistivity measurements had to be condensed to one value per structure. However, since five measurements were performed at each test location, these too had to be condensed to one value. Therefore, to minimize the effect of occasional outliers, the median was calculated at each location. The same process was also applied to subsets 2 and 3. The results that are summarized in Table 10 are based on the median values at each of the 12 test locations. With one exception, there were 12 test locations on each structure.

Because the probability plots showed that the resistivity measurements fit an approximate log-normal, both the mean and the median values were calculated for each deck using the information collected since the median is a measure of central tendency that is much more resistant to the presence of extreme outliers (Ostle et al, 1995). The mean values ranged from as high as 348 kΩ-cm to as low as 31.0 kΩ-cm, while the median values ranged from 349 kΩ-cm to 32.0 kΩ-cm. It is also important to note the high variability of the resistivity data. The coefficient of variation, which is a measure of relative variability, usually calculated only when all values are positive, and expresses the standard deviation of the data as a percentage of the mean, ranged from as low as 7.88% to as high as 120%. Since resistivity is a property of the in situ concrete, unlike clear cover depths or corrosion potentials and linear polarization, it is possible that it may be used to non-destructively evaluate how changes in specifications and construction practices have influenced the final product. Therefore, it is important to have a measure of the variability of this technique to properly assess its field applicability.

Table 10 Resistivities for Structures with a Specified Maximum Water/Cement Ratio of 0.47

Bridge Number_District	Number of Total Observations	Resistivity Mean/Bridge(kΩ-cm)	Resistivity Median/Bridge (kΩ-cm)	Coefficient of Variation
2049_4	12	203	181	50.0
1062_4	12	261	195	77.6
1804_1	12	31.0	32.0	25.5
6042_9	10	178	157	45.2
6101_1	12	116	113	28.5
1800_5	12	318	101	120
2007_2	12	348	238	71.9
2801_9	12	348	349	7.88
1021_3	12	46.4	44.2	29.4
1032_6	12	162	108	108

This approximate lognormal distribution of all the measurements associated with subset 1 is also visible in the probability plots of each individual structure that comprises subset 1. The probability plots are presented in Figures 10 through 12.

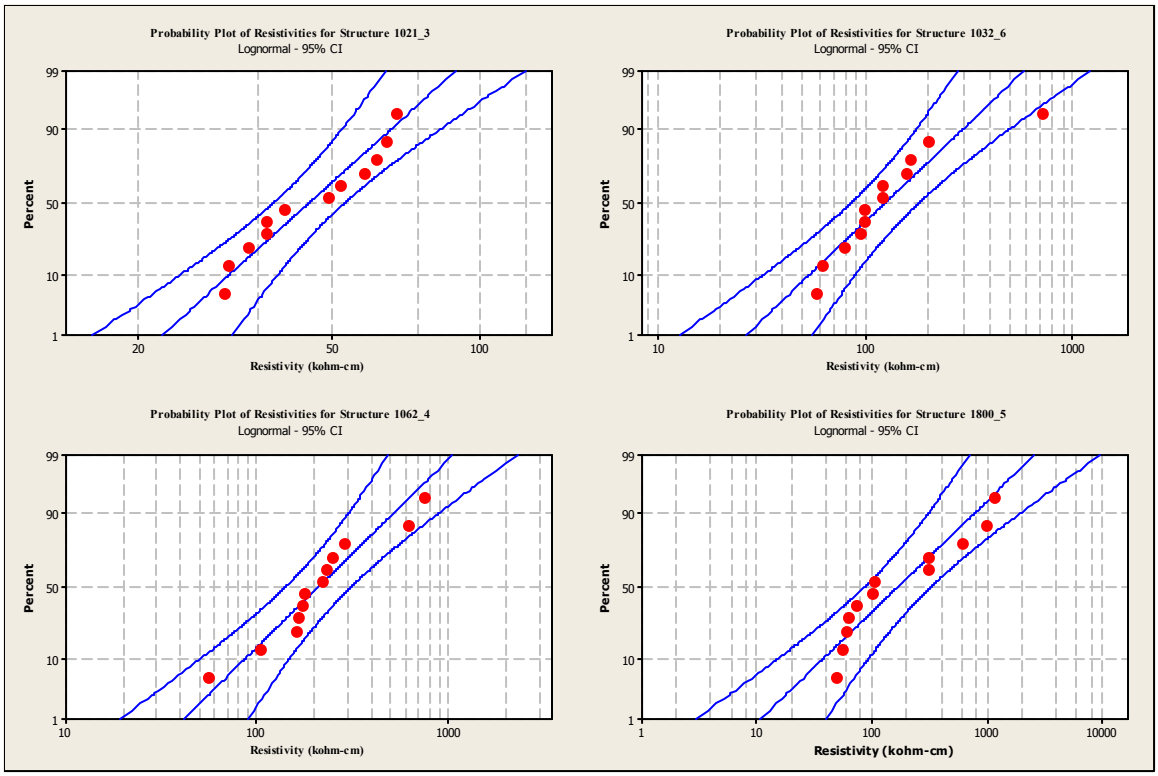

Figure 10 Resistivity Distributions for Structures 1021_3, 1032_6, 1062_4 and 1800_5

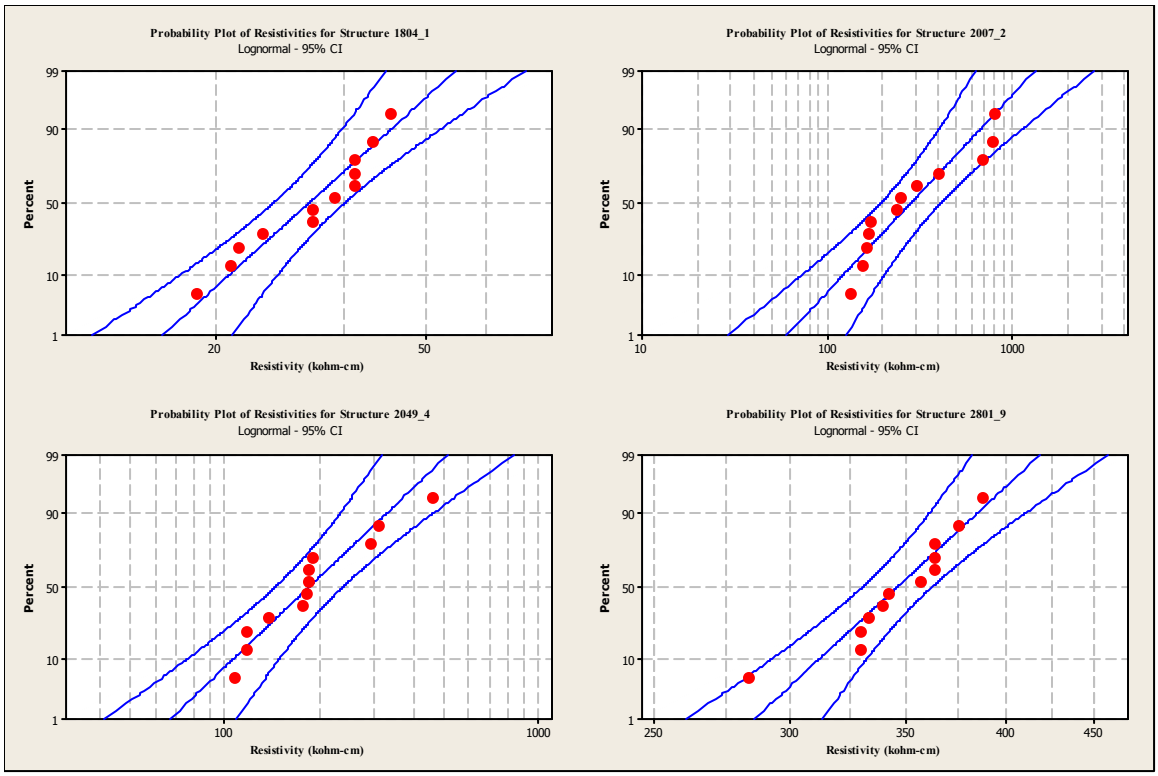

Figure 11 Resistivity Distributions for Structures 1804_1, 2007_2, 2049_4 and 2801_9

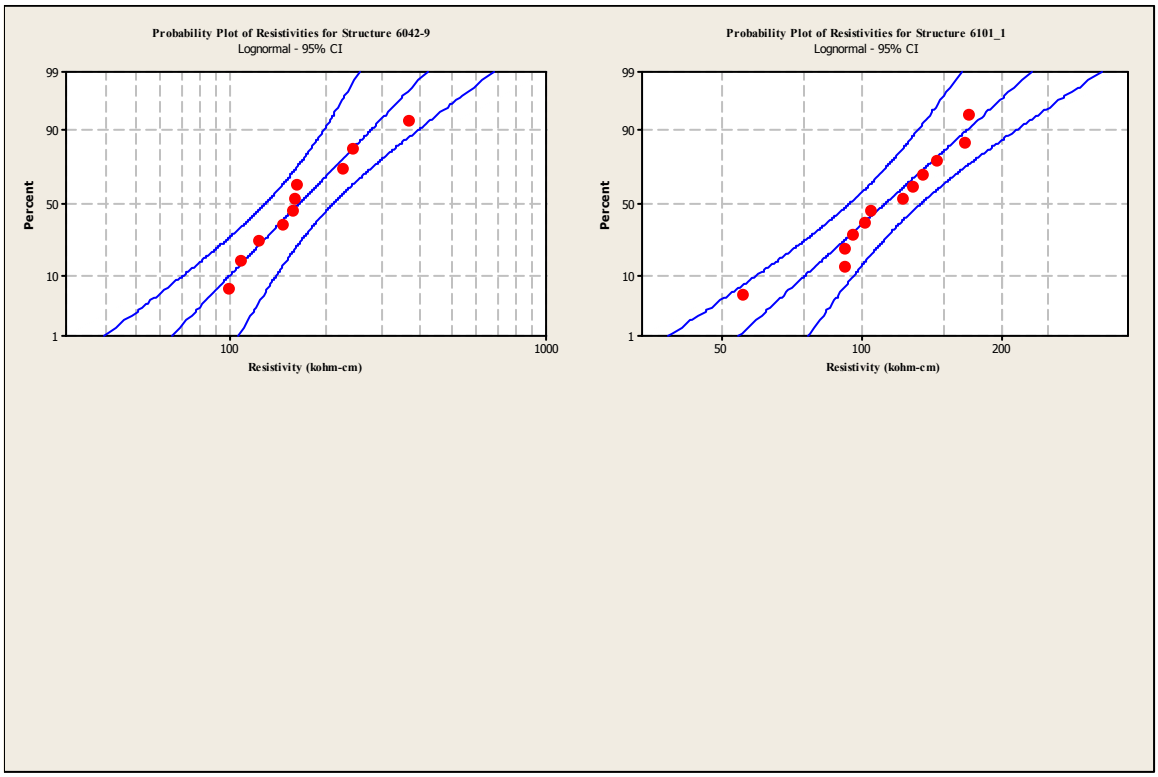

Figure 12 Resistivity Distributions for Structures 6042_9 and 6101_1

Linear Polarization

Since the corrosion current density measurements were collected at specific and not random locations, and were therefore biased, probability plots would not yield an accurate picture of the actual data distribution. Generally, six corrosion current density tests were performed on each structure based on the corrosion potential values obtained. More specifically, two test locations were chosen based on the highest absolute corrosion potential values, two on the lowest absolute corrosion potential values, and finally two test locations were chosen based on values approximately half way between the highest and the lowest absolute corrosion potential values. The actual values collected at each individual location along with the respective resistivity, corrosion potentials and clear cover depth measurements collected at the same locations are presented for each structure in Table 11.

Table 11 Corrosion Current Densities for Structures with a Specified Maximum W/C Ratio of 0.47

Bridge Number	Resistivity Median (kΩ-cm)	Corrosion Potential (-mV)	Corrosion Current Density (μA/cm^2)	Clear Cover Depth (mm)
1021_3	30.3	412	21.75	47
	73.4	186	8.441	56
	44.7	207	13.42	48
	38.3	203	14.67	57
	44.7	209	8.711	61
	31.0	250	20.97	54
1032_6	115	123	3.138	60
	54.3	103	6.898	57
	109	110	6.722	53
	163	144	4.837	57
	28.4	146	5.324	61
	83.0	125	5.375	66
1062_4	259	36.0	1.108	49
	294	60.0	0.839	55
	204	103	1.989	38
	182	87.0	2.268	57
	57.5	89.0	2.527	57
	166	42.0	1.492	58
1800_5	41.5	150	3.894	51
	830	195	3.014	49
	1181	151	3.822	48
	51.1	246	4.049	31
	798	253	7.146	31
	76.6	221	4.029	39
1804_1	22.3	428	11.94	57
	17.9	306	9.880	61
	31.9	220	6.070	56
	38.3	217	5.054	53
	38.3	339	10.90	58
	25.5	269	5.697	61
2007_2	479	326	3.107	38
	239	156	3.232	40
	243	250	3.221	39
	134	187	4.153	36
2049_4	185	104	5.199	52
	140	118	3.925	53
	185	133	3.594	46
	198	51.0	3.833	42
	287	43.0	2.237	58
	638	63.0	3.179	61

Table 11 (continued) Corrosion Current Densities for Structures with a Specified Maximum W/C Ratio of 0.47

Bridge Number	Resistivity Median (kΩ-cm)	Corrosion Potentials (-mV)	Corrosion Current Density (µA/cm2)	Clear Cover Depth (mm)
2801_9	342	104	2.620	42
	358	109	1.502	44
	396	376	5.459	43
	393	212	3.262	*
	370	235	2.289	*
	364	348	4.526	*
6042_9	252	133	3.221	45
	575	108	2.392	60
	169	84.0	9.508	61
	291	114	1.948	60
6101_1	185	83.0	3.376	46
	176	60.0	3.273	47
	51.1	75.0	7.436	50
	112	78.0	5.086	43
	125	32.0	2.123	57
	156	16.0	2.299	53

Chloride Exposure

The chloride exposure data per climatic zone (Table 12, Column 2) was drawn from a previous study conducted by Dr. R.E. Weyers at Virginia Tech (Weyers, R.E., 2004). Average chloride exposure per climatic zone was calculated over a period of three winter seasons, 2001, 2002, 2003, and expressed as an average annual kg-Cl^- /lane-km. Estimating chloride exposure per bridge was facilitated by multiplying climatic exposure values by the AADT value for the bridge (Table 12, Column 3). The hypothesis was that bridges with higher traffic volumes would most likely receive more frequent salt treatment due to the necessity of maintaining safer driving conditions.

Table 12 Chloride Exposure for Structures with a Specified Maximum W/C Ratio of 0.47

Bridge Number_District	Cl^- Exposure (kg/lane-km)	Cl^- Exposure (AADT*kg/lane-km)
1021_3	220	$174 * 10^3$
1032_6	225	$564*10^4$
1062_4	530	$954*10^3$
1800_5	225	$201*10^4$
1804_1	688	$378*10^4$
2007_2	688	$165*10^5$
2049_4	530	$689*10^4$
2801_9	$437*10^2$	$699*10^5$
6042_9	$437*10^2$	$122*10^6$
6101_1	688	$131*10^4$

Corrosion Potentials

Corrosion potential measurements for the 10 bridge decks in subset 1 were by and large normally distributed. Figures 13 through 15 show the distribution of the corrosion potential measurements collected from each individual structure. The number of observations per structure ranged from 32 to 102, and the standard deviation ranged from - 89.86 mV to -28.60 mV. Table 13 also summarizes the percent of measurements above -200 mV, between -200 and -350 mV, and below -350 mV. These boundaries were set by ASTM and a more detailed discussion can be found in the Literature Review section of this work. 100% of the corrosion potential measurements collected from five structures were greater than -200mV. Those bridge decks were 1032_6, 1062_4, 2049_4, 6042_9 and 6101_1. The percentage of measurements greater than -200mV collected from the remaining structures ranged from 34% to 87%. Only three structures yielded corrosion potential measurements more negative than -350mV. These structures were 1804_1, 1021_3 and 2007_2 with cumulative corrosion potential measurements of 3%, 4% and 10%, respectively.

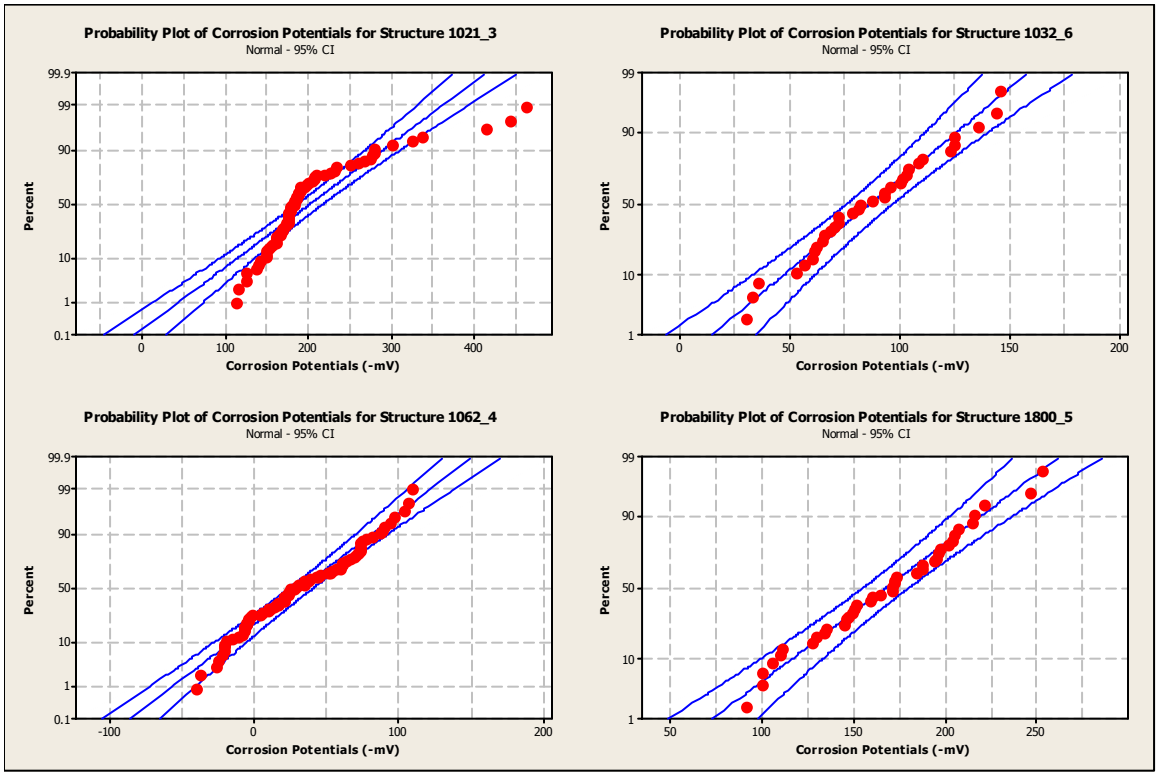

Figure 13 Corrosion Potential Distributions for Structures 1021_3, 1032_6, 1062_4 and 1800_5

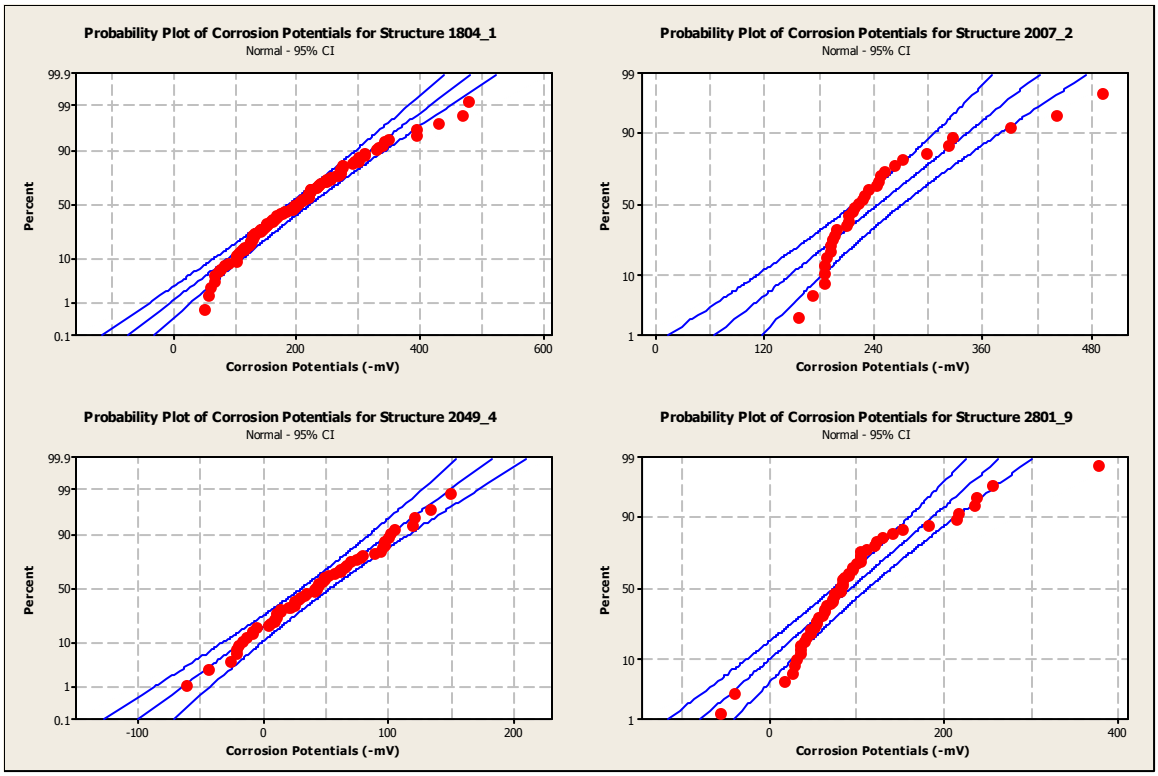

Figure 14 Corrosion Potential Distributions for Structures 1804_1, 2007_2, 2049_4 and 2801_9

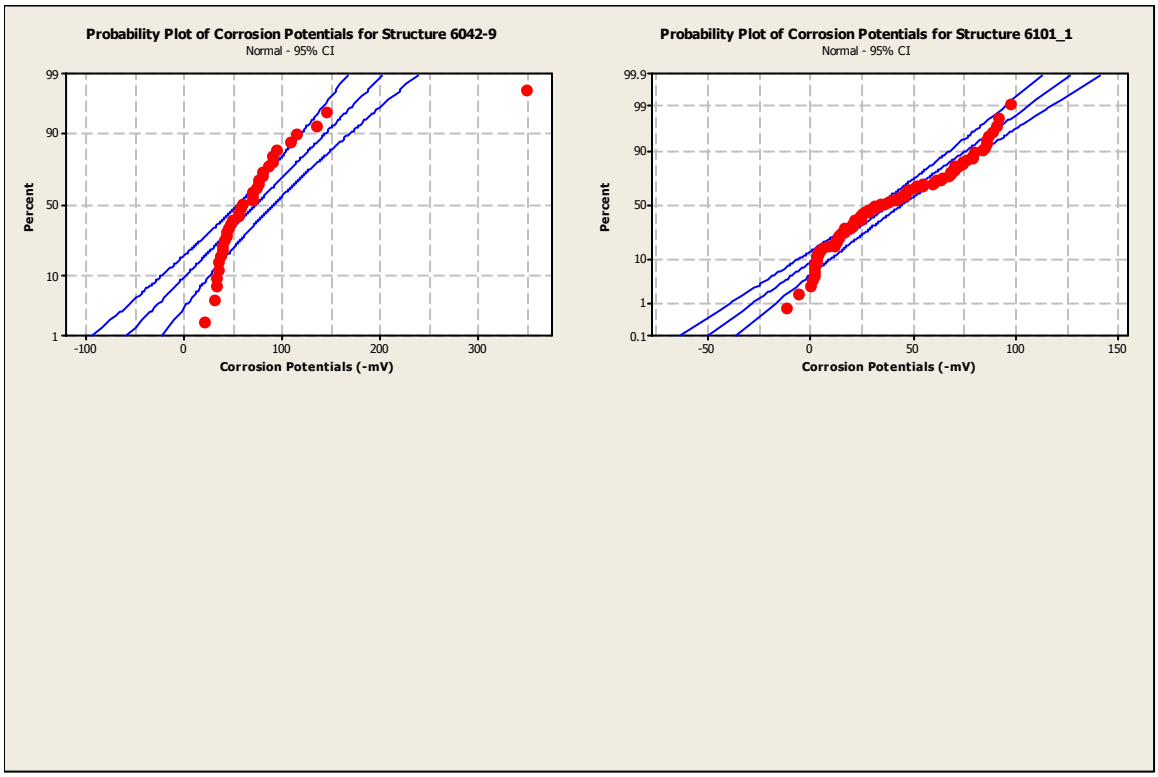

Figure 15 Corrosion Potential Distributions for Structures 6042_9 and 6101_1

Other Data

The remaining structural as well as environmental data, which consisted of structure type (simply supported or continuous), beam material (steel or concrete), traffic volume presented as AADT and AADTT, age, NBIS deck rating and girder spacing are presented in Table 14.

Table 13 Half-cell Potentials for Structures with a Specified Maximum W/C Ratio of 0.47

Bridge Number_District	Number of Observations	Potentials (Cumulative % >=-200mV)	Potentials (% between 200 and 350 mV)	Potentials (Cumulative % <=-350mV)	Potentials Mean/Bridge (-mV)	Standard Deviation (-mV)
2049_4	60	100	0	0	37.60	45.62
1062_4	82	100	0	0	31.14	38.16
1804_1	102	53	44	3	200.8	89.86
6042_9	36	100	0	0	61.89	56.02
6101_1	94	100	0	0	37.76	28.60
1800_5	40	78	22	0	166.7	40.49
2007_2	32	34	56	10	243.3	76.61
2801_9	54	87	13	0	101.1	73.32
1021_3	72	71	25	4	200.3	68.01
1032_6	33	100	0	0	86.06	30.79

Table 14 Physical Parameters for Structures with a Specified Maximum W/C Ratio of 0.47

Bridge Number_District	Beam Material	Superstructure Design	Girder Spacing	NBIS Deck Rating	AADT	AADTT	Age
	Steel/Concrete	Simple/Continuous	mm (in)				Years
2049_4	Concrete	Simple	2362 (93)	6	13000	2730	36
1062_4	Concrete	Simple	2565 (101)	6	1800	306	35
1804_1	Steel	Simple	2616 (103)	6	5500	385	35
6042_9	Steel	Simple	2210 (87)	7	28000	840	35
6101_1	Steel	Simple	2565 (101)	6	1900	19	35
1800_5	Steel	Simple	2489 (98)	7	8900	356	34
2007_2	Steel	Simple	2286 (90)	5	24000	7680	34
2801_9	Steel	Simple	2286 (90)	7	16000	480	34
1021_3	Concrete	Simple	1905 (75)	6	790	55	33
1032_6	Steel	Simple	2794 (110)	6	25000	1500	33

Subset 2: Bridge Decks Constructed Between 1984 and 1991 with Epoxy Coated Bar, Specified Maximum W/C Ratio of 0.45

Cover Depths

As previously stated for subset 1, for data analysis purposes, it was necessary to condense the large number of measurements available for each structure into one value. The clear cover depth number of observations, the mean, the standard deviation, and the percent of observations less than 51 mm for each individual structure in subset 2 is summarized in Table 15. The structures in subset 2 had a mean clear cover depth ranging from 50 to 73 mm. For the 16 structures studied, 59%, 48% and 46% of the measurements performed on three bridge decks, 1031_9, 1014_9 and 1920_7, respectively, were less than 51 mm. The remaining structures exhibited measurements less than 51 mm ranging from 0% to 24% cumulative.

Table 15 Cover Depths for Structures with a Specified Maximum W/C Ratio of 0.45

Bridge Number_District	Number of Observations	Cover Depth Mean/Bridge (mm.)	Standard Deviation (mm)	Cover Depths % < 51 mm.
1019_8	120	64	5.8	0
2547_5	80	65	6	0
1020_2	114	55	6.5	24
2820_1	80	73	5.7	0
1133_8	76	69	4	0
1139_9	79	61	8.4	13
1014_9	40	50	3.6	48
1003_3	240	57	5	10
1132_1	84	55	7	24
1098_9	80	57	5.5	15
1133_1	78	62	4.5	1
1031_9	80	50	6.1	59
1007_4	67	61	3.4	0
6051_1	103	57	6.8	24
1920_7	80	51	7.3	46
2901_4	80	68	7.5	4

As shown in Figures 16 through 19, the clear cover depth measurements for each individual structure in subset 2 were nearly normally distributed.

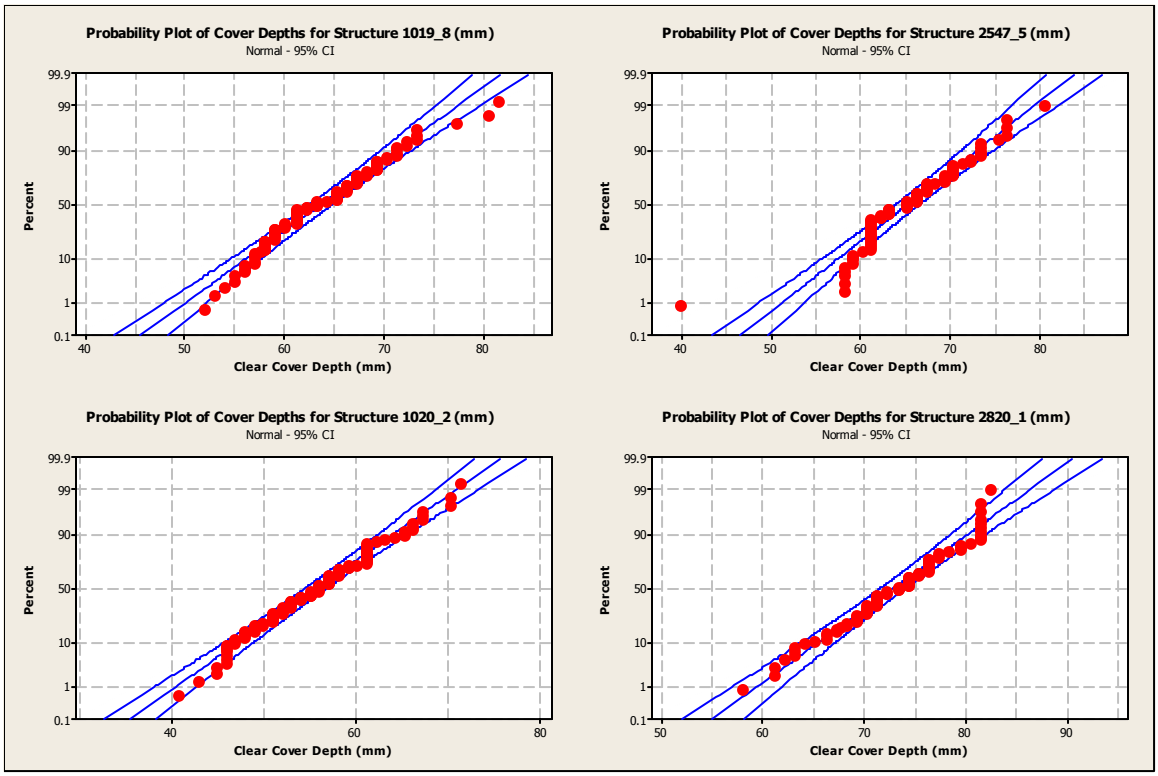

Figure 16 Cover Depth Distributions for Structures 1019_8, 2547_5, 1020_2 and 2820_1

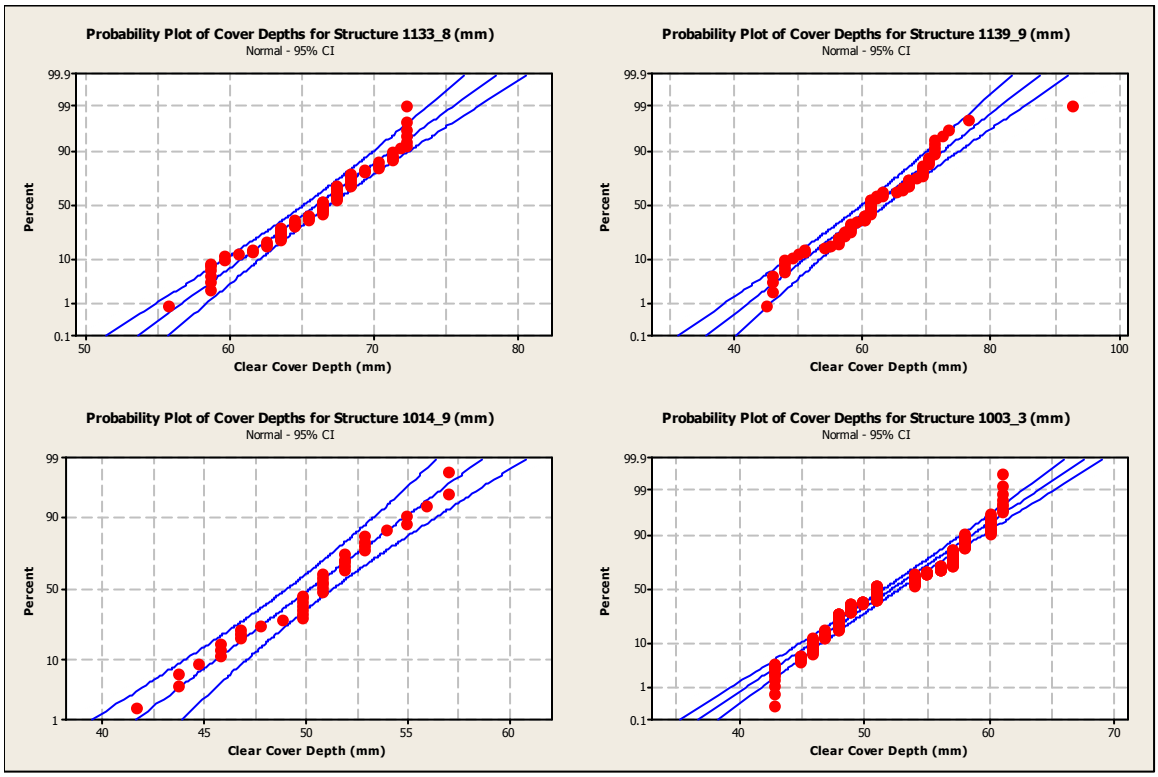

Figure 17 Cover Depth Distributions for Structures 1003_1, 1014_9, 1133_8 and 1139_9

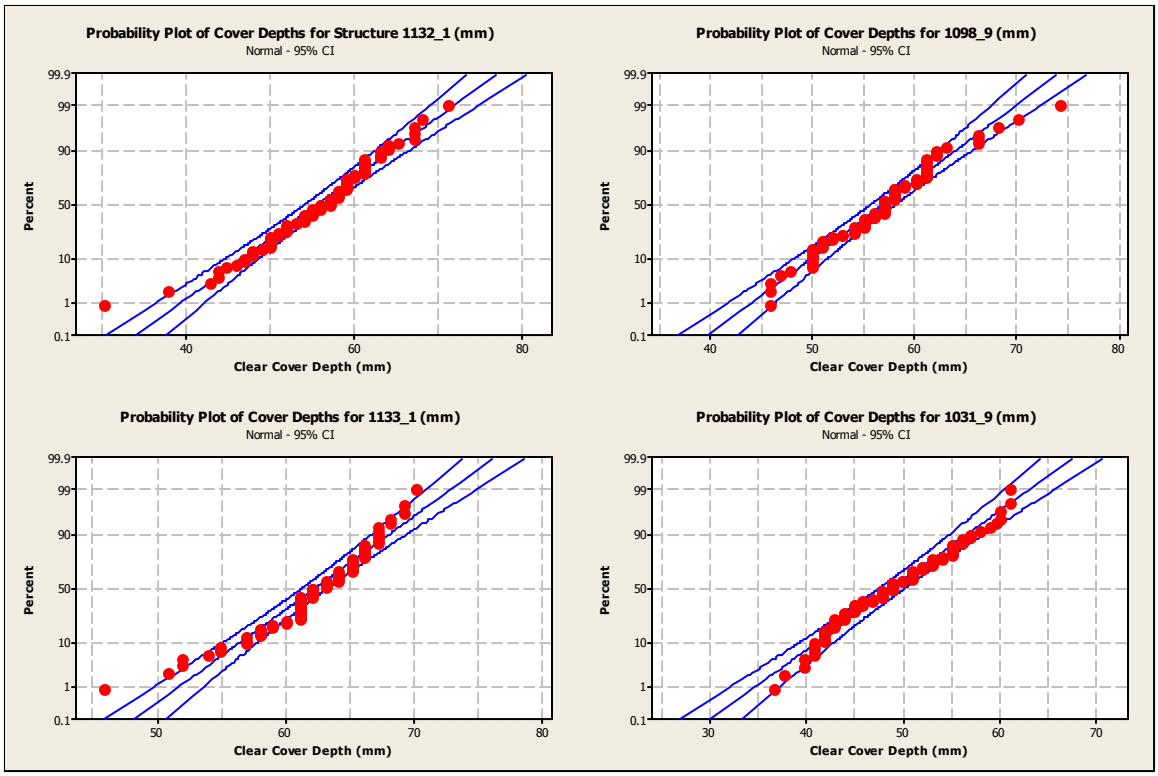

Figure 18 Cover Depth Distributions for Structures 1132_1, 1098_9, 1133_1 and 1031_9

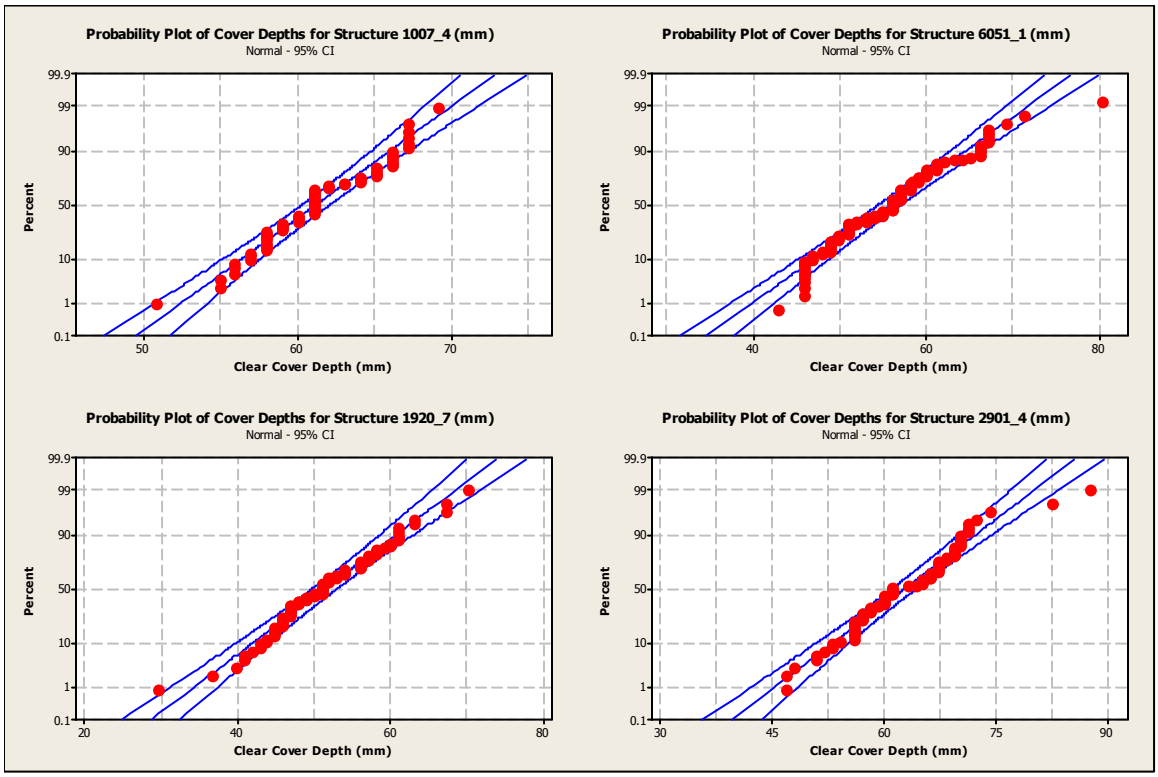

Figure 19 Cover Depth Distributions for Structures 1007_4, 6051_1, 1920_7 and 2901_4

Resistivity Measurements

The results of the resistivity measurements are summarized in Table 16. Twelve locations were tested on each structure with the exception of one structure, 1098_9, where ten locations were tested. This was due to the unforeseen appearance of inclement weather. The mean values ranged from as high as 156 kΩ-cm to as low as 12.8 kΩ-cm, while the median values ranged from 157 kΩ-cm to 12.7 kΩ-cm. The coefficient of variation ranged from as low as 7.35% to as high as 41.5%.

Table 16 Resistivities for Structures with a Specified Maximum W/C Ratio of 0.45

Bridge Number_District	Number of Observations	Resistivity Mean/Bridge (kΩ-cm)	Resistivity Median/Bridge (kΩ-cm)	Coefficient of Variation
1019_8	12	30.1	30.2	14.4
2547_5	12	85.1	76.2	32.4
1020_2	12	85.6	82.3	16.4
2820_1	12	156	157	21.7
1133_8	12	31.4	30.3	7.35
1139_9	12	22.5	21.3	29.6
1014_9	12	70.9	68.6	20.6
1003_3	12	14.4	13.6	37.6
1132_1	12	12.8	12.7	19.4
1098_9	10	111	111	29.8
1133_1	12	13.1	12.8	16.1
1031_9	12	29.6	30.5	19.9
1007_4	12	25.9	24.4	41.5
6051_1	12	15.2	15.4	20.1
1920_7	12	24.6	24.2	27.8
2901_4	12	38.9	36.6	38.2

As with the resistivity data collected on the bridge decks in subset 1, the resistivity data in this particular subset also has an approximate lognormal distribution. The distribution of the resistivity data is presented in Figures 20 through 23.

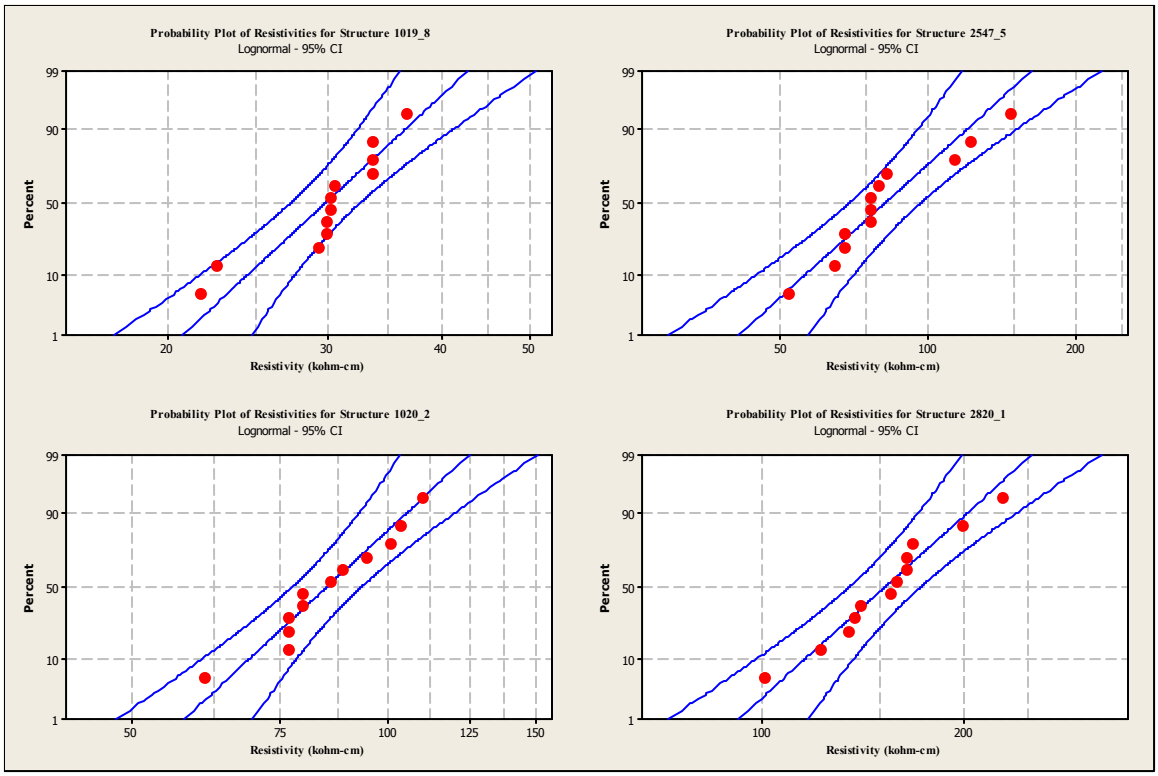

Figure 20 Resistivity Distributions for Structures 1019_8, 2547_5, 1020_2 and 2820_1

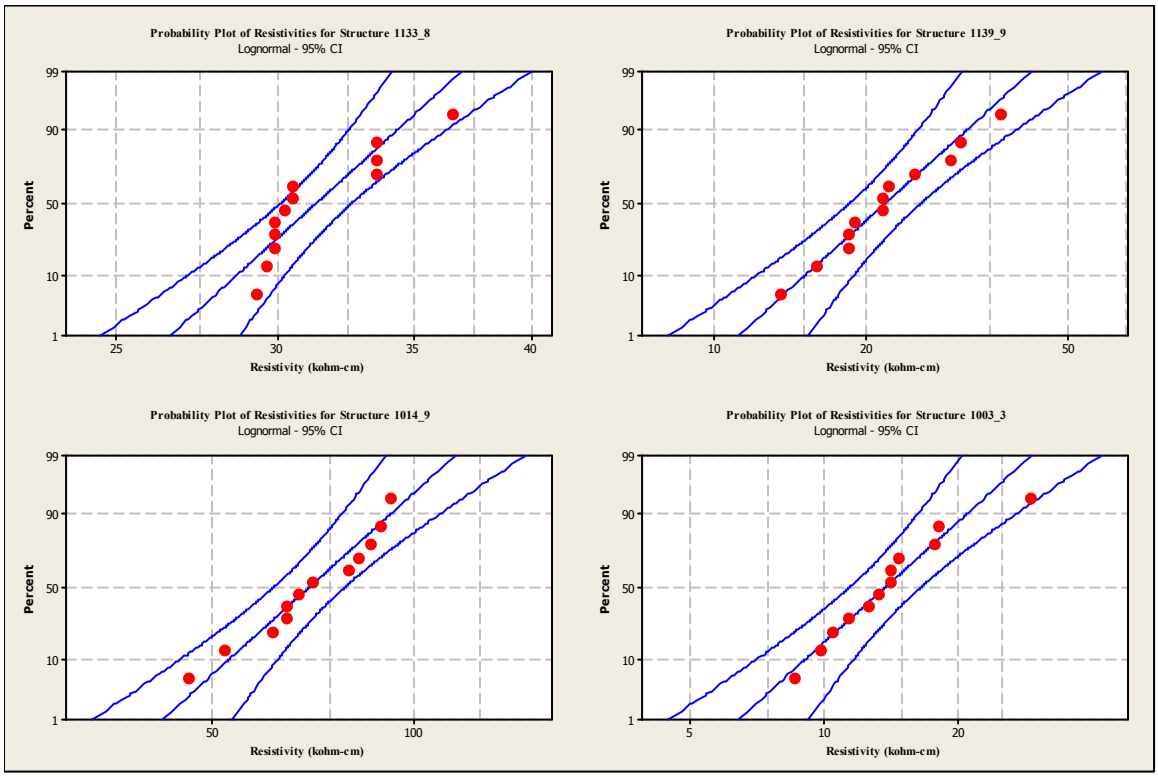

Figure 21 Resistivity Distributions for Structures 1133_8, 1139_9, 1014_9 and 1003_3

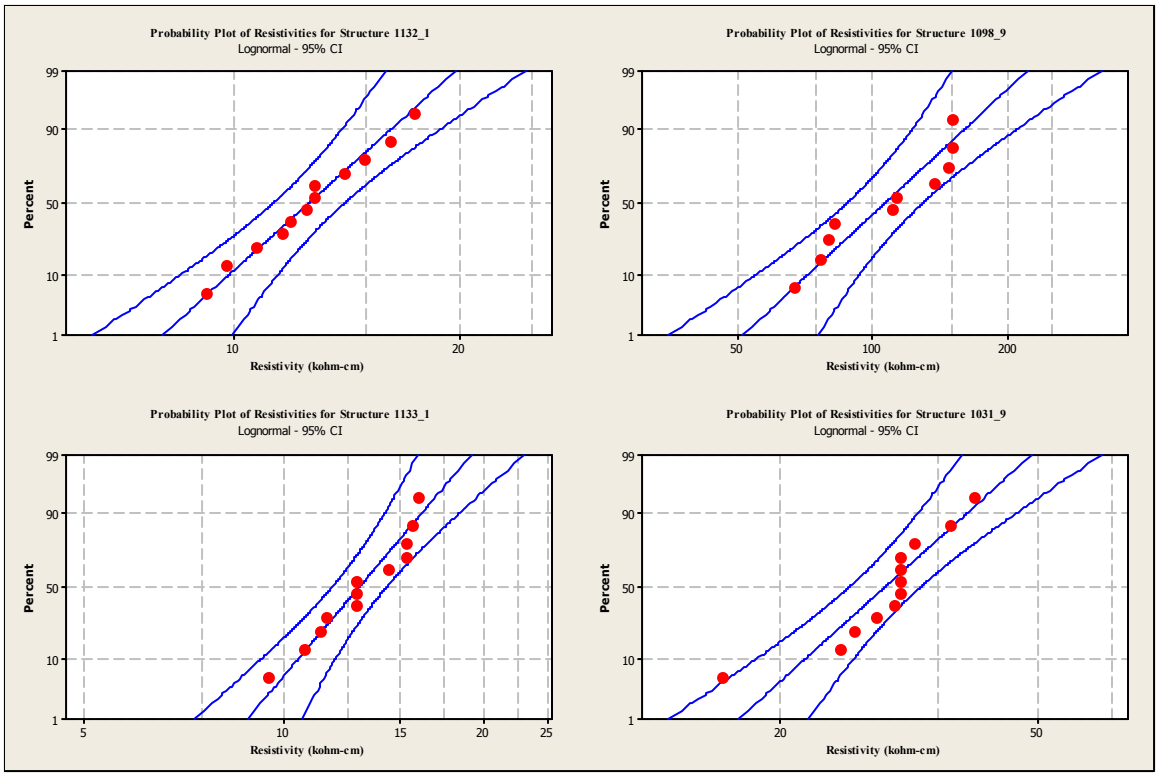

Figure 22 Resistivity Distributions for Structures 1132_1, 1098_9, 1133_1 and 1031_9

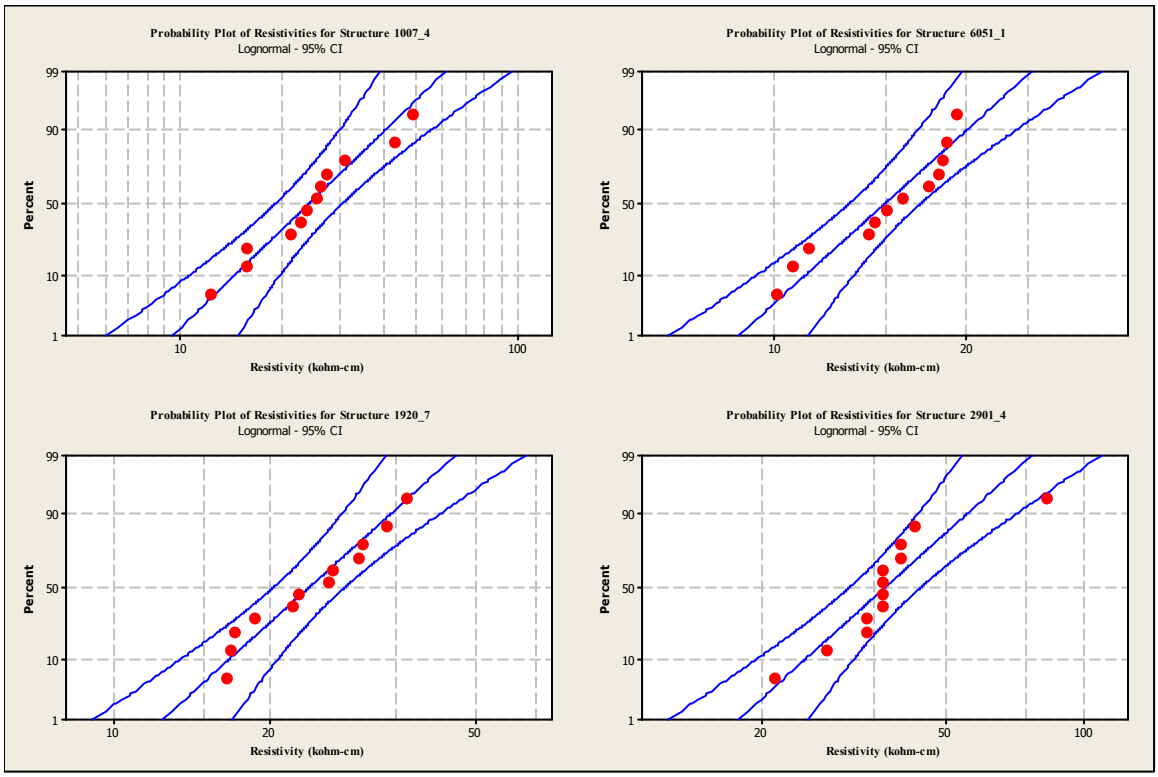

Figure 23 Resistivity Distributions for Structures 1007_4, 6051_1, 1920_7 and 2901_4

Linear Polarization

As with the structures in subset 1, since the corrosion current density measurements were collected at specific and not random locations, probability plots would not yield an accurate picture of the actual data distribution. Six corrosion current density tests were performed on each structure based on the corrosion potential values obtained. More specifically, two test locations were chosen based on the highest absolute corrosion potential values, two on the lowest absolute corrosion potential values, and finally two test locations were chosen based on values approximately half way between the highest and the lowest absolute corrosion potential values. The actual values collected at each individual location along with the respective resistivity, corrosion potentials and clear cover depth measurements collected at the same locations are presented for each structure in Table 17.

Table 17 Corrosion Current Densities for Structures with a Specified Maximum W/C Ratio of 0.45

Bridge Number	Resistivity Median (kΩ-cm)	Corrosion Potentials (-mV)	Corrosion Current Density (μA/cm^2)	Clear Cover Depth (mm)
1132_1	13.4	251	16.13	60
	13.1	269	25.54	30
	13.1	211	18.69	50
	16.9	298	17.61	47
	11.5	452	25.19	56
	11.5	435	23.69	58
2820_1	137	154	10.68	69
	163	144	8.069	76
	47.9	169	11.03	75
	150	141	9.736	81
	76.6	184	9.166	*
	112	210	5.956	*
1020_2	95.8	243	7.229	46
	60.7	296	11.68	56
	115	170	3.128	53
	82.9	176	5.147	58
	92.6	344	8.483	59
	92.6	387	13.02	58
1003_3	13.7	200	9.518	59
	18.5	284	7.291	56
	8.94	325	26.36	64
	11.8	246	22.22	59
	15.3	244	19.88	57
	13.1	295	15.69	54
1014_9	86.2	289	2.527	49
	70.2	235	2.693	52
	57.5	159	2.620	49
	54.3	152	2.331	48
	70.2	214	2.537	55
	63.8	262	1.813	47

Table 17 (continued) Corrosion Current Densities for Structures with a Specified Maximum W/C Ratio of 0.45

Bridge Number	Resistivity Median (kΩ-cm)	Corrosion Potentials (-mV)	Corrosion Current Density (μA/cm^2)	Clear Cover Depth (mm)
2901_4	38.3	342	7.519	61
	54.3	245	9.052	65
	57.5	250	9.322	53
	54.3	304	9.726	71
	82.9	315	10.89	*
	89.4	277	11.71	*
2547_5	76.6	131	1.667	61
	67.0	118	1.512	61
	121	181	2.579	58
	*	*	*	61
	*	*	*	62
	*	*	*	59
1920_7	22.3	213	10.69	37
	22.7	287	26.50	47
	34.8	241	15.70	52
	31.9	386	0.632	57
	31.9	437	0.622	54
	35.1	405	0.518	46
1133_8	31.3	124	1.657	75
	31.6	221	2.217	71
	35.1	220	1.937	71
	31.9	134	1.906	72
	30.9	172	2.123	61
	35.1	178	1.699	67
1019_8	35.1	331	2.227	59
	44.7	379	19.17	59
	31.2	357	2.569	56
	31.3	341	3.179	61
	31.9	364	2.631	59
	31.6	332	2.818	61
1031_9	31.6	257	0.756	44
	25.9	291	0.839	43
	27.1	270	0.984	52
	16.9	260	0.766	48
	34.2	231	0.705	43
	29.4	200	0.683	55
1139_9	29.4	386	0.849	58
	22.3	473	1.284	46
	17.6	527	1.035	70
	19.8	345	0.880	61
	19.1	306	0.787	58
	31.9	273	0.736	61
1133_1	11.1	403	5.779	61
	14.0	211	4.091	65
	15.9	208	3.863	59
	12.1	265	3.967	59
	10.2	299	4.039	51
	14.7	313	25.01	64

Table 17 (continued) Corrosion Current Densities for Structures with a Specified Maximum W/C Ratio of 0.45

Bridge Number	Resistivity Median (kΩ-cm)	Corrosion Potentials (-mV)	Corrosion Current Density (μA/cm^2)	Clear Cover Depth (mm)
6051_1	15.6	193	0.549	57
	21.7	187	0.456	61
	15.6	296	0.300	66
	10.5	285	0.342	54
	9.89	289	2.496	49
	10.9	305	2.455	67
1007_4	18.8	380	0.383	64
	19.1	388	0.373	62
	25.5	294	0.819	61
	31.9	276	0.984	64
	44.7	199	3.293	59
	60.7	211	3.242	69
1098_9	121	321	0.911	66
	60.7	309	1.202	61
	44.7	313	1.347	59
	156	310	1.450	58
	144	299	1.429	61
	86.2	270	1.367	62
1014_9	86.2	289	2.527	49
	70.2	235	2.693	52
	57.5	159	2.620	49
	54.3	152	2.330	47
	70.2	214	2.537	55
	63.8	262	1.813	47

Chloride Exposure

The chloride exposure data was calculated as described for subset 1 and is summarized in Table 18. The chloride exposure as calculated per environmental zone ranged from 225 kg/lane-km to 4369 kg/lane-km, while the chloride exposure calculated taking into consideration the traffic volume for each individual structure ranged from $757*10^3$ AADT*kg/lane-km to $267*10^6$ AADT*kg/lane-km.

Table 18 Chloride Exposure for Structures with a Specified Maximum W/C Ratio of 0.45

Bridge Number_District	Cl^- Exposure (kg/lane-km)	Cl^- Exposure (AADT*kg/lane-km)
1019_8	671	$738*10^4$
2547_5	530	$122*10^5$
1020_2	688	$646*10^4$
2820_1	688	$172*10^5$
1133_8	671	$637*10^4$
1139_9	4369	$830*10^5$
1014_9	4369	$786*10^5$
1003_3	530	$127*10^4$
1132_1	688	$756*10^4$
1098_9	4369	$267*10^6$
1133_1	688	$757*10^4$
1031_9	4369	$830*10^5$
1007_4	530	$122*10^5$
6051_1	688	$757*10^3$
1920_7	4369	$367*10^5$
2901_4	225	$406*10^4$

Corrosion Potentials

Although the corrosion potential measurements in subset 2 were collected on bridge decks reinforced with epoxy coated steel, the data was nearly normally distributed. Figures 24 through 27 demonstrate that the corrosion potential data for individual structures are also generally normally distributed.

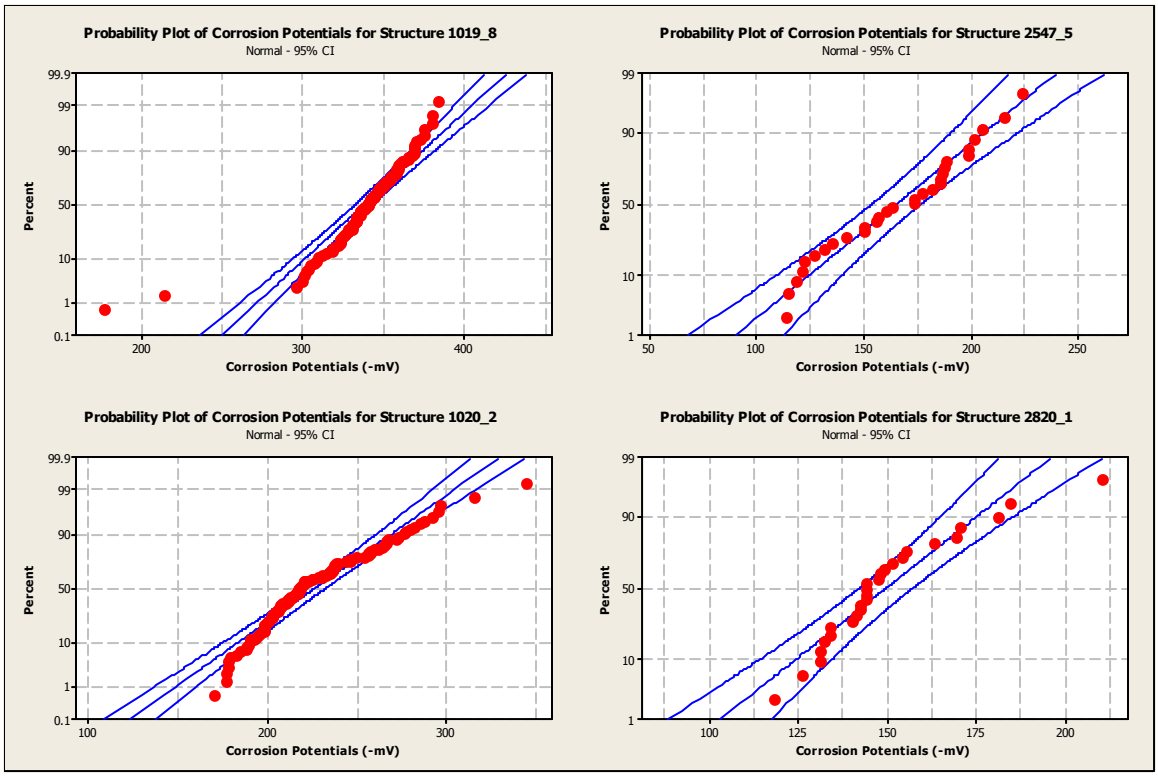

Figure 24 Corrosion Potential Distributions for Structures 1019_8, 2547_5, 1020_2 and 1021_2

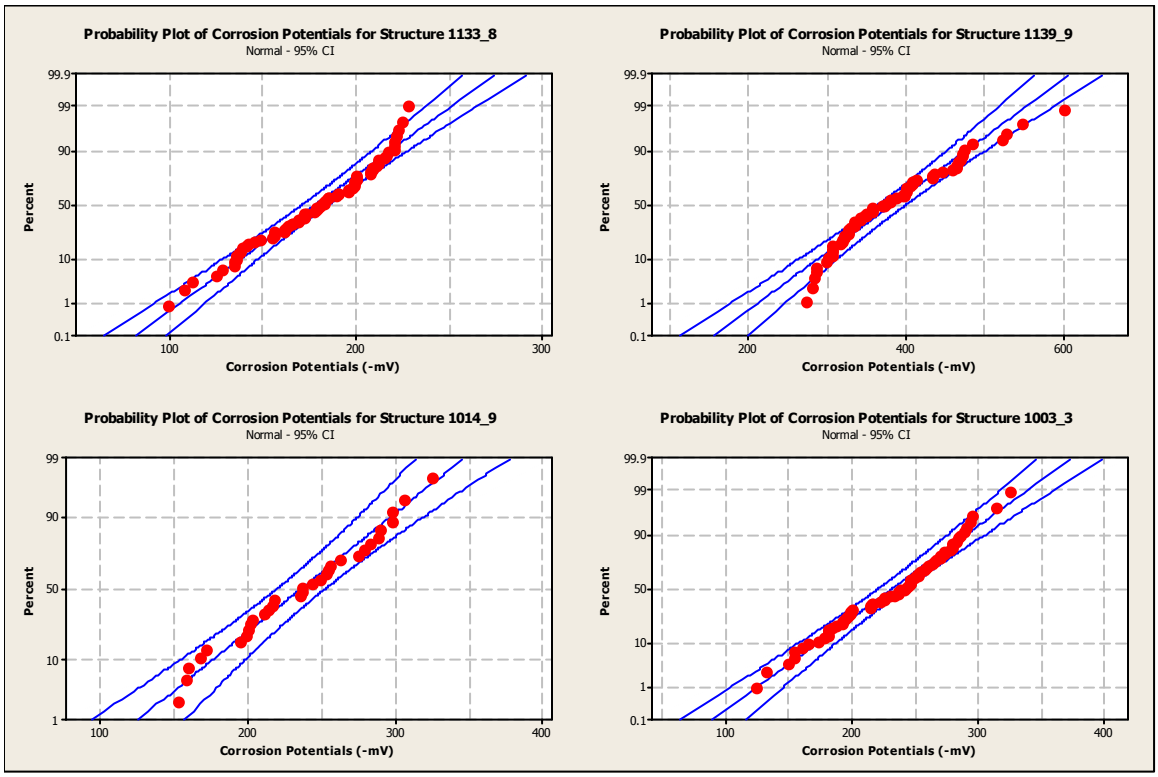

Figure 25 Corrosion Potential Distributions for Structures 1133_8, 1139_9, 1014_9 and 1003_3

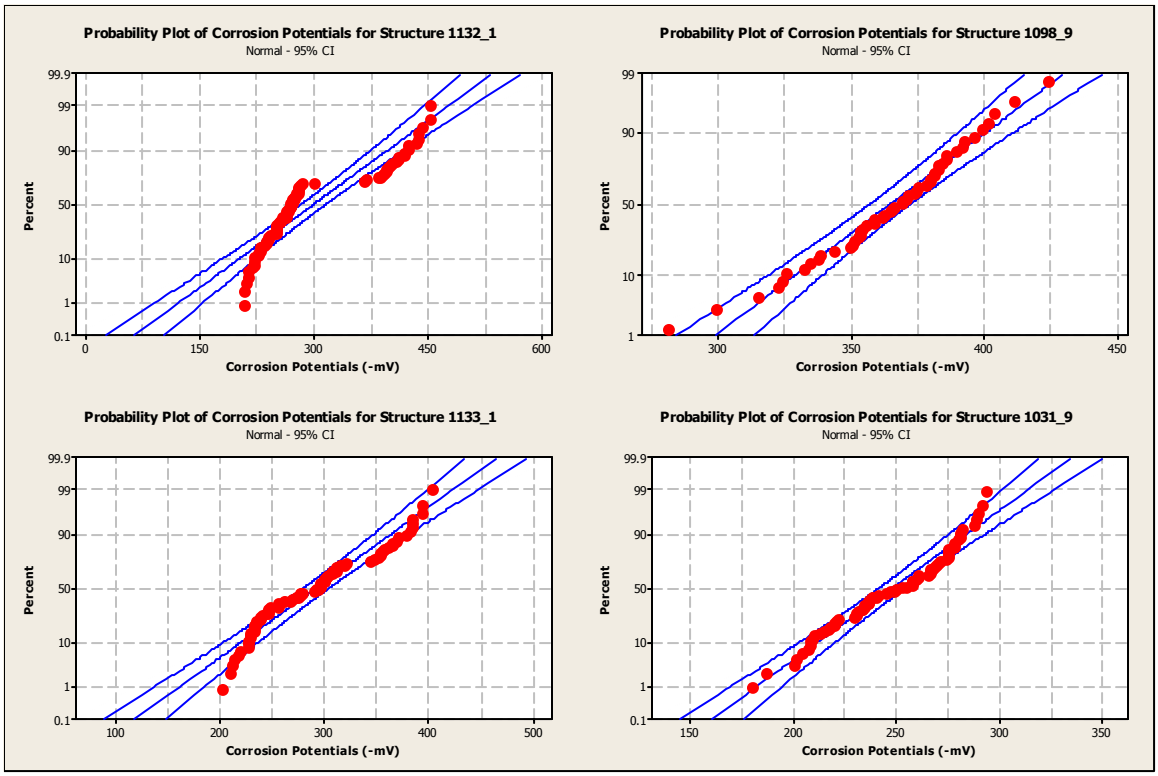

Figure 26 Corrosion Potential Distributions for Structures 1132_1, 1098_9, 1133_1 and 1031_9

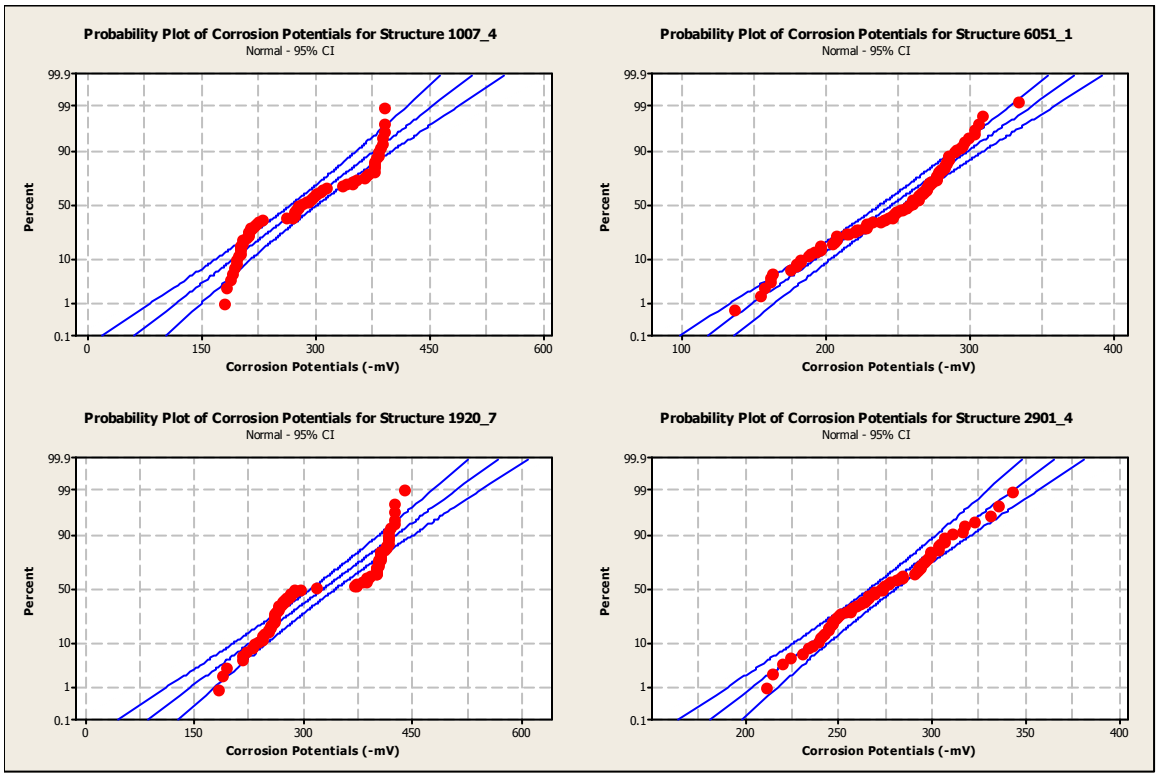

Figure 27 Corrosion Potential Distributions for Structures 1007_4, 6051_1, 1920_7 and 2901_4

The corrosion potential data is summarized in Table 19. The number of measurements ranged from 27 to 112. The standard deviation ranged in value from -77.93 mV to -19.90 mV. Table 18 also summarizes the percent of measurements above -200 mV, between -200 and -350 mV, and below -350 mV. The percentage of measurements greater than -200mV collected from the structures ranged from 0% to 96%. Six structures yielded corrosion potential measurements more negative than -350mV. The cumulative corrosion potential measurements of these structures ranged from 23% to 83%.

Other Data

The remaining structural as well as environmental data, which consisted of structure type (simply supported or continuous), beam material (steel or concrete), traffic volume presented as AADT and AADTT, age, NBIS deck rating and girder spacing are presented in Table 20.

Table 19 Half-cell Potentials for Structures with a Specified Maximum W/C Ratio of 0.45

Bridge Number_District	Number of Observation	Potentials (Cumulative % >=-200mV)	Potentials (% between 200 and 350)	Potentials (Cumulative % <=-350mV)	Potentials Mean/Bridge (-mV)	Standard Deviation
1019_8	102	0	70	30	339.7	28.39
2547_5	30	87	13	0	164.3	32.07
1020_2	112	23	77	0	223.4	33.15
2820_1	27	96	4	0	149.2	19.90
1133_8	76	75	25	0	177.6	31.10
1139_9	64	0	44	56	380.0	73.02
1014_9	32	25	75	0	235.1	47.21
1003_3	68	32	68	0	230.2	45.77
1132_1	84	0	71	29	296.9	75.43
1098_9	52	0	17	83	363.9	28.04
1133_1	78	0	77	23	289.9	56.00
1031_9	73	0	100	0	247.5	28.15
1007_4	67	15	85	0	282.9	72.18
6051_1	103	17	83	0	244.8	41.43
1920_7	80	4	49	48	324.7	77.93
2901_4	70	0	100	0	272.5	29.77

Table 20 Physical Parameters for Structures with a Specified Maximum W/C Ratio of 0.45

Bridge Number_District	Beam Material	Superstructure Design	Girder Spacing	NBIS Deck Rating	AADT	AADTT	Age
	Steel/Concrete	Simple/Continuous	mm (in)				Years
1019_8	Steel	Continuous	2870 (113)	7	11000	550	20
2547_5	Steel	Simple	3251 (128)	6	23000	1380	20
1020_2	Steel	Continuous	2718 (107)	7	9400	1034	18
2820_1	Concrete	Simple	2667 (105)	6	25000	7500	18
1133_8	Steel	Continuous	2896 (114)	7	9500	2660	17
1139_9	Steel	Simple	2438 (96)	7	19000	950	17
1014_9	Concrete	Simple	2057 (81)	8	18000	1620	17
1003_3	Steel	Simple	2972 (117)	7	2400	240	15
1132_1	Steel	Continuous	2743 (108)	6	11000	990	15
1098_9	Steel	Continuous	2261 (89)	7	61000	3050	15
1133_1	Steel	Simple	2743 (108)	7	11000	990	15
1031_9	Steel	Continuous	3048 (120)	7	19000	950	14
1007_4	Steel	Simple	2819 (111)	8	23000	1380	14
6051_1	Steel	Simple	2235 (88)	6	1100	22	14
1920_7	Concrete	Simple	2286 (90)	6	8400	588	13
2901_4	Concrete	Continuous	2311 (91)	7	18000	5040	13

Subset 3: Bridge Decks Constructed Between 1984 and 1991 with Epoxy Coated Bar, Specified Maximum W/Cm Ratio of 0.45 with Supplementary Cementing Material (Slag, Flyash)

Cover Depths

The clear cover depth number of observations, the mean, the standard deviation, and the percent of observations less than 51 mm for each individual structure in subset 3 are summarized in Table 21. The structures in subset 3 had a mean clear cover depth ranging from 54 to 67 mm. For the 11 structures studied, 38% of the measurements performed on one bridge deck, 1000_3, were less than 51 mm, while the remainder of the measurements less than 51 mm ranged from 0% to 25%. Three structures: 2815_1, 2812_5 and 2819_1, had no clear cover depths less than 51 mm. Also, as shown in Figures 28 through 30, the clear cover depth measurements for each individual structure in subset 3 were generally normally distributed.

Table 21 Cover Depths for Structures with a Specified Maximum W/CM Ratio of 0.45

Bridge Number_District	Number of Observations	Cover Depth Mean/Bridge (mm.)	Standard Deviation (mm)	Cover Depths % < 51 mm.
2815_1	104	64	5.5	0
2819_1	114	67	6.2	0
1002_9	82	66	8.7	5
1152_1	60	63	14	25
1002_8	68	58	6.5	12
1021_2	48	62	4.2	2
1017_3	48	54	5.1	25
1042_8	56	59	11	20
2812_5	40	64	4.1	0
1000_3	50	52	5.1	38
6058_9	40	59	4.3	10

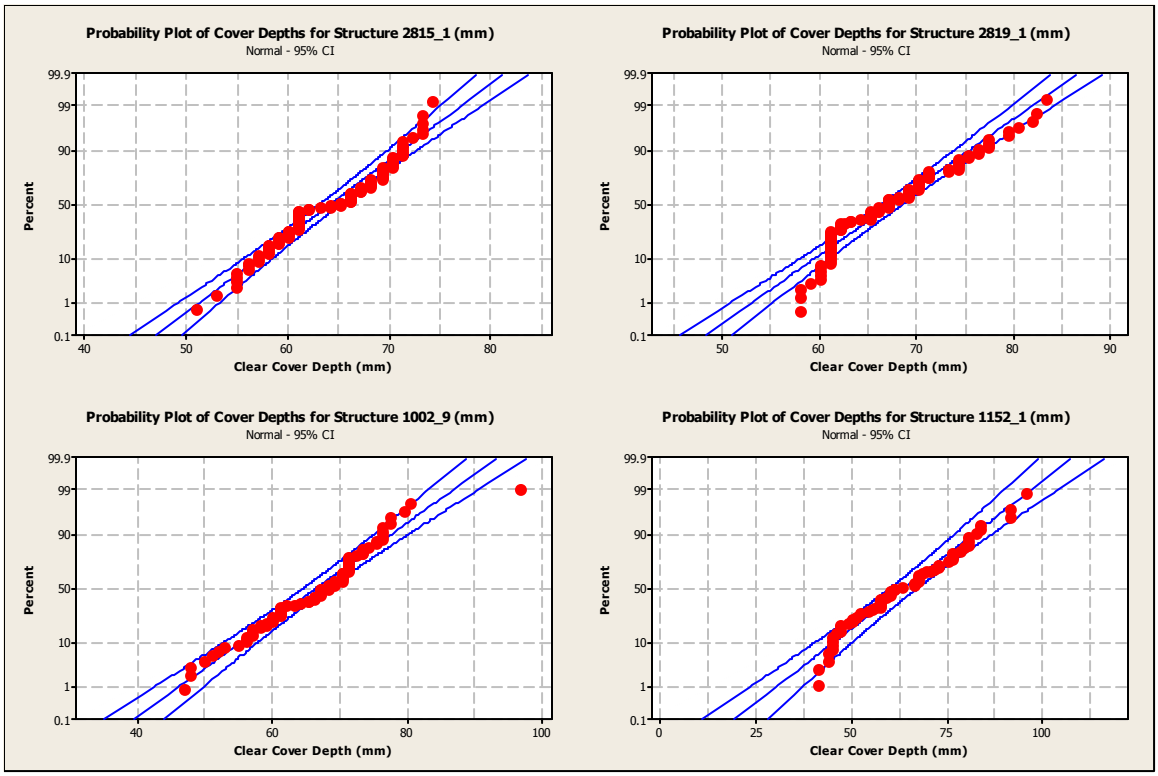

Figure 28 Cover Depth Distributions for Structures 2815_1, 2819-1, 1002_9 and 1152_1

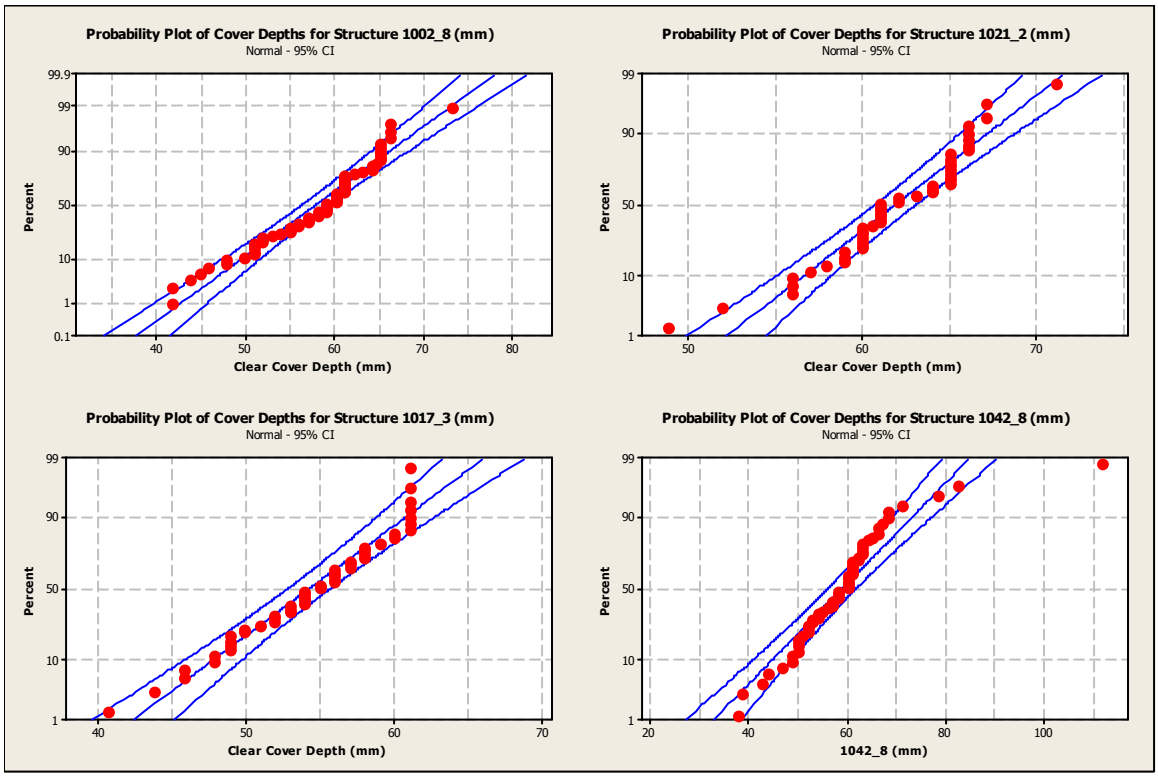

Figure 29 Cover Depth Distributions for Structures 1002_8, 1021_2, 1017_3 and 1042_8

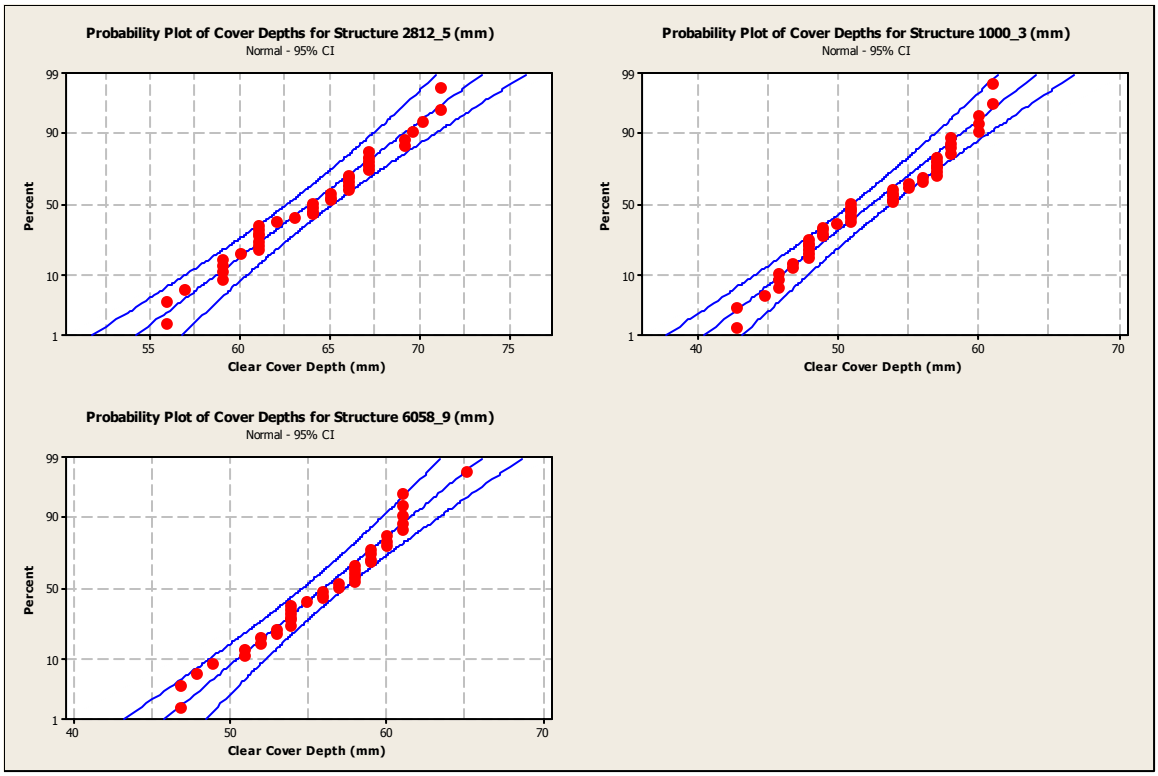

Figure 30 Cover Depth Distributions for Structures 2812_5, 1000_3 and 6058_9

Resistivity Measurements

The resistivity measurements are summarized in Table 22. The mean values ranged from as high as 298 kΩ-cm to as low as 29.6 kΩ-cm and the median values ranged from 299 kΩ-cm to 30.2 kΩ-cm. The coefficient of variation ranged from 8.60% to 38.5%. Due to the unforeseen appearance of inclement weather or short structure length, several structures yielded less than twelve test locations as follows: seven locations were tested on structure 1152_1, and eight locations were tested on structures 1021_2, 1017_3, 1042_8, and 1000_3.

Table 22 Resistivities for Structures with a Specified Maximum W/CM Ratio of 0.45

Bridge Number_District	Number of Observations	Resistivity Mean/Bridge(kΩ-cm)	Resistivity Median/Bridge (kΩ-cm)	Coefficient of Variation
2815_1	12	298	299	16.8
2819_1	12	135	131	19.1
1002_9	12	50.8	48.8	38.1
1152_1	7	149	146	7.26
1002_8	12	103	89.9	38.5
1021_2	8	152	152	10.9
1017_3	8	139	140	8.60
1042_8	8	29.6	30.2	17.1
2812_5	12	37.9	36.6	16.3
1000_3	8	163	157	9.97
6058_9	12	53.9	54.9	20.1

As demonstrated for subsets 1 and 2, the resistivity data in this particular subset has a lognormal distribution as well. The distribution of the resistivity data is presented in Figures 31 through 33. With two exceptions: structures 2815_1 and 1042_8, the individual probability plots presented in Figures 31 through 33 demonstrate that the resistivity measurements for subset 3 also have a general lognormal distribution.

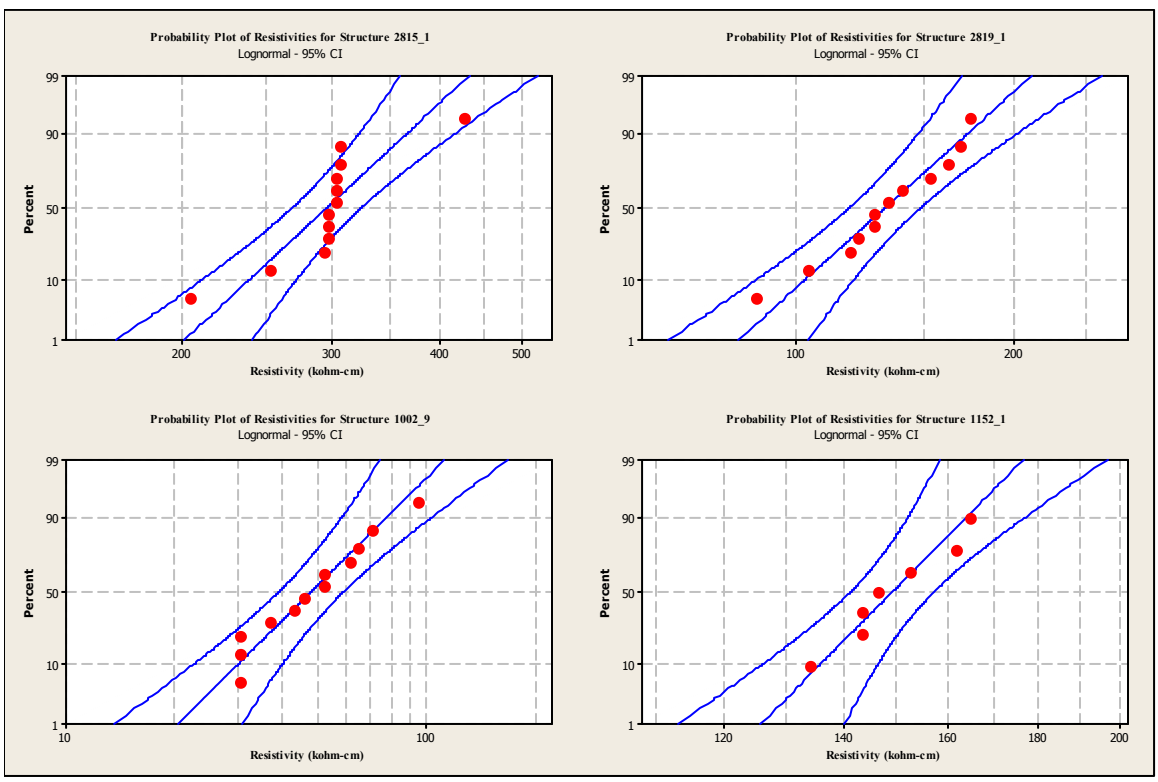

Figure 31 Resistivity Distributions for Structures 2815_1, 2819_1, 1002_9 and 1152_1

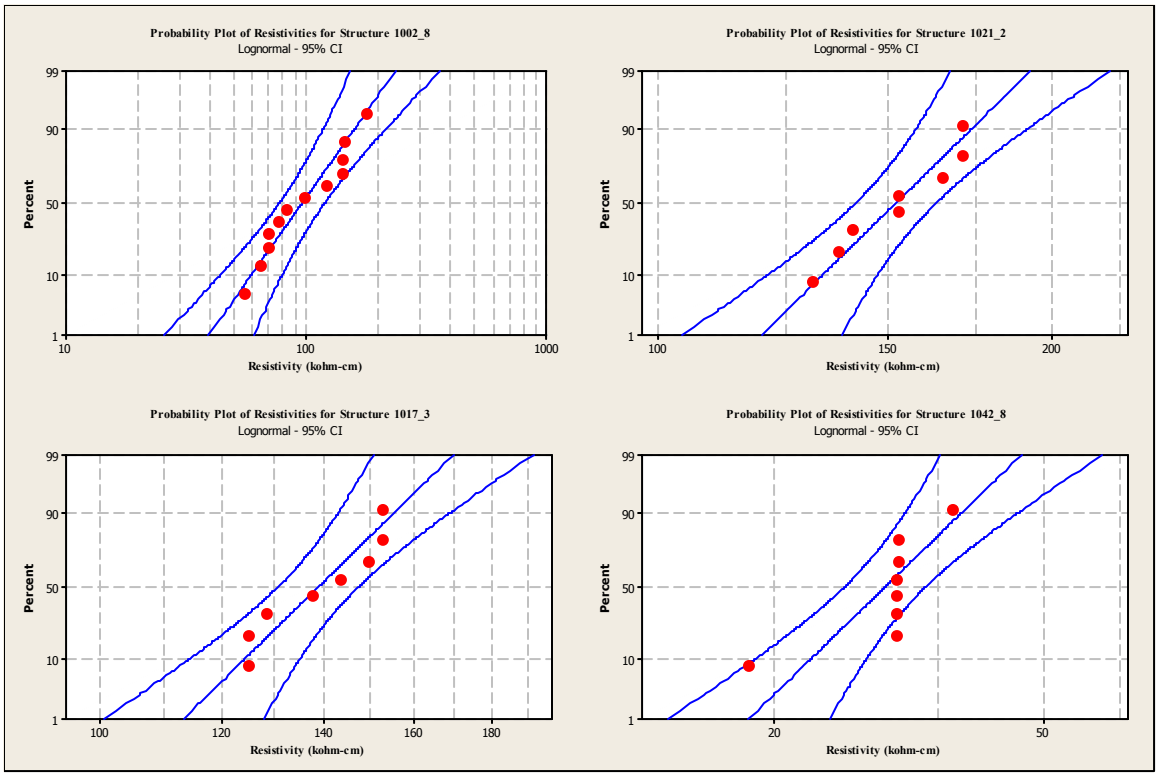

Figure 32 Resistivity Distributions for Structures 1002_8, 1021_2, 1017_3 and 1042_8

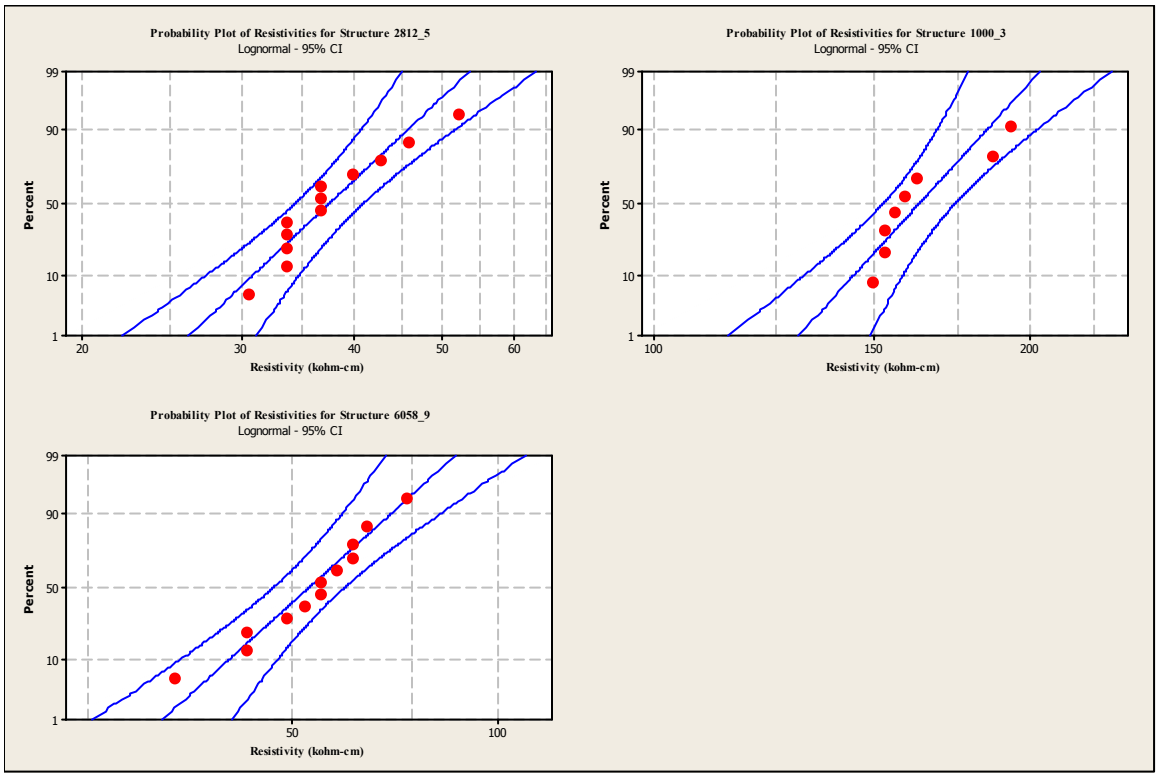

Figure 33 Resistivity Distributions for Structures 2812_5, 1000_3 and 6058_9

Linear Polarization

As with the structures in subsets 1 and 2, since the corrosion current density measurements were collected at specific and not random locations, probability plots would not yield an accurate picture of the actual data distribution. Six corrosion current density tests were performed on each structure based on the corrosion potential values obtained. The actual values collected at each individual location along with the respective resistivity, corrosion potentials and clear cover depth measurements collected at the same locations are presented for each structure in Table 23.

Table 23 Corrosion Current Densities for Structures with a Specified Maximum W/CM Ratio of 0.45

Bridge Number	Resistivity Median (kΩ-cm)	Corrosion Potentials (-mV)	Corrosion Current Density (μA/cm^2)	Clear Cover Depths (mm)
1152_1	163	245	0.518	91
	131	107	7.923	45
	166	328	2.201	59
	134	356	0.829	71
	*	*	*	72
	*	*	*	49
2815_1	306	290	2.445	59
	310	149	2.061	62
	163	318	8.917	61
	252	222	4.432	61
	351	394	4.247	70
	316	313	2.806	69
1021_2	217	285	0.642	66
	137	328	0.580	58
	169	312	0.414	61
	134	277	0.404	49
2819_1	128	168	8.328	83
	140	169	11.76	67
	176	188	9.084	61
	92.6	235	8.803	63
	92.6	202	9.912	59
	150	240	5.261	61
1000_3	169	319	2.341	46
	166	237	2.050	47
	137	255	2.186	59
	188	283	2.331	51
1017_3	134	313	0.736	59
	150	277	0.705	52
	137	230	0.725	49
	121	242	0.911	54

Table 23 (continued) Corrosion Current Densities for Structures with a Specified Maximum W/CM Ratio of 0.45

Bridge Number	Resistivity Median (kΩ-cm)	Corrosion Potentials (-mV)	Corrosion Current Density (μA/cm^2)	Clear Cover Depths (mm)
2812_5	35.1	222	6.867	66
	25.5	243	8.607	67
	44.7	190	6.939	69
	31.9	262	6.981	64
	31.9	198	4.163	66
	60.7	290	3.138	61
1002_8	89.4	334	4.992	61
	70.2	310	3.261	55
	70.2	256	3.616	49
	76.6	320	4.909	61
	73.4	258	3.315	61
	51.1	318	4.619	65
1042_8	31.6	697	2.779	49
	31.9	370	5.092	59
	38.3	393	6.076	49
1002_9	51.1	157	1.667	59
	31.9	161	2.009	69
	28.7	256	4.536	48
	35.1	308	4.609	61
	115	282	4.754	80
	57.5	265	3.635	71
6058_9	35.1	278	0.891	58
	54.3	200	0.964	57
	60.7	255	1.212	54
	76.6	206	0.932	56
	47.9	266	0.964	59
	38.3	264	0.901	59

Chloride Exposure

The chloride exposure data was calculated as described in the previous sections and is summarized in Table 24. The chloride exposure as calculated per environmental zone ranged from 688 kg/lane-km, while the chloride exposure calculated per structure based on the Annual Average Daily Traffic (AADT) ranged from $963*10^4$ AADT*kg/lane-km to $271*10^6$ AADT*kg/lane-km.

Table 24 Chloride Exposure for Structures with a Specified Maximum W/CM Ratio of 0.45

Bridge Number_District	Cl^- Exposure (kg/lane-km)	Cl^- Exposure (AADT*kg/lane-km)
2815_1	688	$172*10^5$
2819_1	688	$963*10^3$
1002_9	4369	$271*10^6$
1152_1	688	$103*10^5$
1002_8	671	$671*10^4$
1021_2	220	$572*10^4$
1017_3	220	$211*10^4$
1042_8	671	$255*10^4$
2812_5	225	$271*10^4$
1000_3	220	$196*10^4$
6058_9	4369	$218*10^6$

Corrosion Potentials

The corrosion potential measurements for subset 3 were also collected on bridge decks reinforced with epoxy coated steel, as was subset 2. Figures 34 through 36 show that the corrosion potential data for individual structures are also generally normally distributed.

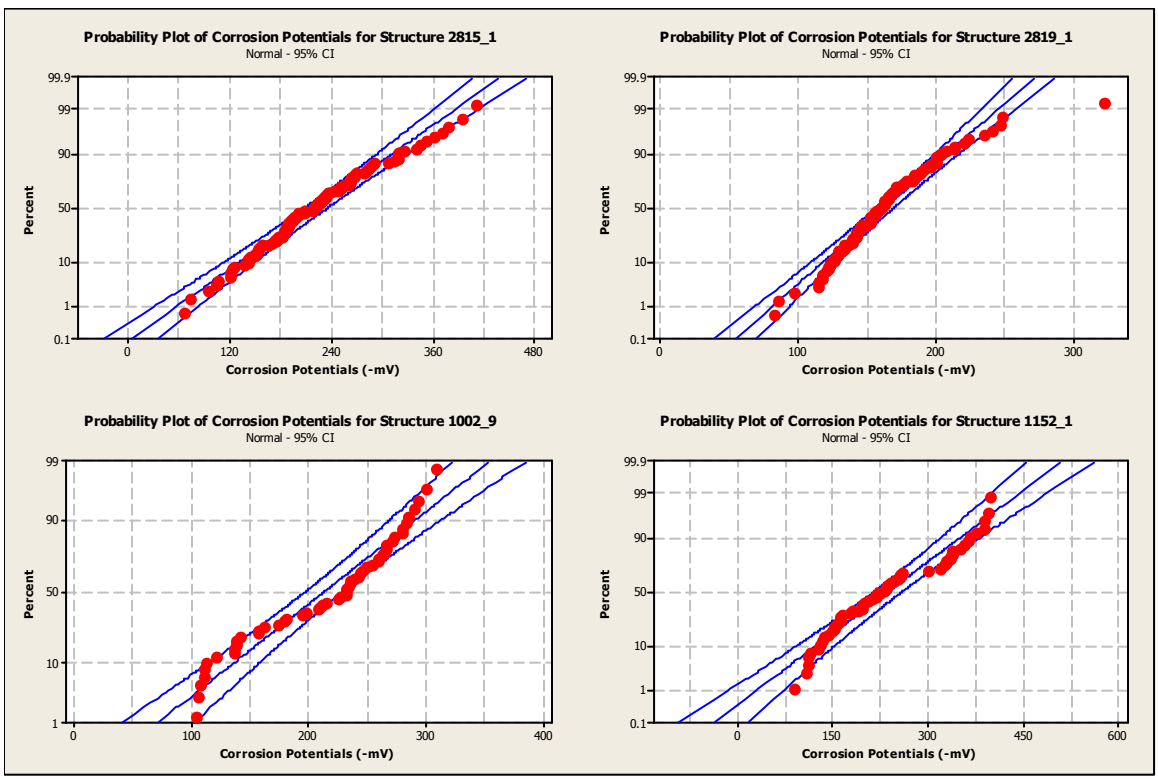

Figure 34 Corrosion Potential Distribution for Structures 2815_1, 2819_1, 1002_9 and 1152_1

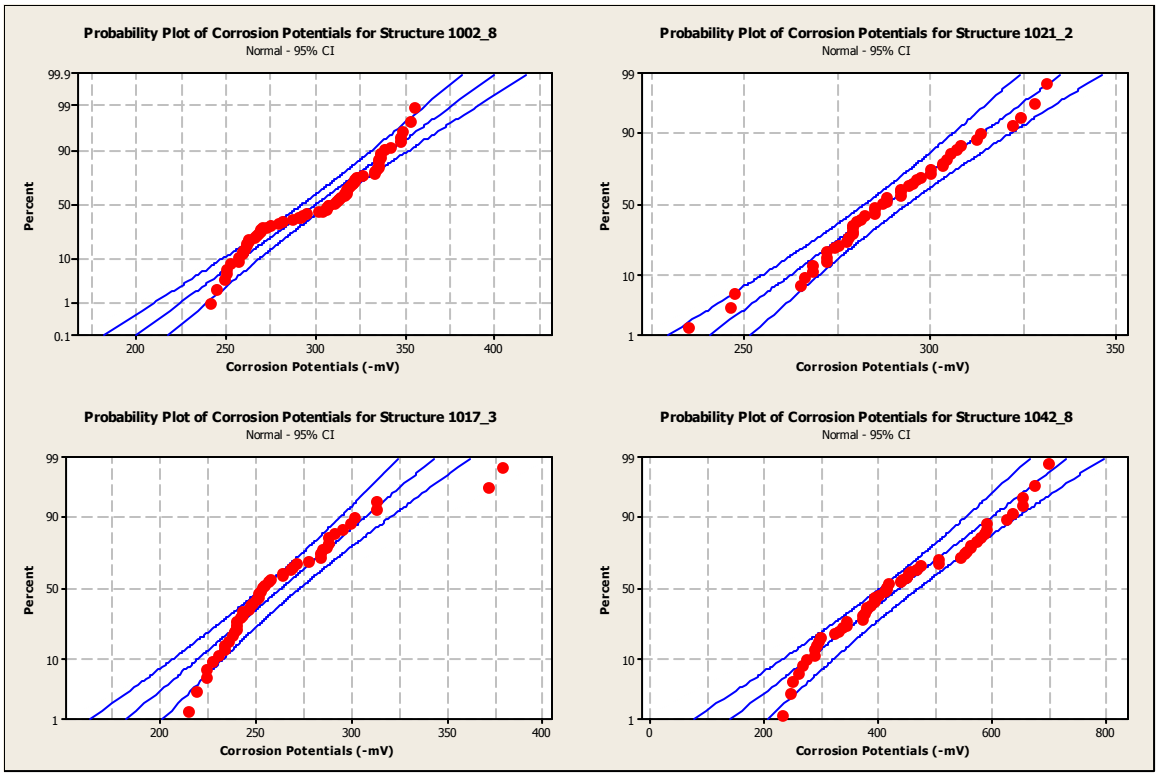

Figure 35 Corrosion Potential Distribution for Structures 1002_8, 1021_2, 1017_3 and 1042_8

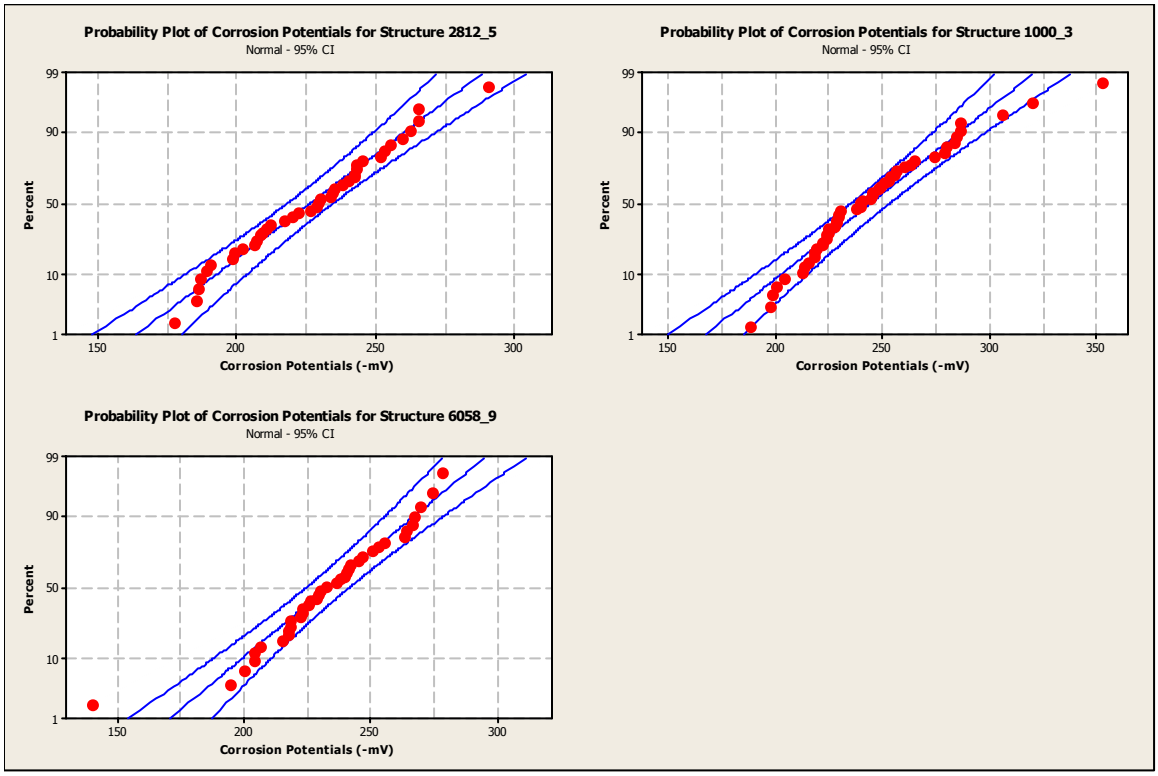

Figure 36 Corrosion Potential Distribution for Structures 2812_5,1000_3 and 6058_9

The corrosion potential data is summarized in Table 25. The number of measurements ranged from 27 to 112. The standard deviation ranged in value from -126.3 mV to -26.62 mV. Table 25 also summarizes the percent of measurements above -200 mV, between -200 and -350 mV, and below -350 mV. The percentage of measurements greater than -200mV collected from the structures ranged from 0% to 90%. Six structures yielded corrosion potential measurements more negative than -350mV. The cumulative corrosion potential measurements of these structures ranged from 2% to 73%. However, it is important to note that these values were not well distributed from 2% to 73%, but instead five structures had values between 2% and 13%, while only one structure had cumulative corrosion potential measurements of 73%.

Other Data

The remaining structural as well as environmental data, which consisted of structure type (simply supported or continuous), beam material (steel or concrete), traffic volume presented as AADT and AADTT, age, NBIS deck rating and girder spacing are presented in Table 26.

Table 25 Half-cell Potentials for Structures with a Specified Maximum W/CM Ratio of 0.45

Bridge Number_District	Number of Observations	Potentials (Cumulative % >=-200mV)	Potentials (% between 200 and 350)	Potentials (Cumulative % <=-350mV)	Potentials Mean/Bridge (-mV)	Standard Deviation
2815_1	103	48	48	5	219.9	70.1
2819_1	114	90	10	0	161.7	35.05
1002_9	54	37	63	0	212	60.47
1152_1	60	42	45	13	233.5	88.35
1002_8	70	0	97	3	299.2	32.34
1021_2	48	0	100	0	288.5	20.29
1017_3	48	0	96	4	262.7	34.41
1042_8	55	0	27	73	434.3	126.3
2812_5	40	20	80	0	225.8	26.62
1000_3	50	8	90	2	243.5	32.72
6058_9	38	3	97	0	232.6	26.66

Table 26 Physical Parameters for Structures with a Specified Maximum W/CM Ratio of 0.45

Bridge Number_District	Beam Material	Superstructure Design	Girder Spacing	NBIS Deck Rating	AADT	AADTT	Age
	Steel/Concrete	Simple/Continuous	mm (in)				Years
2815_1	Steel	Simple	2616 (103)	6	25000	7500	18
2819_1	Steel	Continuous	2438 (96)	6	1400	28	18
1002_9	Steel	Simple	3581 (141)	7	62000	1240	17
1152_1	Concrete	Simple	1168 (46)	6	15000	1050	17
1002_8	Steel	Continuous	1981 (78)	6	10000	500	16
1021_3	Concrete	Simple	1473 (58)		26000	4420	15
1017_3	Steel	Simple	2896 (114)	7	9600	384	14
1042_8	Concrete	Simple	2210 (87)	7	3800	304	14
2812_5	Steel	Continuous	2438 (96)	7	12000	480	13
1000_3	Steel	Simple	2972 (117)	7	8900	356	13
6058_9	Steel	Continuous	3404 (134)	7	50000	1500	13

Variability of Non-destructive Measurements

To address the issue of whether the non-destructive tests may be applied to determine how the general quality of construction has changed over a period of three decades and several changes in construction specifications, resistivity and clear cover depths are presented in Figures 37 through 40. Percentage values for each test were calculated based on generally accepted interpretation guidelines as they applied to each subset.

Specifically, for clear cover depth VDOT increased the specified minimum clear cover depth from 43mm (1.69 in) specified during the 1969 to 1972 construction era to 63mm (2.5 in) minus zero, plus 13mm (0.5 in) for the construction periods between 1972 to present (2004). In addition to the VDOT specifications, the data collected from the three bridge deck subsets (i.e. the two construction eras mentioned previously) were also compared to AASHTO specified minimum of 50.8mm (2.0 in).

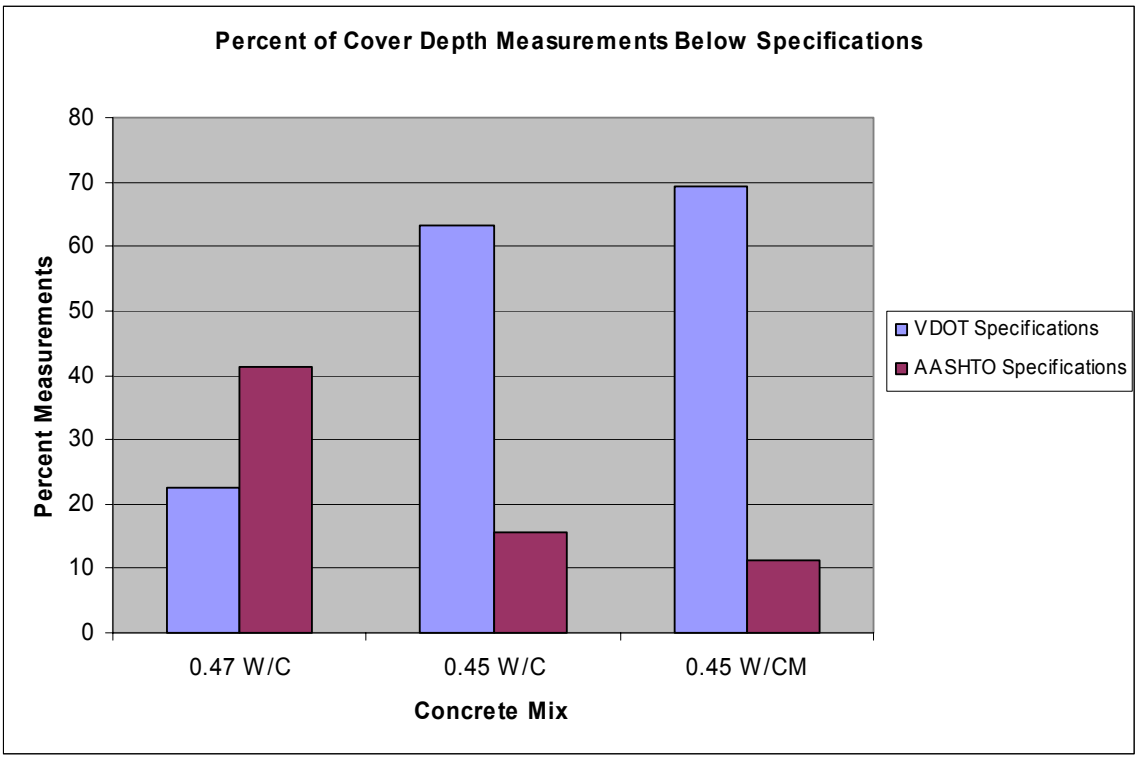

Figure 37 Percent of Cover Depth Measurements Less than Specifications Particular to Each Construction Era

There are no generally agreed upon interpretation guidelines or standards for resistivity measurements; however, some interpretation guidelines have been recommended. Of those, the three guidelines considered for this study have been recommended by Bungey, Feliu and Manning, see Figures 38, 39, and 40, respectively.

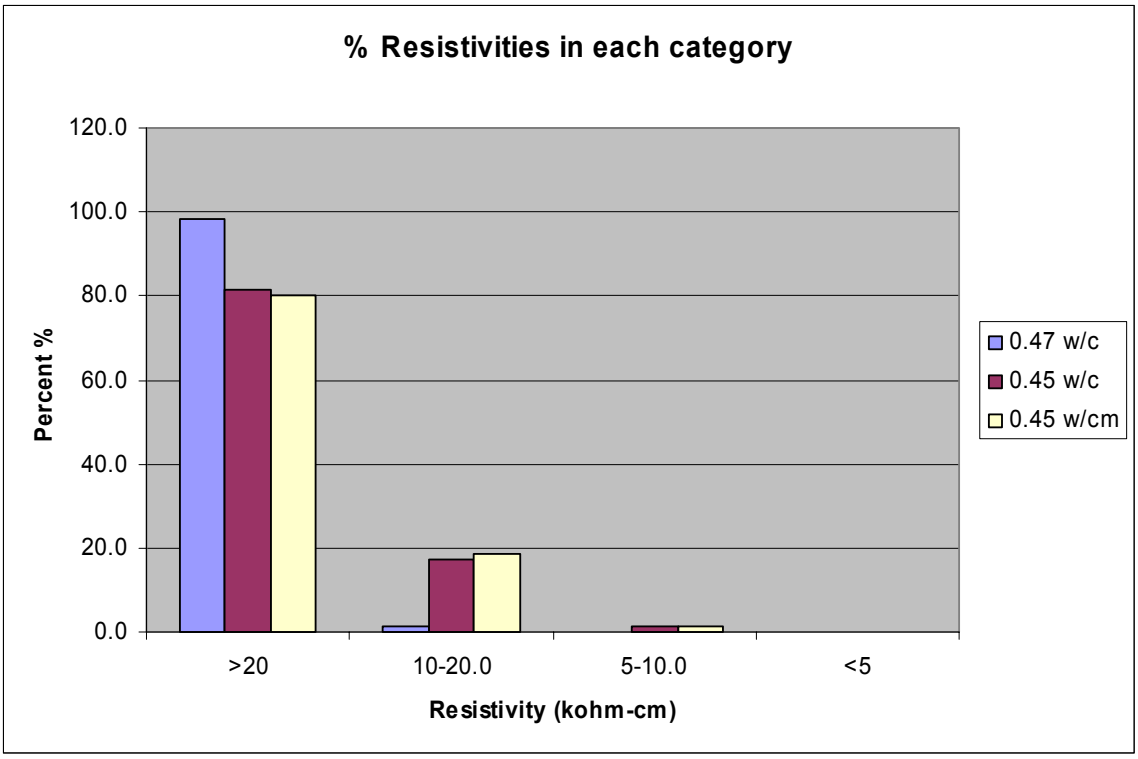

Figure 38 Comparison of Resistivities Using the Guidelines Recommended by Bungey, J.H.

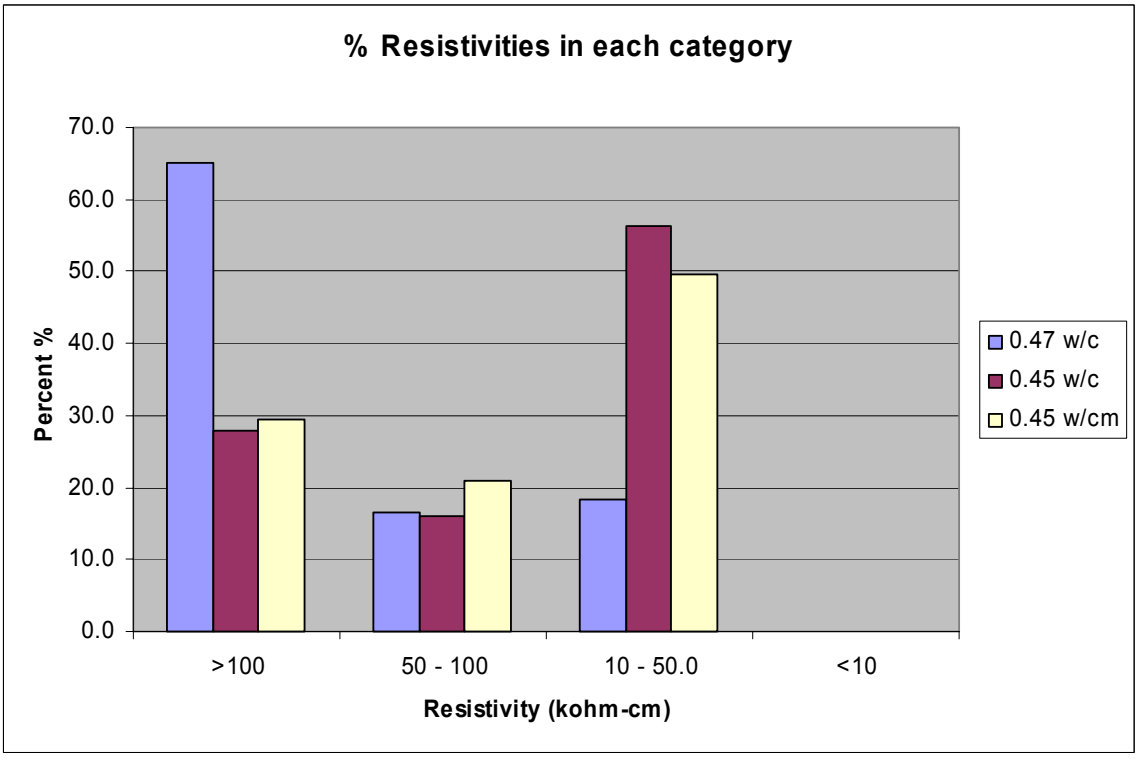

Figure 39 Comparison of Resistivities Using the Guidelines Recommended By Feliu et al.

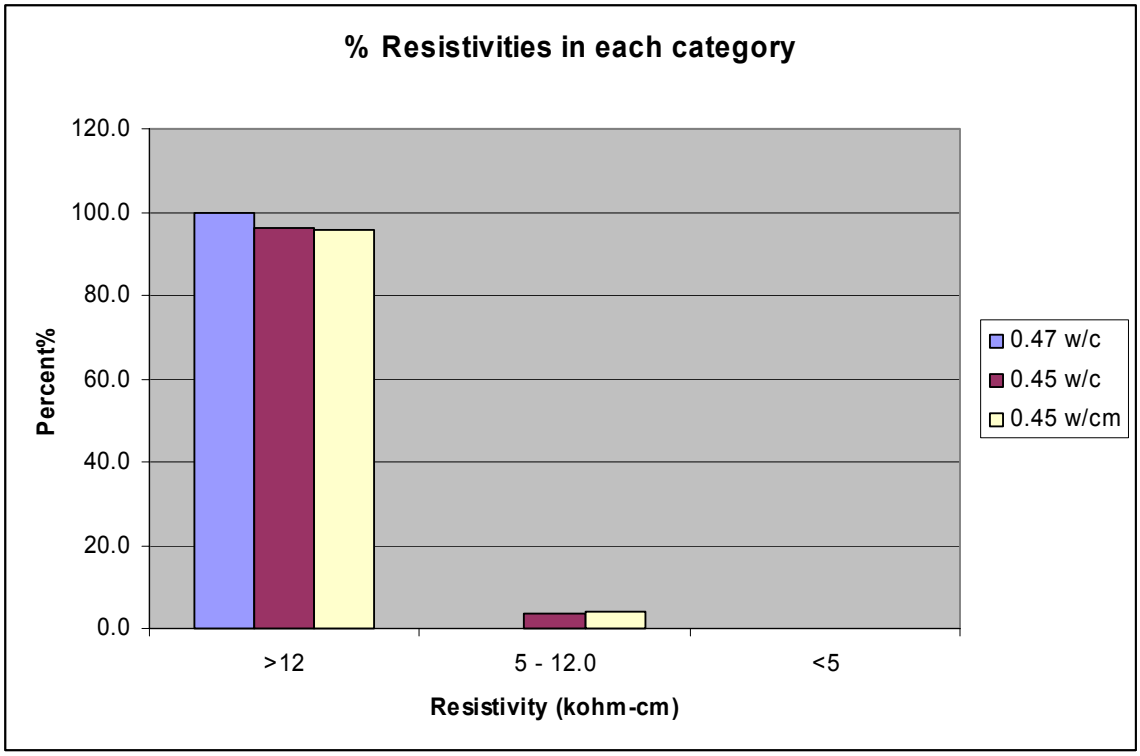

Figure 40 Comparison of Resistivities Using the Guidelines Recommended By Manning, D.G.

The trend that is immediately visible is that the bridge decks with the higher w/c ratio (i.e. older decks) consistently have higher resistivity values. Since the resistivity of concrete is a general measure of the moisture content, as well as the size, continuity and tortuosity of the pore system within the cement paste (Revie, R.W., 2000), Figures 38 through 40 would indicate that the older decks with a higher w/c ratio have a lower permeability than the newer decks with lower w/c or w/cm ratios. Also, there appears to be no significant difference between the resistivity values collected on structures in subsets 2 and 3 (i.e. subsets built with concrete having w/c 0.45 and w/cm 0.45, respectively).

ANALYSIS AND DISCUSSION

To complete the primary objective of this study it was necessary to condense the non-destructive test measurements to one value per structure, whereas the number of measurements used to complete the secondary objectives was controlled by the non-destructive test with the least number of data points per structure (i.e. corrosion current density measurements). Therefore the secondary objective draws from a significantly larger pool of data. The sample population was divided into two subsets necessary to compare the effects of epoxy coating as well as the change in the concrete mixture on nondestructive measurements such as resistivity, half-cell potentials and linear polarization. Since there is a very large amount of raw data, it was necessary to abbreviate the data presented in this chapter. The raw field data is available for review in the Appendix.

NBIS Deck Rating Influencing Factors

The statistical analysis was performed to identify which of the environmental, structural and NDT factors are related to the NBIS deck rating. The parameters considered in the statistical analysis were as follows:

Non-destructive Testing Parameters:

1. Concrete resistivity
2. Corrosion potentials
3. Clear cover depth

Environmental Exposure Parameters:

1. Cars AADT
2. Trucks AADT
3. Total AADT
4. Chloride exposure by environmental zone
5. Chloride exposure by traffic volume
6. Age

Structural Parameters:

1. Girder type
2. Girder design
3. Girder spacing
4. Concrete mixture
5. Reinforcement type
6. Cracking severity

To examine how these parameters relate to the NBIS rating, correlation tests were performed on single point values calculated for each structure. More specifically, a median value was calculated using the 12 resistivity data points, the six corrosion current

density data points and the various number of corrosion potential data points. The correlation p-values, which were obtained using Minitab software, are presented in Table 27. The selection was based on a 90% or higher probability that a relationship exists (i.e. a p-value ≤ 0.1).

Table 27 NBIS Deck Rating Prediction Factors

Response	Predictor	P-Value
NBIS Deck Rating	Resistivity	0.008
	Corrosion Potentials	0.068
	Age	0.012
	Cl^- Exposure/Environmental Zone	0.046
	AADT Cars	0.000

Since the NBIS deck rating is a discrete value, to evaluate which one of the remaining predictors in Table 27 is the most influential, a classification tree was built using S-Plus statistical software, see Figure 41.

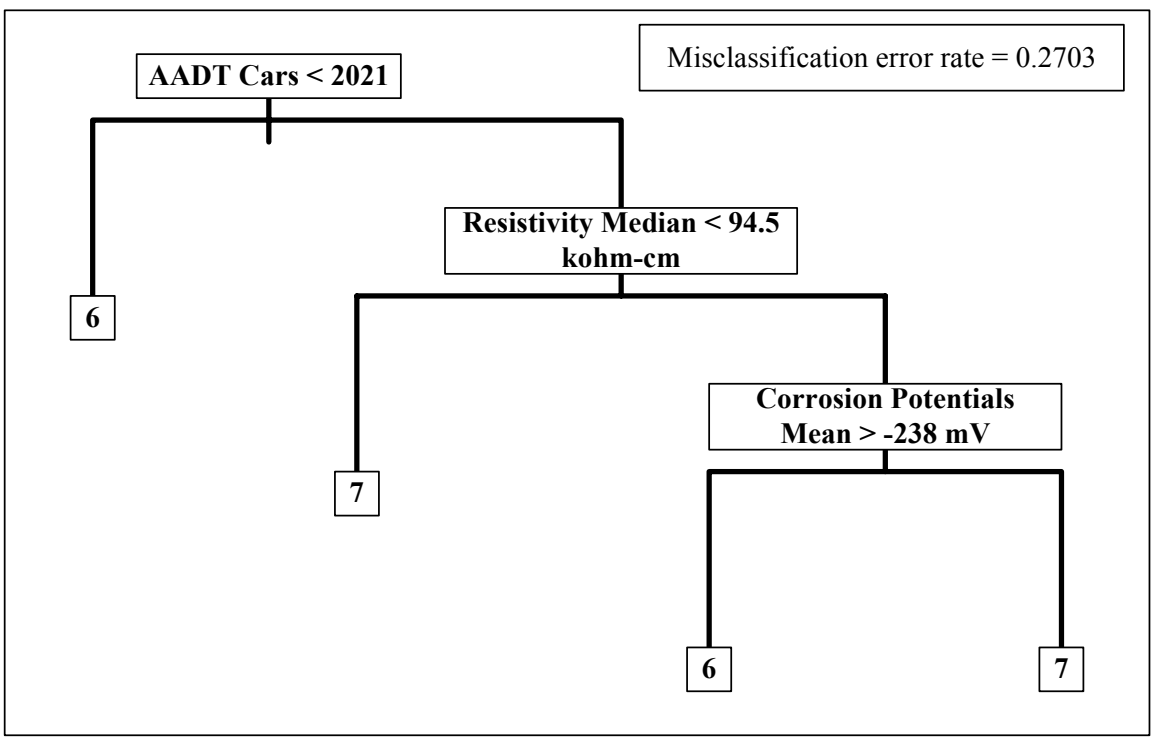

Figure 41 Deck Rating Classification Tree Using Table 27 Predictors

As illustrated in Figure 41, the principal deciding factor is the Annual Average Daily Car Traffic (AADCT), followed by resistivity and corrosion potentials mean. Therefore, according to the classification tree, any structure with an AADCT less than 2021 vehicles receive an NBIS rating of 6. An interpretation could be low volume routes with AADCT values less than 2021, which include most non-US routes as well as secondary routes, may receive lower ratings based on factors outside the NBIS guidelines, which refers

only to visible damage such as cracks, spalls and other defects (Hartle, R.A. et al 1995). Based on our survey results for the structures with AADCT less than 2021 which have a NBIS rating of 6, none of the structures have any visible spalls or delaminations. Furthermore, the measured visible cracking in linear meters of cracking per surveyed area (m/m^2) is not consistent, ranging in value from 0.281 m/m^2 to 0.766 m/m^2 for structures having received an NBIS rating of 6, while structures that received a rating of 7 may exhibit far more cracking, an order of magnitude greater in some cases. Decks with resistivities less than 94.5 kΩ-cm receive an NBIS rating of 7. This could be explained by the fact that the newer structures that were part of this study have lower resistivities that the older structures. This claim is also supported by bar charts in Figures 38 through 40. Finally, based on the classification tree in Figure 41, structures where the average measured corrosion potential is more negative, or the absolute value is greater than 238 mV; receive an NBIS rating of 6. If the results are interpreted according to the ASTM C 876-91 guidelines, then structures where the average measured corrosion potential is less negative than -200 mV have a 90% probability of no active corrosion taking place and consequently less visible damage. The overall correct classification rate for the classification tree in Figure 41 is 73%.

Since resistivity and corrosion potentials are not in the regular inspection program; these two parameters appear as NBIS deck rating predictors because they are strongly correlated to concrete deck cracking, which is the primary NBIS prediction factor in Figure 42. As part of this study, a correlation p-value of 0.034 was obtained between resistivity and cracking frequency, and a correlation p-value of 0.004 was obtained between resistivity and corrosion potentials. Both these correlation p-values, shown in Table 28, indicate the strong possibility that a relationship exists between these parameters and that resistivity may affect the ultimate level of cracking present.

Table 28 Resistivity Correlation p-values

Correlation Parameters		**P-Value**
Resistivity	Cracking Frequency	0.034
Resistivity	Corrosion Potentials	0.004

A second classification tree was created for the NBIS deck rating using all predictor parameters previously listed at the beginning of this section. The predictor parameters used included single point values of the non-destructive tests, environmental exposure parameters and structural parameters regardless of whether a potential relationship was previously detected in the Minitab analysis.

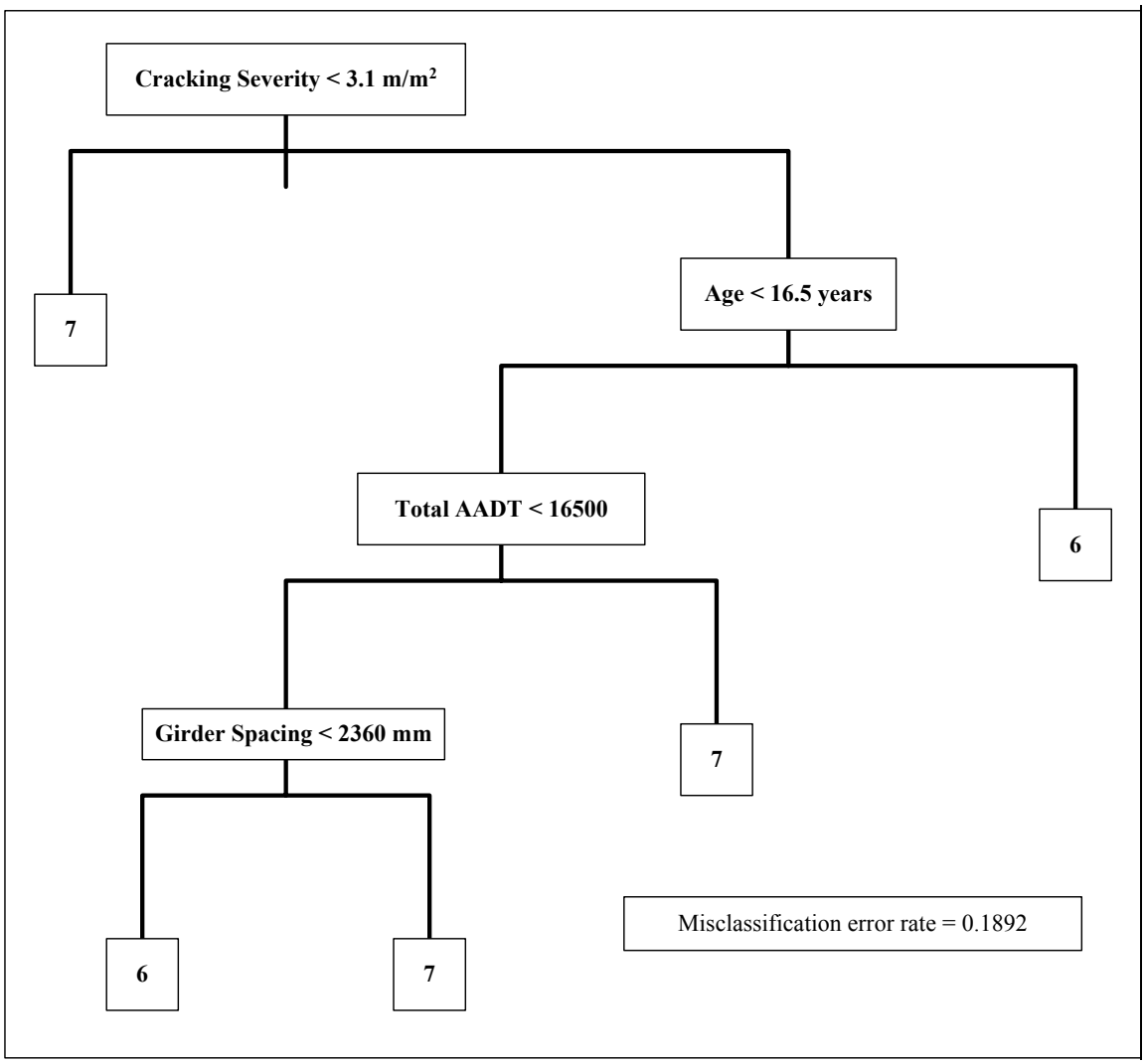

Figure 42 Deck Rating Regression Tree Using All Predictor Parameters

As illustrated by the second classification tree, Figure 42, the principal deciding factor is the amount of cracking shown at the top of the classification tree, followed by age, Annual Average Daily Traffic and girder spacing. The analysis supports the assertion that visible damage – in this case cracking – is the controlling parameter with respect to the NBIS deck rating. This is immediately followed by age, with structures older than 16.5 years at the time of inspection receiving a rating of 6. The next deciding factor is the total Annual Average Daily Traffic, with structures having an AADT value greater than 16500 receiving an NBIS rating value of 7. This can be explained by the fact that by and large, the structures carrying a higher traffic volume are also newer and therefore may exhibit less visible damage. Lastly, structures with a girder spacing of less than 2360 mm receive a rating of 6, while structures with girder spacing larger than 2360 mm receive a rating of 7. This may be tied into the previous statement, where structures with larger girder spacing carry larger traffic volumes, but are also generally newer and therefore exhibit less visible damage. Another possible explanation may be that structures with higher traffic volumes receive less attention during the inspection process due to safety concerns; however, this aspect was not specifically investigated in this

project. As an example, this model is used to determine the predicted NBIS deck rating value for a structure built in 1989. Start at the top node. The measured cracking severity is greater than the cutoff value of 3.1 m/m^2, so the right branch is followed. The age of the structure is less than 16.5 years, so the left branch is followed. The inspector would continue moving down the tree until he/she arrives at a terminal node that gives the predicted value. The correct classification rate for the tree in Figure 42 is 81%.

Applicability of Non-Destructive Corrosion Measurements to Epoxy Coated Steel

Bridge Decks Constructed Between 1968 and 1971 with Bare Bar and Specified Maximum W/C Ratio of 0.47.

To determine if the non-destructive corrosion measurement methods of CSE half-cell potentials, linear polarization and resistivity are applicable to structures reinforced with ECR, a baseline was established using the bridge decks reinforced with bare steel.

As was shown in the Results section of this study, the CSE half-cell potentials were approximately normally distributed for all three subsets. The normal distribution of the corrosion potentials was expected for the structures in subset 1, since these structures are reinforced with bare steel (ASTM C 876-91). However, the fact that the corrosion potentials measured on the structures in subsets 2 and 3 were normally distributed as well may be an indicator that the epoxy coating is not as dielectric as previously thought (Geenen F.M., 1991). Since a closed circuit, or continuity, is required for the test to be applicable (ASTM C 876-91), the normal distribution of the measurements performed on structures reinforced with epoxy coated steel indicates that the epoxy coating does not provide the expected electron barrier (Geenen F.M., 1991 and Manning D.G., 1996).

The resistivity measurements exhibit approximate log-normal distributions as shown in the Results section. The large number of observations: 590, 855 and 650 resistivity measurements in subsets 1, 2 and 3 respectively, support the conclusion that the distribution of data is proper. Furthermore, based on Ohm's Law, which states:

$$E = IR \qquad \text{Equation 13}$$

Where: E = Electrical potential (mV)
I = Current (μA)
R = Resistivity (kΩ)

A linear relationship should exist between the three parameters, corrosion potential (E), corrosion current density (i_{corr}) as (I) and resistivity as (R) (Feliu, S. et al 1996). To examine these relationships, correlation tests were performed on paired data points. More specifically, the number of data points available for this analysis was controlled by the test with the least number of test locations per deck. In this case, therefore, the number of data points available for analysis was controlled by the corrosion current density values, of which there were no more than six per structure. The correlation

values obtained are presented in Table 29. Scatter diagrams of these relationships are presented in Figures 43 through 47.

Table 29 Correlation and Probability Parameters for Structures with a Specified Maximum W/C Ratio of 0.47

Correlation Parameters		R-Value	P-Value
Resistivity	Corrosion Current Density	-0.360	0.006
Resistivity	Corrosion Potentials	-0.133	0.329
Corrosion Potentials	Corrosion Current Density	0.527	0.000
E/R	Corrosion Current Density	0.680	0.000

As shown in Table 29, the potential values show a positive correlation R-value of 0.527 with a p-value of 0.000 with the corrosion current density values. Therefore, an increase of the half cell potential absolute value results in an increase in current linearly. Furthermore, a p-value of 0.006 indicates that a strong relationship exists between resistivity and corrosion current density values, although not necessarily a linear relationship. Referring to Ohm's Law, if we consider voltage to be a constant, then the current is inversely proportional to the resistivity, or:

$$I \approx \frac{1}{R} \qquad \text{Equation 14}$$

Based on the relationship illustrated by Equation 14, an R^2-value of 0.449 is obtained. The scatter plot of this relationship along with the regression line is illustrated in Figure 44. Andrade and Alonso support these results, although they caution that the scatter found invalidates the deduction of i_{corr} values from single resistivity ones (Andrade C et al, 1996). It's also important to note that Andrade and Alonso do not specify which linear polarization instrument was used, as there are two instruments commercially available, Gecor and 3LP. For this study, the 3LP device was used. The Gecor device, which was developed by Andrade, is different in that it "has a guard ring electrode which is used to confine the influence area of the counter electrode by actively confining the polarization current during the measurement process" (Liu, Y. 1996).

Under closer inspection, Figure 43 clearly shows that as resistivity decreases, corrosion current density increases. This relationship is supported by others. Previous studies have shown that the electrical resistance of concrete affects the ionic flow between the anode and the cathode, and therefore the rate at which corrosion can occur (Gowers, K.R. et al 1999). The relationship between corrosion potentials and resistivity shown in Figure 45 is not as well defined. Although no definite relationship may be inferred from the scatter plot, the general trend of the data indicates that as resistivity increases, the corrosion potential decreases. The scatter plot in Figure 46 illustrates the relationship between corrosion potentials and corrosion current density. Much better defined than the previously examined scatter plots, this scatter plot indicates that as corrosion potential increases, so does the corrosion current density. This relationship is supported by Ohm's Law discussed previously. If the concrete resistivity (R) is taken as a constant, then the remaining relationship between corrosion potential (E) and corrosion current density

(i_{corr}) is linear as shown in Figure 46. Lastly, the relationship between measured and calculated values of corrosion current density is examined in Figure 47. The calculated values were obtained using Ohm's Law, where R and E were the measured resistivity and corrosion potential values, respectively. As expected, the plot shows a linear relationship between the measured and calculated values. The scatter in this case, as well as the scatter in Figures 43, 44 and 45, is most likely due to the high variability of the resistivity measurements.

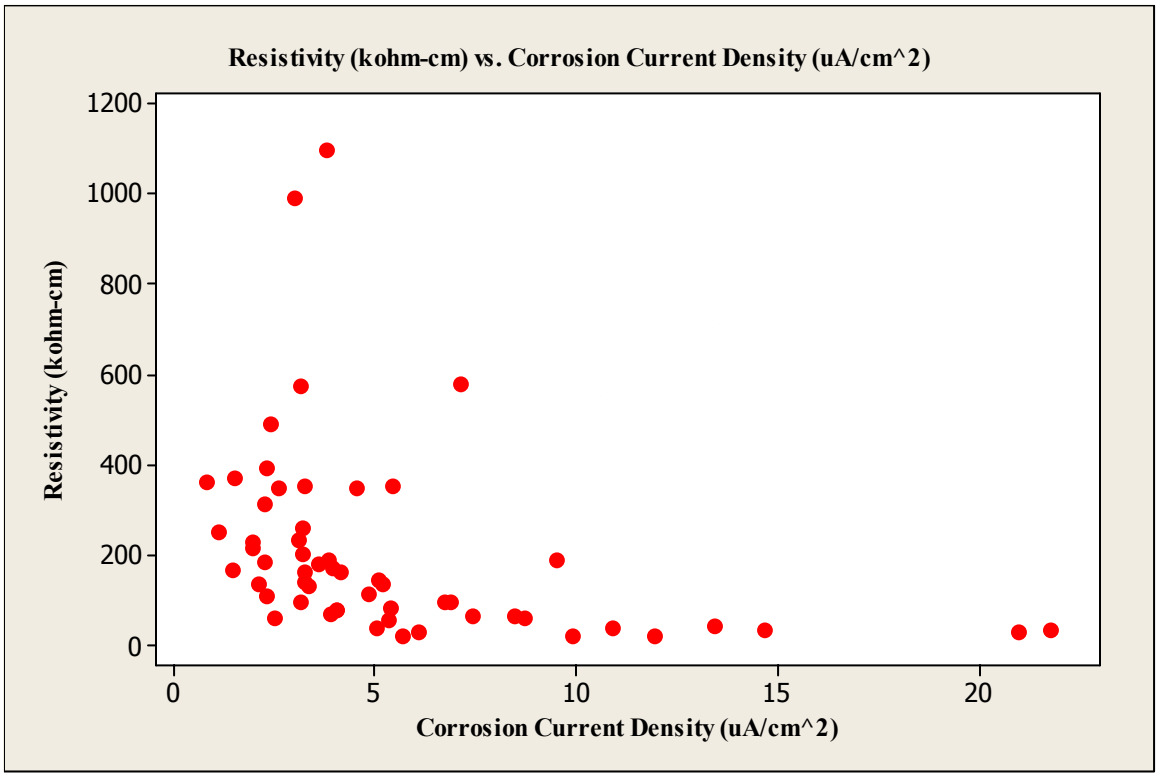

Figure 43 Resistivity versus Corrosion Current Density for Structures with a Specified Maximum W/C Ratio of 0.47

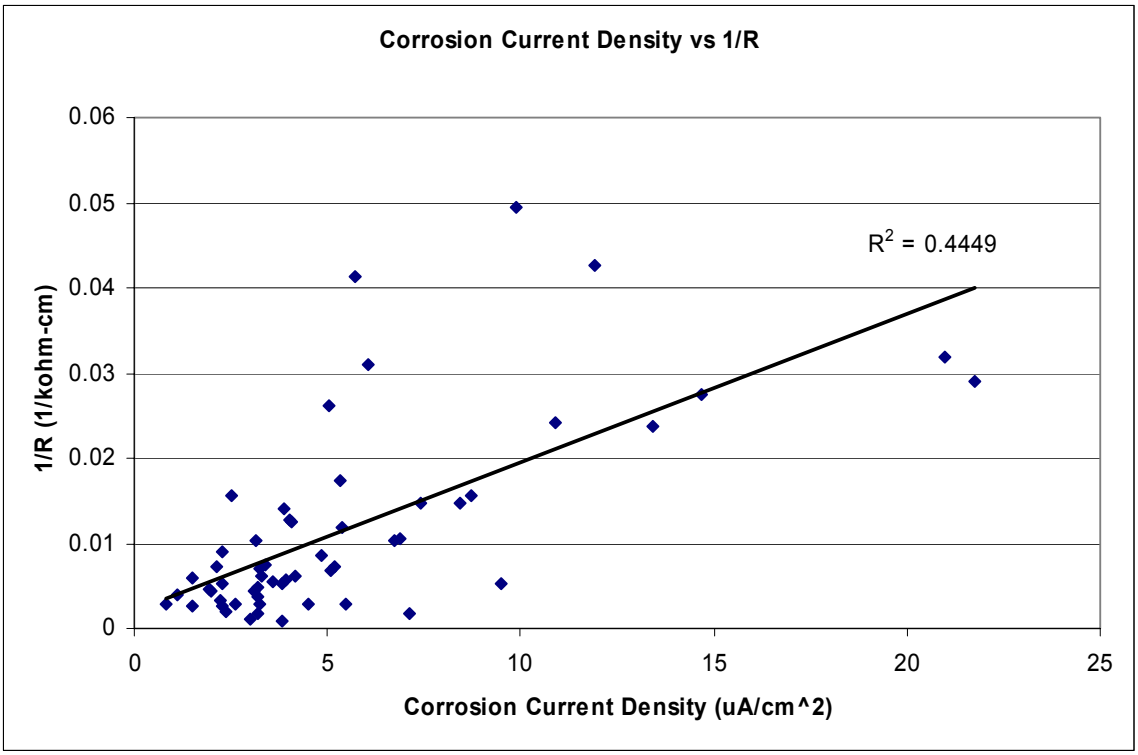

Figure 44 1/Resistivity versus Corrosion Current Density

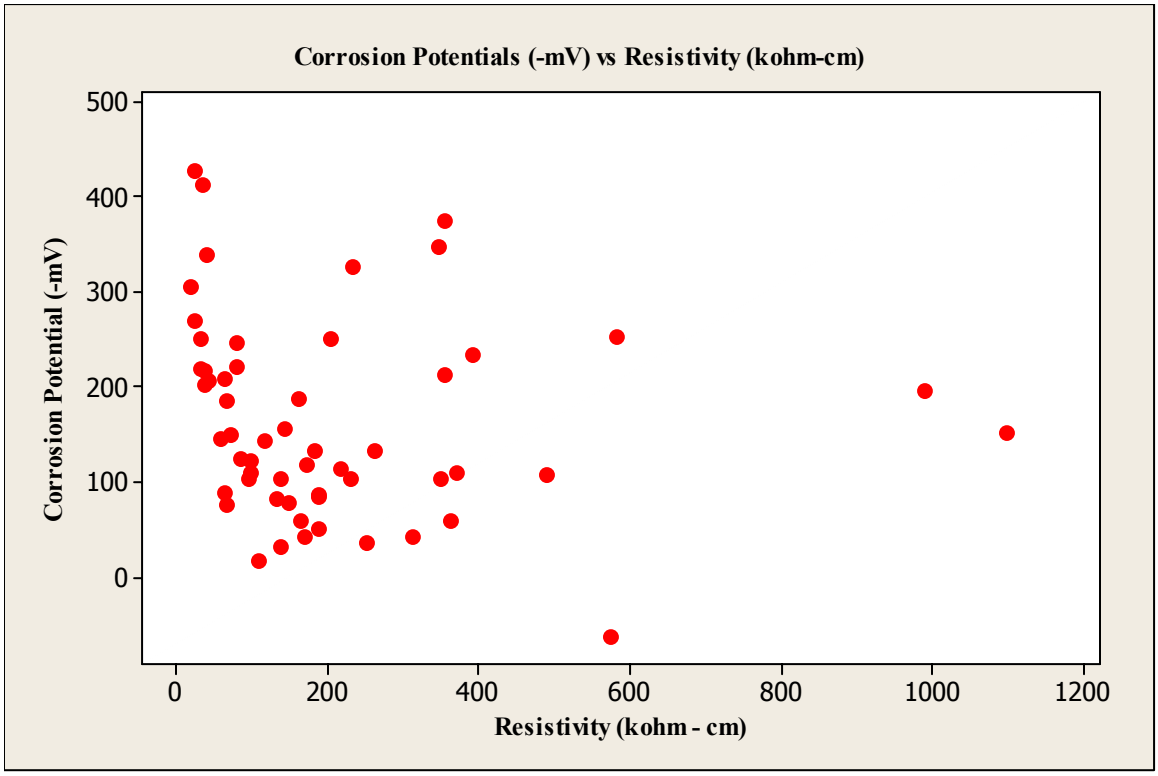

Figure 45 Corrosion Potentials versus Resistivity for Structures with a Specified Maximum W/C Ratio of 0.47

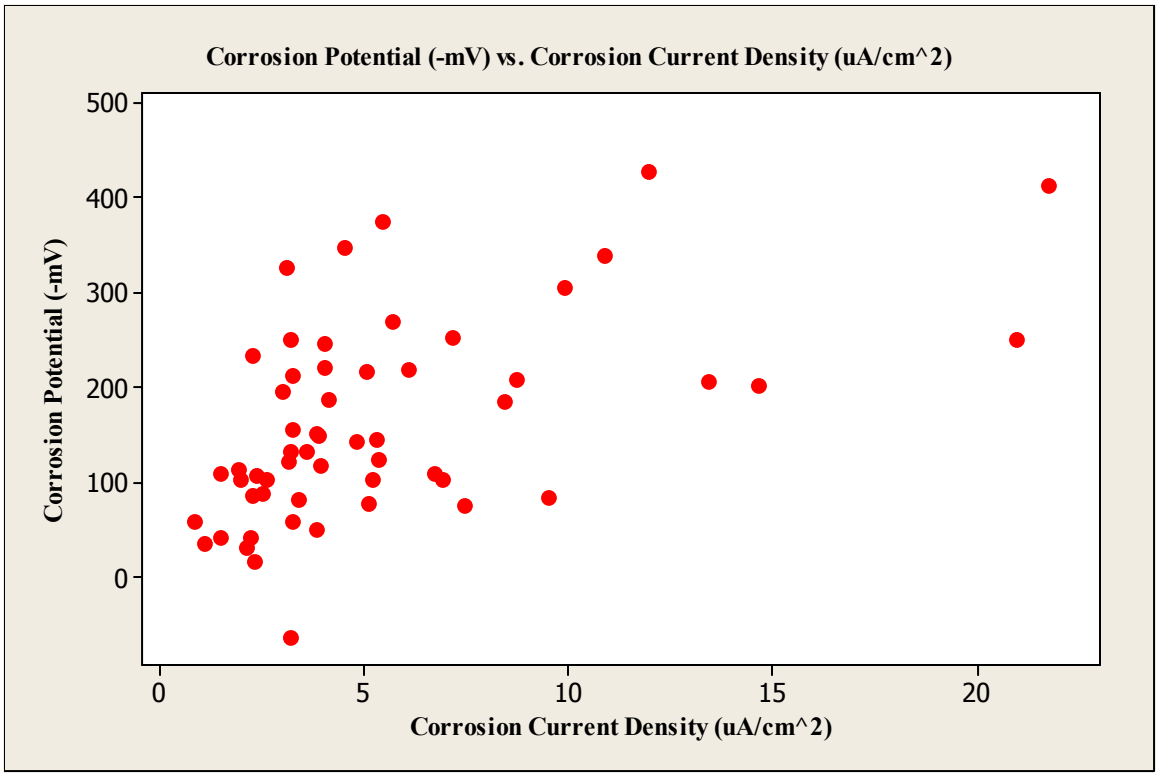

Figure 46 Corrosion Potentials versus Corrosion Current Density for Structures with a Specified Maximum W/C Ratio of 0.47

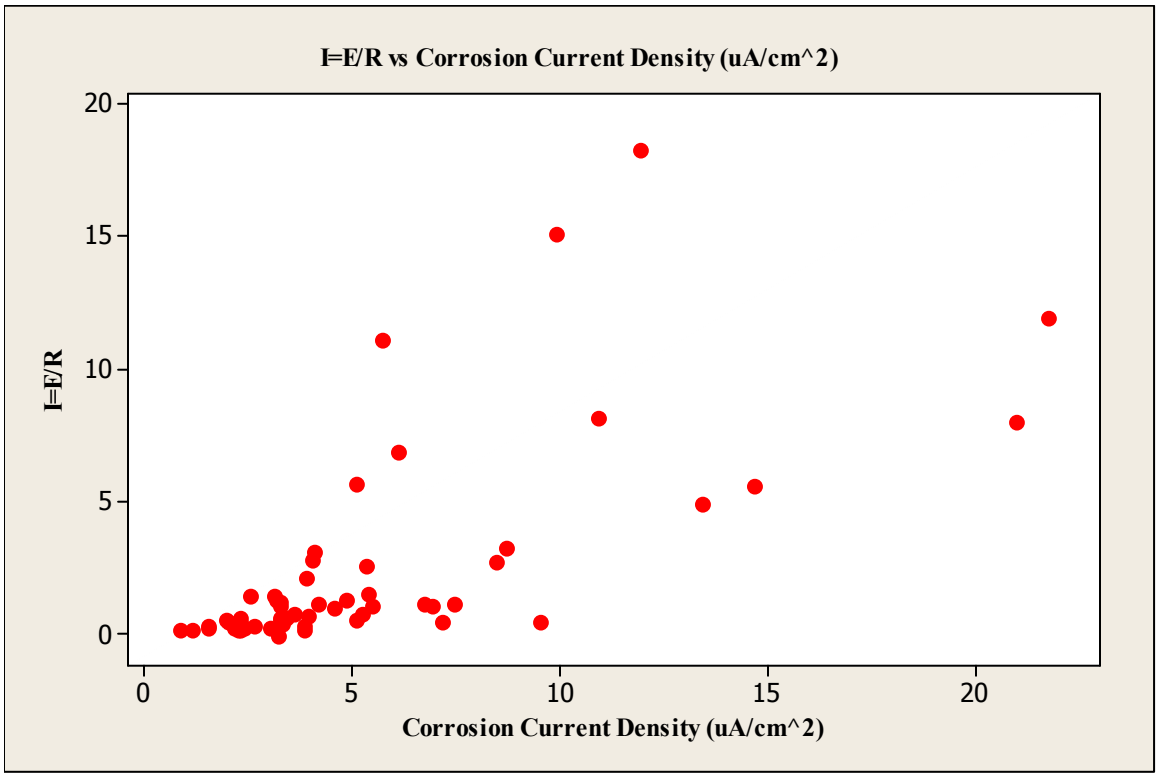

Figure 47 Corrosion Current Density versus I=E/R for Structures with a Specified Maximum W/C Ratio of 0.47

Bridge Decks Constructed Between 1972 and Present with Epoxy Coated Bars and Specified Maximum W/C (Cm) Ratio of 0.45.

Similarly, the distributions of the non-destructive test parameters for the combined 0.45 w/c and 0.45 w/cm subsets exhibit the same shape indicating the possibility that half-cell potentials may be used on structures reinforced with epoxy coated steel. However, the trends exhibited in the correlation analyses performed between resistivity and corrosion current density, half-cell potentials and corrosion current density, and resistivity and half cell potentials that were visible in subset 1 are weaker or non-existent in the structures reinforced with epoxy coated steel. Whereas there were three correlations with p-values less than 0.1 in subset 1, there were only two in the combined data set of subsets 2 and 3.

The correlation values obtained are presented in Table 30 and the scatter diagrams of these correlations are presented in Figures 48 through 51. The relationship between resistivity and corrosion current density is maintained, albeit with a higher p-value of 0.024 and a lower R-value of -0.182. This relationship is illustrated in Figure 48, which by and large shows that as the resistivity increases, the corrosion current density decreases. The p-values obtained in the statistical analysis indicate that the probability of a possible relationship between resistivity and corrosion potentials, as well as corrosion potentials and corrosion current density is low, with p-values of 0.145 and 0.576, respectively. However, examining the scatter plots of these relationships, the expected relationships can be discerned. As the resistivity increases, the corrosion potential will decrease, see Figure 49. The scatter plot of the corrosion potentials versus the corrosion current density shows that the linear relationship between the two parameters is generally maintained, see Figure 50. Lastly, the plot of the calculated corrosion current density values versus the measured field values shows that a linear relationship between the two values exists, see Figure 51.

Since the variability of the resistivity measurements is generally lower in the structures built with a specified minimum w/c and w/cm ratio of 0.45, one conclusion that may be drawn from Figures 48 through 51 is that the scatter of the non-destructive measurements of corrosion activity is influenced by the epoxy coating present on the reinforcing steel.

Table 30 Correlation and Probability Parameters for Structures with a Specified Maximum W/C (Cm) Ratio of 0.45

Correlation Parameters		**R-Value**	**P-Value**
Resistivity	Corrosion Current Density	-0.182	0.024
Resistivity	Corrosion Potentials	-0.118	0.145
Corrosion Potentials	Corrosion Current Density	0.045	0.576
E/R	Corrosion Current Density	0.372	0.000

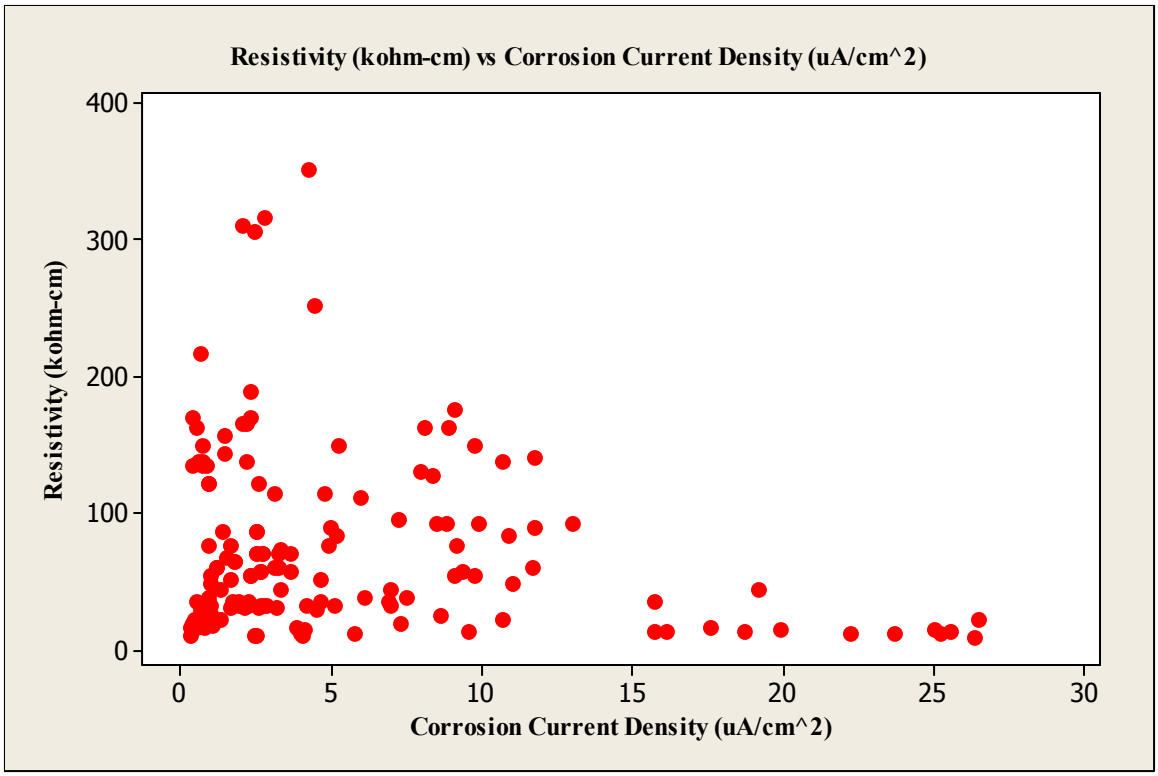

Figure 48 Resistivity versus Corrosion Current Density for Structures with a Specified Maximum W/C (CM) Ratio of 0.45

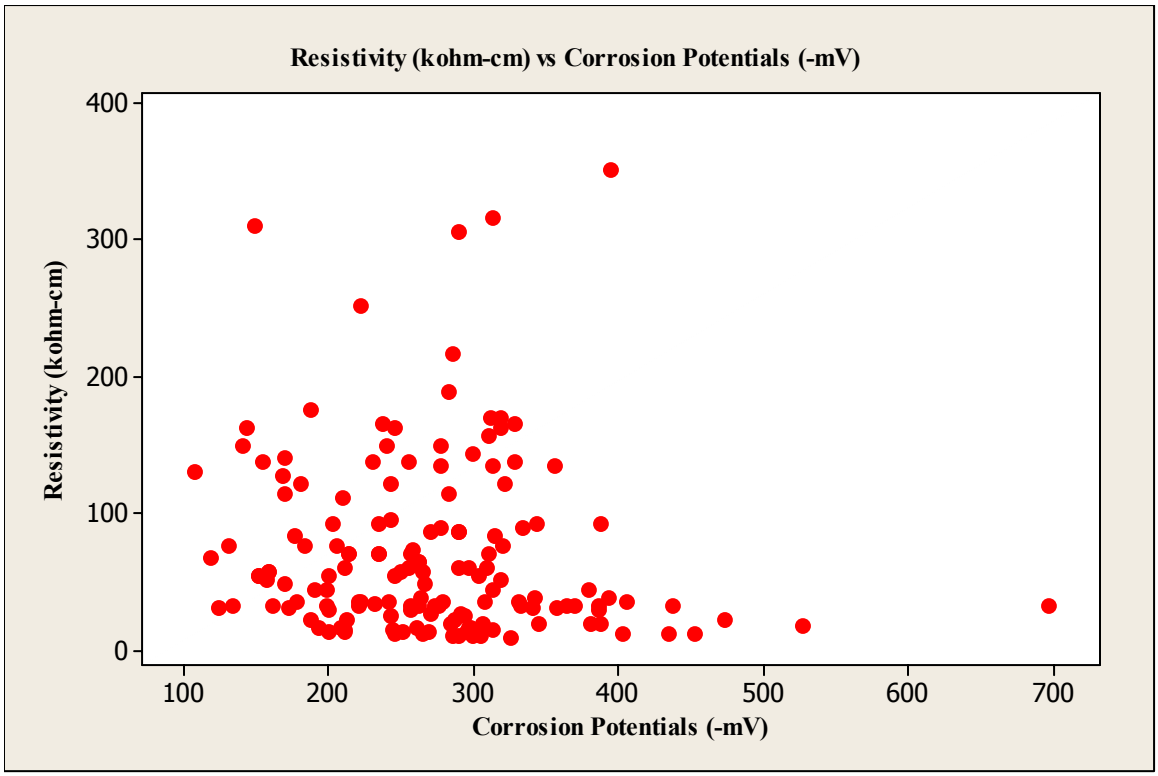

Figure 49 Resistivity versus Corrosion Potentials for Structures with a Specified Maximum W/C (CM) Ratio of 0.45

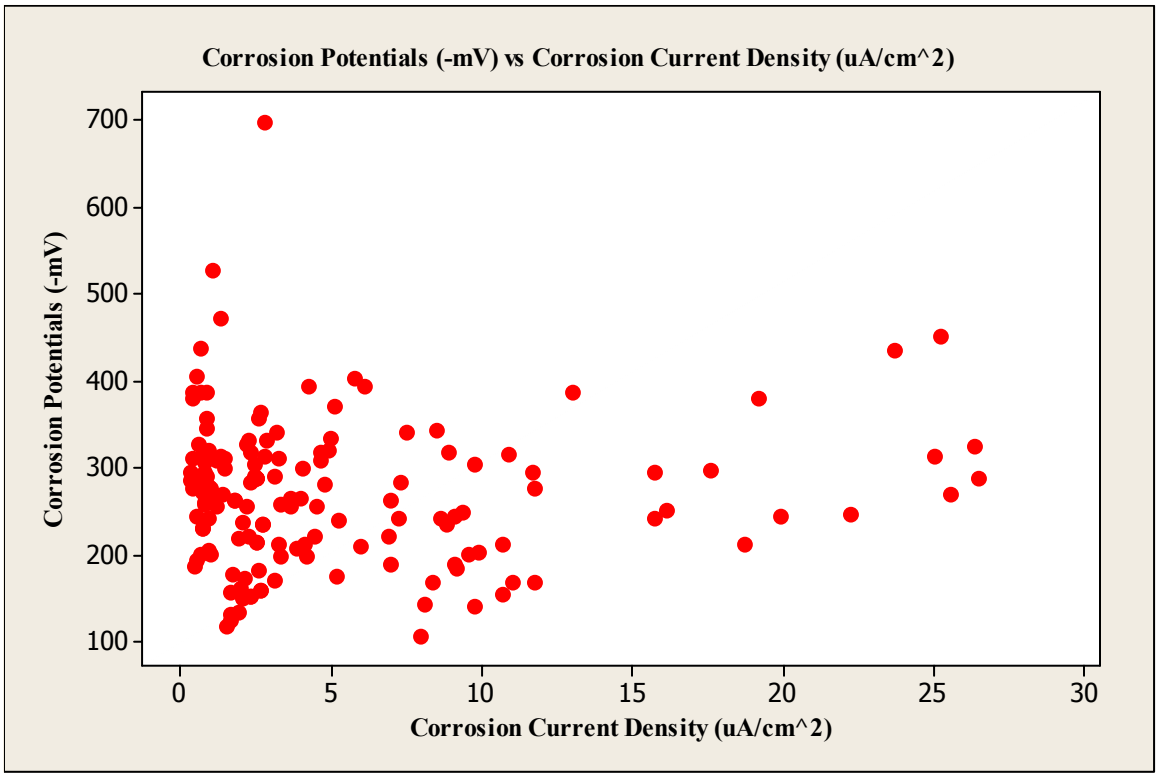

Figure 50 Corrosion Potentials versus Corrosion Current Density for Structures with a Specified Maximum W/C (CM) Ratio of 0.45

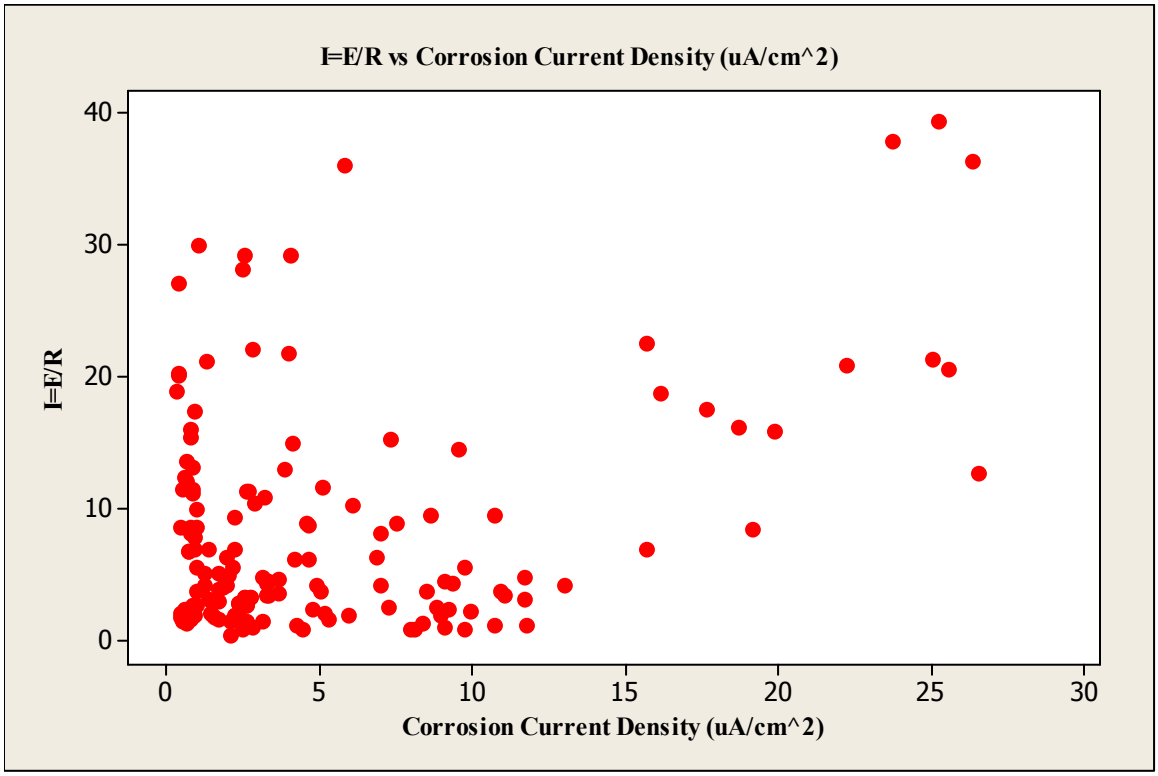

Figure 51 I=E/R versus Corrosion Current Density for Structures with a Specified Maximum W/C (Cm) Ratio of 0.45

Assessing Construction Quality Using Non-Destructive Test Methods

To assess how the general quality of construction has changed over the years two NDT testing methods were considered: concrete resistivity and reinforcing steel clear cover depth. For clarity purposes, each testing method will be analyzed separately.

1. Resistivity Measurements:

It is generally accepted that resistivity measurements are a relatively good indicator of concrete permeability in spite of the fact that there "is no quantification of permeation measures based on resistivity measurements (Bryant JW, 2001)." It is surprising therefore that older structures built with a specified maximum w/c ratio of 0.47 consistently have higher resistivities than newer structures built with maximum specified w/c ratios of 0.45 with and without pozzolans since these newer construction specifications were implemented specifically to decrease the permeability of the concrete, and consequently the susceptibility to chloride induced corrosion.

Furthermore, it is important to note that based on an analysis of variance (ANOVA), there is a significant difference between the measurements performed on structures built with a maximum specified w/c ratio of 0.47 and structures built with a maximum specified w/c or w/cm ratio of 0.45 as seen in Figure 52. This conclusion is based on the fact that the P-value in the ANOVA summary table in Figure 52 is less than 0.05. This conclusion is further supported graphically in Figure 52. There is a clear difference between the means of the resistivity measurements performed on structures built with a maximum specified w/c ratio of 0.47 and structures built with a maximum specified w/c or w/cm ratio of 0.45.

```
Source    DF         SS       MS      F      P
Factor     2   13855405  6927703  61.51  0.000
Error   2092  235599406   112619
Total   2094  249454811

Individual 95% CIs For Mean Based on Pooled StDev
Level                N   Mean  StDev  --+---------+---------+---------+-------
Resistivity 0.47   590  258.9  620.9                                 (---*----)
Resistivity 0.45   855   82.2   86.5    (---*--)
Resistivity 0.45   650   73.1   57.3  (---*---)
                                       --+---------+---------+---------+-------
                                        60       120       180       240
```

Figure 52 Resistivity ANOVA

A possible explanation for the significantly higher standard deviation for the group of measurements associated with subset 1 as well as the individual high coefficient of variation values for the structures in subset 1 is that the surface paste in the older structures has been worn sufficiently by traffic to expose a significant amount of aggregate. The aggregate, by and large, has a resistivity an order of magnitude and more than the hydrated portland cement paste (Bryant, J.W. 2001). Although the probe spacing on the resistivity meter was maintained at 51 mm as recommended by others to measure the average resistivity of the concrete paste and aggregate (Millard, et al, 1990), lack of quality surface paste can lead to highly variable measurements. This is caused by

probe contact with the aggregate and not with the portland cement paste. Other factors that can affect resistivity measurements are temperature, concrete relative humidity (moisture condition), type of cementitious material (e.g. cement, supplementary cementitious material), w/cm ratio and degree of hydration (Bryant, J.W. 2001), since the total porosity and the concentration of ions are influenced by the w/cm ratio (Hughes, B.P. et al. 1985).

2. Cover Depths:

VDOT cover depth specifications of 63 mm for structures built 20 years ago and newer, and 43 mm for structures older than 20 years allow for higher than specified clear cover depths, but do not allow for less than specified (R.E. Weyers et al 2003, AASTHO 1994, VDOT 1994). Based on a plot of the percent of clear cover depth measurements less than 51 mm (~ 2.00 in) for each structure versus the year each deck was built, with the exception of three decks, the structures in all three subsets appear to have an equal percentage of measurements less than 51 mm (~2.00 in), see Figure 53.

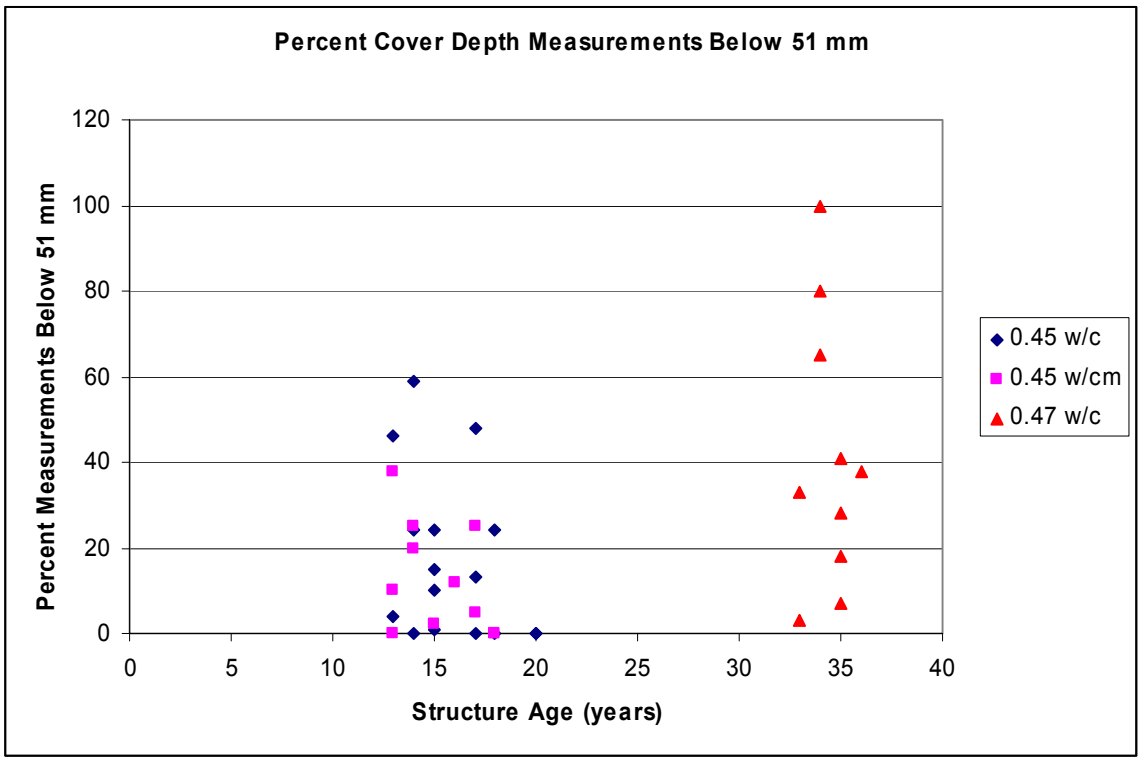

Figure 53 Percent Cover Depth Measurements Less Than 51mm

However, where only approximately 20 % of the cover depth measurements were less than specifications (43 mm) in the older structures built with maximum specified water/cement ratios of 0.47, the majority, approximately 70%, of the cover depth measurements for the structures built with maximum specified water/cement ratios of 0.45 with and without pozzolans and reinforced with epoxy coated steel were less than the minimum specified clear cover depth of 63 mm as shown in Figure 37. Furthermore, Figure 54 shows that even though the quality control has improved with an overall standard deviation decreasing from 11 mm for subset 1 to 9.5 and 8 mm for subsets 2 and

3, respectively, the VDOT specifications of 63 mm -0/+13 mm were still not met consistently.

Similar to resistivity measurements, it is important to note that based on ANOVA, there is also a significant difference between the measurements performed on structures built with a maximum specified w/c ratio of 0.47 and structures built with a maximum specified w/c or w/cm ratio of 0.45 as seen in Figure 54. This conclusion is based on the fact that the P-value in the ANOVA summary table in Figure 54 is less than 0.05. This conclusion is further supported graphically in Figure 54. There is a clear difference between the means of the clear cover depth measurements performed on structures built with a maximum specified w/c ratio of 0.47 and structures built with a maximum specified w/c or w/cm ratio of 0.45.

```
Source    DF        SS       MS       F      P
Factor     2   34487.3  17243.6  193.65  0.000
Error   2748  244698.7     89.0
Total   2750  279185.9

Level                 N    Mean   StDev
CD 0.47 W/C (mm)    728  52.202  10.756
CD 0.45 W/C (mm)   1157  60.230   9.510
CD 0.45 W/CM (mm)   866  60.224   8.049

Individual 95% CIs For Mean Based on Pooled StDev
Level              ----+---------+---------+---------+-----
CD 0.47 W/C (mm)   (--*--)
CD 0.45 W/C (mm)                                      (-*-)
CD 0.45 W/CM (mm)                                    (--*-)
                   ----+---------+---------+---------+-----
                    52.5      55.0      57.5      60.0
```

Figure 54 Clear Cover Depth ANOVA

Examining the data from the view point that the Virginia Department of Transportation increased the required clear cover depth from 43 mm to 63 mm in order to increase the projected service life of bridges by minimizing the amount of reinforcing steel with a clear cover depth less than 51 mm, Figure 53 shows that on a global level there have not been any major improvements in construction quality with respect to clear cover depth. It's important to point out that Figure 53 can be misleading since subset 1 has 10 structures, while subsets 2 and 3 have 16 and 11 structures, respectively. Furthermore, where there were no structures in subset 1 that had 0% measurements less than 51 mm, there were 5 structures in subset 2 and 3 structures in subset 3 that had 0% measurements less than 51 mm. This is important to note because some of the 0% data points overlap at the bottom of the plot giving the impression that the three subsets behave in a similar fashion.

Looking at the mean and the standard deviation of the percent of measurements less than 51 mm gives a better indication of the level of improvement in quality control with respect to clear cover depth, see Table 31.

Table 31 Mean and Standard Deviation of % Cover Depths < 51 mm

Study Subset	Mean of % Cover Depths < 51 mm	Standard Deviation
1	41.3	31.5
2	16.8	19.4
3	12.5	12.9

Where subset 1 had a mean of 41.3% and a standard deviation of 31.5%, subsets 2 and 3 showed averages of 16.8% and 12.5% and standard deviations of 19.4% and 12.9%, respectively. This analysis shows a clear initial improvement between subsets 1 and 2, followed by slightly less improvement between subsets 2 and 3.

CONCLUSIONS

Based on the tree classification, the determining factor in the assignment of an NBIS deck rating value was the visible damage to the bridge deck, as required in the NBIS rating guide, measured in linear meters of cracking per area surveyed. Further analysis however, showed that in the field this parameter is not consistently applied with some structures receiving higher ratings than other structures with far less visible deterioration supporting the assertion that the current inspection guidelines are applied subjectively. One limitation of this study was narrow range of rating values available. The structures used in this study had only three rating values – 6, 7, and 8 – out of theoretically ten and realistically five possible rating values. This study showed that there is a need for specific quantitative inspection guidelines which address all forms of visible damage, since the current guidelines are overly broad.

The comparison of measurements distributions does not eliminate the possibility that these non-destructive test methods may be applicable to structures reinforced with ECR. With respect to corrosion potentials, this conclusion is based on the fact that the field readings obtained appeared to be reasonable – the readings were stable and had the correct polarity sign – as well as the approximate normal distribution as specified in ASTM C 867-91. The same test however could not be performed on the linear polarization method since the data was biased. Instead, the only analysis tool available was the possible relationship as indicated by Ohm's Law. It is important to note that the test based on Ohm's law, which governs the relationships between resistance, current and potential, generally failed when applied to the measurements collected from structures reinforced with epoxy coated steel at p-value threshold of 0.10. However, the expected relationships were generally visible in the scatter plots of the electrical measurements. Therefore, due to the limited amount of information related to the linear polarization testing of epoxy coated bars as well as a complete lack of information regarding the influence of epoxy coatings on corrosion current density calculations, the conclusion is that the 3LP device could possibly be used on structures reinforced with epoxy coated bars following more research into the effects of the epoxy coating on the corrosion current density measurements.

With respect to current quality of construction, it appears that the benefits of the increase in the specified clear cover depth and lower water/cement ratio as well as the addition of pozzolans, may be lost due to other factors such as poor quality control during the batching or construction processes. This conclusion is supported by the fact that in the newer structures, more than 60% of the clear cover depth measurements indicate clear cover depth lower than the current VDOT specified minimum of 63 mm (2.5 in) as opposed to less than of quarter of measurements in the structures built approximately three decades ago when the specified minimum cover depth was 43 mm (1.69 in). Analyzing the same data, however, using the AASHTO standard of 51 mm (~ 2.00 in) clear cover depth as opposed to the VDOT standard of 63 mm (2.5 in) a clear improvement in the number of measurements below 51 is visible. The analysis of variance test also shows that standard deviation in each subset decreased slightly.

Furthermore, lower resistivity measurements in the newer structures (i.e. subsets 2 and 3) may point to higher permeability of the concrete decks leading to premature chloride induced corrosion of the reinforcing steel. However, it's important to note that the resistivity readings obtained on the structures in subset 1 are suspect because of possible high surface contact resistance.

RECOMMENDATIONS

Further investigation is necessary to evaluate the bridge inspection procedures as related to the NBIS rating. Exact rating guidelines based on specific levels of deterioration have to be established to eliminate the current level of subjectivity associated with the NBIS rating system. In addition, the NBIS rating scale would also have to be re-evaluated, whereby the extreme values are eliminated while the remaining values are scaled such that they are more sensitive to changes in deck conditions, and therefore provide a more meaningful damage assessment.

Since the results of this study show that non-destructive tests may be applicable to epoxy coated reinforcing steel, further investigation is necessary to study the impact epoxy coatings have on non-destructive tests such as corrosion potentials and linear polarization. Moreover, the results of this study may be further refined using the data from the tests currently being performed by the VTRC mentioned in the Methods and Materials section of this work. Once those effects are better understood, it will be necessary to establish interpretation guidelines for the tests mentioned above.

Lastly, this study showed that there were some improvements with respect to clear cover depth, however, benefits associated with changes in construction specifications such as of lower water/cement ratios and the use of pozzolans may be lost due to current construction practices. Therefore, better field quality control measures need to be implemented to realize all the potential benefits such as increased service life and lower maintenance costs.

REFERENCES

Anderson-Cook, Christine M. et al (2002). "Differentiating Soil Types Using Electromagnetic Conductivity and Crop Yield Maps." Soil Science Society of America Journal, vol. 66, n. 5, Sept.-Oct. 2002, p. 1562-1570.

Andrande,C. et al (1996). "Corrosion Rate Monitoring in the Laboratory and On-Site." Construction and Building Materials, vol. 10, n. 5, 1996, p. 315 – 328.

Andrande, C. et al (2002). "Standardization to a Reference of 25°C, of Electrical Resistivity for Mortars and Concretes in Saturated or Isolated Conditions." ACI Material Journal, vol. 99, n. 2, March – April 2002, p. 119 – 128.

ASTM (1991), "C 876-91, Standard Test Method for Half-Cell Potentials of Uncoated Reinforcing Steel in Concrete", ASTM Annual Book of ASTM Standards, vol. 04.02n. (Concrete and Aggregates).

ASHTO LRFD Bridge Design Specifications, Section 5.12.3, 1994.

Atimay, E. and Ferguson, P.M. (1974). "Early Chloride Corrosion of Reinforcing – A Test Report." Materials Performance, v. 13, n. 12, p. 18-21.

Babaei K and Hawkins N (1988). "Evaluation of Bridge Deck Protective Strategies." Concrete International, Vol. 10 No. 12, pp. 56-66.

Baweja, Daksh et al (1998). "Chloride – Induced Steel Corrosion in Concrete: Part 1 – Corrosion Rates, Corrosion Activity, and Attack Areas." ACI Materials Journal, vol. 95, n. 3, May – June 1998, p. 207 – 217.

Beasley, Kimball J. (2003). "Failure of Exposed Concrete Caused by Corrosion of Embedded Steel." Journal of Performance of Constructed Facilities, ASCE, August 2003, p.107 – 108.

Beeby, A. W. (1970). "An Investigation of Cracking in Reinforced Concrete Slabs Spanning One Way – Static Loading." CIRIA Research Report 21, March 1970, p. 5-6, 43-45.

Bennett, J. "Corrosion of Reinforcing Steel in Concrete and its Prevention by Cathodic Protection." Anti-Corrosion Methods and Materials, v. 33, n. 11, October 1986, p. 12 – 17.

Bentz, Dale P. et al. (1991) "Simulation Studies of the Effects of Mineral Admixtures on the Cement Paste-Aggregate Interfacial Zone." ACI Materials Journal, vol. 88, n. 5, September – October 1991, p. 518 – 529.

Brown, Michael C. (2003). "Linear Cracking and Chloride Penetration of Concrete Bridge Decks." VTRC Research Proposal, March 2003.

Brown, Michael C. (2002) " Corrosion Protection Service Life of Epoxy Coated Reinforcing Steel in Virginia Bridge Decks." Dissertation in Civil and Environmental Engineering, Virginia Polytechnic Institute and State University.

Bryant, James W. Jr. (2001) "Non-Invasive Permeability Assesment of High-Performance Concrete Bridge Deck Mixtures." Dissertation in Civil and Environmental Engineering, Virginia Polytechnic Institute and State University.

Bungey, J.H. (1989) "Testing of Concrete in Structures." 2nd Edition, Chapman & Hall, New York.

Castellote, Martha et al (2002). "Standardization, to a Reference of 25 °C, of Electrical Resistivity for Mortars and Concretes in Saturated or Isolated Conditions." ACI Materials Journal, March – April 2002, p. 119 – 128.

Clear, Kenneth C. et. al.(1995). "Performance of Epoxy-Coated Reinforcing Steel in Highway Bridges." National Academy Press, Washington, D.C., 1995.

Clear, Kenneth C. (1989). " Measuring Rate of Corrosion of Steel in Field Concrete Structures." Kenneth C. Clear, Inc. Concrete Materials and Corrosion Specialists, Sterling, Virginia 1989.

Clemeña, Gerardo G. (1992). "Benefits of Measuring Half – Cell Potentials and Rebar Corrosion Rates in Condition Surveys of Concrete Bridge Decks." Virginia Transportation Research Council, Report Number VTRC 92-R16.

Coleman, Hal (2004). VDOT Salem District Bridge Engineer. Personal comunication, April 2004.

Crank J (1975). "The Mathematics of Diffusion." Second Edition, Oxford University Press, Great Britain

Deshpande, P.G. et al (2002). "Corrosion Performance of Polymer-Coated, Metal-Clad, and Other Rebars as Reinforcements in Concrete: Literature Review." FHWA Report Number: FHWA/TX – 03/4904 – 1.

Elsener, B et al (1993). "Inspection and Monitoring of Reinforced Concrete Structures – Electrochemical Methods to Detect Corrosion." Insight – non – Destructive Testing and Condition Monitoring, vol. 36, n. 7, July 1994, p. 502 – 506.

Feliu, S. et al (1996). "Techniques to Assess the Corrosion Activity of Steel Reinforced Concrete Structures." ASTM STP 1276.

Ferraris, Chiara F. et al (2001). "The Influence of Mineral Admixtures on the Rheology of Cement Paste and Concrete." Cement and Concrete Research, vol. 31, n. 2, p.245 – 255.

FHWA (1995). "Recording and Coding Guide for the Structure Inventory and Appraisal of the Nation's Bridges." Report No. FHWA-PD-96-001.

Fitch MG et al (1995). "Determination of End of Functional Service Life for Concrete Bridge Decks." Transportation Research Record, n. 1490, p. 60 – 66.

Fontana, Mars Guy (1986). "Corrosion Engineering." McGraw-Hill Company, 1986.

Fulton, F.S. et al (1974). "The Properties of Portland Cements Containing Milled Granulated Blastfurnace Slag", The Portland Cement Institute, Johannesburg, South Africa.

Geenen, F. M. (1991). " Characterization of Organic Coatings With Impedance Measurements." Doctoral Dissertation, Delft University of Technology

Gowers, K. R. et al (1999). "Measurement of Concrete Resistivity for Assesment of Corrosion Severity of Steel Using Wenner Technique." ACI Materials Journal, vol. 96, n. 5, September – October 1996, p. 536 – 541.

Griffith, Andrew et al (1999). "Epoxy Coating Reinforcement Study." State Research Project #527, Oregon Department of Transportation Research Group.

Hartle, R.A. et al (1995). "Bridge Inspector's Training Manual 90." FHWA – PD – 91 – 015.

Hughes, B.P. et al (1985). "New Technique For Determining The Electrical Resistivity of Concrete." Magazine of Concrete Research, 37(133), pp. 243 – 248.

Huston, Alvin I (1993). "Carbonation in Canadian Buildings." CMHC Technical Series 93 – 207.

Kirkpatrick, Trevor J. (2001) "Impact of Specification Changes on Chloride Induced Corrosion Service Life of Virginia Bridge Decks." Master's Thesis in Civil and Environmental Engineering, Virginia Polytechnic Institute and State University.

Kirkpatrick, T.J., Weyers, R.E., Anderson-Cook, C., and Sprinkel, M.M. (2002). "A Model toPredict the Impact of Specification Changes on the Chloride-Induced Service Lifeof Virginia Bridge Decks." VTRC 03-CR4, Virginia Transportation Research Council, Charlottesville, VA, 2002.

Lambert, Paul (1998). "Reinforced Concrete – History, Properties & Durability." Corrosion Prevention Association, Oct. 1998.

Law, D.W. et al (2003). "Evaluation of Corrosion Loss of Steel Reinforcing Bars in Concrete Using Linear Polarization Resistance Measurements." Non-Destructive Testing in Civil Engineering (NDT-CE), Oct 2003, v. 8, n. 10

Lewis, D.W. (1985). "Discussion of Admixtures for Concrete." Concrete International: Design and Construction, v. 27, n. 5, May 1985, p. 64 – 65.

Lohtia, R.P. (1995). "Concrete Admixtures Handbook" Noyes Publications, Park Ridge, NJ.

Liu, Y. (1996). "Modeling the Time-to-Corrosion Cracking of the Cover Concrete in Chloride Contaminated Reinforced Concrete Structures." Doctoral Dissertation, Virginia Polytechnic Institute & State University.

Malhotra, V.M. et al (2004). "Nondestructive Testing of Concrete. Second Edition." CRC Press LLC. West Conshohocken, PA.

Manning, David G. (1995). "Detecting Defects and Deterioration in Highway Structures." National Cooperative Highway Research Program Synthesis of Highway Practice 118.

Mehta, P. Kumar (1993). " Concrete Structures, Properties and Materials." Prentice Hall, Englewood Cliffs, NJ.

Millard, S. et al (1990). "Assessing electrical resistivity of concrete structures for corrosion durability studies." Proceedings of third international symposium on corrosion of reinforcement in concrete construction. Elsevier Science, 1990, pp. 303 – 313.

Morris, W. et al (2001). "Corrosion of Reinforcing Steel Evaluated by Means of Concrete Resistivity Measurements." Corrosion Science, v. 44, p. 81 – 99.

Morris, W. et al (1996). "Practical Evaluation of Resistivity of Concrete in Test Cylinders Using a Wenner Array Probe." Cement and Concrete Research, vol. 26 n. 12, October 1996, p. 1779 – 1787.

Montemor, M.F. et al (2000). "Effect of Flyash on Concrete Reinforcement Corrosion Studies by EIS." Cement and Concrete Composites, vol. 22, January 2000, p. 175 – 185.

Nagi, Mohamad A. and Whiting, David A. (2003). "Electrical Resistivity of Concrete—A LiteratureReview." R&D Serial No. 2457, Portland Cement Association, Skokie, Illinois, USA, 57 pages.

Naish, C. C. et al (1988). " Variability of Potentials Measured on Reinforced Concrete Structures." Materials Performance, vol. 27, n. 4, April 1988, p. 45 – 48.

Ostle, B. et al (1995). "Engineering Statistics: The Industrial Experience." Wadsworth, November 1995.

Polder, Rob B. et al (2002). "Characterisation of Chloride Transport and Reinforcement Corrosion in Concrete Under Cyclic Wetting and Drying by Electrical Resistivity." Cement and Concrete Composites, vol. 24, 2002, p. 427 – 435.

Pyc, Wioleta Agata (1998). "Field Performance of Epoxy-Coated Reinforcing Steel in Virginia Bridge Decks." Doctoral Dissertation in Civil and Environmental Engineering, Virginia Polytechnic Institute and State University.

Ramachandran, V.S. (1995). "Concrete Admixtures Handbook" Noyes Publications, Park Ridge, NJ.

Revie, R.W. (2000). "Uhlig's Corrosion Handbook." 2nd ed., John Wiley & Sons, Inc., New York, NY, 2000.

Sagüés, A.A. et al (1990). "Marine Environment Corrosion of Epoxy-Coated Reinforcing Steel." Page, C.L., Treadaway, K.W.J., and Bamforth, P.B. Corrosion of Reinforcement in Concrete, 539-550. Applied Elsevier Science Ltd.

Sagüés, A.A. et al (1996). "Practical Evaluation of Resistivity of Concrete in Test Cylinders Using a Wenner Array Probe." Cement and Concrete Research, vol. 26, n.12, p. 1779 – 1787.

Seymour, R.B. et al (1990). "Handbook of Organic Coatings: A Comprehensive Guide for the Coatings Industry." New York & London, Elsevier.

Sohanghpurwala, A.A. et al (1999). "Condition and Performance of Epoxy Coated Rebars in Bridge Decks." Public Roads, November/December 1999.

Smith, J.L. et al (2000). "Materials and Methods for Corrosion Control of Reinforced and Prestressed Concrete Structures in New Construction." FHWA Report Number: FHWA – RD – 00 – 081.

Takewaka, K. et al. (2003). "Simulation Model for Deterioration of Concrete Structures due to Chloride Attack." Journal of Advanced Concrete Technology, v. 1, n. 2, 2003, p. 139-146.

Trethewey, K.R. et al. (1988). "Corrosion for Students of Science and Engineering." Longman Scientific & Technical, p. 228 – 230.

Turner, H.M. (1998). "Conversion Between Network-Level and Project-Level Units of Measure for Use in a Bridge Management System." VTRC Report 99-R4. "Corrosion Protection: Concrete Bridges." http://www.tfhrc.gov/structur/corros/introset.htm. Last accesed Oct 20, 2003.

Vermani, P and Clemena, G. (2001). "Fighting Corrosion in Reinforced Concrete Bridge Decks." The Road Ahead, Virginia Transportation Research Council, Charlottesville, VA, June 2001, pp. 1-7.

Virginia Department of Transportation Road and Bridge Specifications, Section 406, January 1994.

Weed, R.M. (1974). "Recommended Depth of Cover for Bridge Deck Steel." Transportation Research Record, n. 500, p. 32 – 35.

Weyers, RE et al (1993). "Concrete Bridge Protection, Repair, and Rehabilitation Relative to Reinforcement Corrosion: A Methods Application Manual." SHRP-S-360, Strategic Highway Research Program.

Weyers, R.E. and Liu, Y. (1998). "Modeling the Time-to-Corrosion Cracking in Chloride Contaminated Reinforced Concrete Structures." ACI-Materials-Journal, v. 95, n. 6, 1998, pp 675-681.

Weyers, R.E. et al (2003). "Bridge Deck Cover Depth Specifications." Concrete International, February 2003, v. 25, n. 2, pp. 61 – 64.

Weyers, R.E., Personal Communication with Richard E. Weyers, January, 2004.

Young, Francis J. et al (1998). "The Science and Technology of Civil Engineering Materials." Prentice Hall, Upper Saddle River, NJ.

Zemajtis, J., R.E. Weyers, M.M. Sprinkel, and W.T. McKeel, Jr. (1996). "Epoxy-Coated Reinforcement - A Historical Performance Review." VTRC 97-IR1, Virginia Transportation Research Council, pp. 4.

Zemajtis, J. (1998). "Modeling the Time to Corrosion Initiation for Concretes with Mineral Admixtures and/or Corrosion Inhibitors in Chloride-Laden Environments." Dissertation in Civil and Environmental Engineering, Virginia Polytechnic Institute and State University.

Zhang, Jieying et al (2000). "Validation of Resistivity Spectra From Reinforced Concrete Corrosion by Kramers – Kronig Transformations." Cement and Concrete Research, vol 31, 2001, p. 603 – 607.